Activity of the Aurora kinase B inhibitor AZD1152 in Acute Myeloid Leukaemia

MARTIN GRUNDY, BSc.

Thesis submitted to the University of Nottingham

for the degree of Doctor of Philosophy

DECEMBER 2012

Abstract

Aurora kinases play an essential role in orchestrating chromosome alignment, segregation and cytokinesis during mitotic progression, with both aurora-A and B frequently over-expressed in a variety of human malignancies including those of leukaemic origin. Acute myeloid leukaemia (AML) is a heterogeneous clonal disorder of haematopoietic progenitor cells whose prognosis is particularly poor and where standard induction therapy has changed little over the past thirty years. This thesis evaluated the effects of AZD1152-hQPA (barasertib-hQPA), a highly selective inhibitor of aurora-B kinase, in AML cell lines and primary samples. Inhibition of phospho-Histone H3 (pHH3) on serine 10 can be used as a biomarker for AZD1152-hQPA activity and an assay was optimized to measure pHH3 in our cell lines and primary samples. AZD1152-hQPA inhibited pHH3 in our cell lines resulting in polyploid cells, apoptosis, and cell death, irrespective of cellular p53 status.

Over-expression of the ATP-binding cassette (ABC) drug transporter proteins P-glycoprotein (Pgp) and Breast cancer resistance protein (BCRP) is a major obstacle for chemotherapy in many tumour types with Pgp conferring particularly poor prognosis in AML. A cell line which over-expresses Pgp was developed by selecting for daunorubicin (DNR) resistance in OCI-AML3 cells. Pgp and also BCRP expressing AML cell lines were found to be resistant to AZD1152-hQPA and it was found that AZD1152-hQPA is effluxed by these transporters. pHH3

inhibition by low dose AZD1152-hQPA was seen in all of the primary samples tested with Pgp and BCRP positive samples being less sensitive. However, 50% inhibition of pHH3 by AZD1152-hQPA was achieved in 94.6% of these samples.

The FLT3-ITD-expressing MOLM-13 and MV4-11 cell lines were particularly sensitive to AZD1152-hQPA. Internal tandem duplications (ITDs) within the FLT3 tyrosine kinase receptor are found in approximately 25% of AML patients and are associated with a poor prognosis. It was demonstrated that AZD1152-hQPA directly targets phosphorylated FLT3 in the FLT3-ITD cell lines along with inhibiting its downstream target pSTAT5. FLT3-ITD primary samples were particularly sensitive to clonogenic inhibition and pSTAT5 down-regulation after treatment with AZD1152-hQPA compared with FLT3 wild-type (WT) samples.

List of Publications

1.

Mol Cancer Ther. 2010 Mar;9(3):661-72.

The FLT3 internal tandem duplication mutation is a secondary target of the aurora B kinase inhibitor AZD1152-HQPA in acute myelogenous leukemia cells.

Grundy M, Seedhouse C, Shang S, Richardson J, Russell N, Pallis M.

Department of Academic Haematology, University of Nottingham, Nottingham.

2.

BMC Cancer. 2011 Jun 16;11:254.

P-glycoprotein and breast cancer resistance protein in acute myeloid leukaemia cells treated with the aurora-B kinase inhibitor barasertib-hQPA.

Grundy M, Seedhouse C, Russell NH, Pallis M.

Department of Academic Haematology, The University of Nottingham, Clinical Sciences Building, Hucknall Road, Nottingham, NG5 1PB, UK.

Acknowledgements

Firstly I would like to say thank you to my project supervisors, Dr Monica Pallis and Professor Nigel Russell, for all their help and guidance throughout my PhD. In particular, I would like to say a huge thank you to Dr Monica Pallis for giving me this research project and for her support, expert advice and ideas throughout the course of this PhD and during the writing of this thesis.

I would also like to thank all staff and students, past and present in the Academic Haematology Department at the Nottingham University Hospitals City Campus for making my PhD an enjoyable experience. I'd particularly like to thank Dr Claire Seedhouse for her expert technical advice and to Shilli Shang for her assistance and tireless enthusiasm in the department.

Outside of the department, I would like to thank Dr Kirsten Mundt and Dr Elizabeth Anderson of AstraZeneca UK for their enlightening discussions throughout the course of this PhD and to Robert Moss in the Oncology department for his technical assistance.

On a more personal note, I would like to thank my wife Rebecca for her love, support and encouragement and for giving me my daughter Sophia who provides me with endless cuddles and smiles.

List of Abbreviations

^{3}H-Tdr	Tritiated Thymidine
7-AAD	7-Amino-actinomycin D
ABC	ATP-Binding Cassette
ABCB1	Gene encoding the ATP-Binding Cassette Sub-Family B Member 1 protein (Pgp)
ABCC1	Gene encoding the ATP-Binding Cassette Sub-Family G Member 2 protein (MRP1)
ABCG2	Gene encoding the ATP-Binding Cassette Sub-Family G Member 2 protein (BCRP)
AIM-1	Aurora-B Protein
ALL	Acute Lymphoblastic Leukaemia
ALM	Activation loop mutation
AML	Acute Myeloid Leukaemia
APL	Acute Promyelocytic Leukaemia
Ara-c	Cytosine Arabinoside
ATO	Arsenic Trioxide
ATP	Adenosine Triphosphate
ATRA	All-trans Retinoic Acid
AZD1152-hQPA	AZD1152-Hydroxyquinazoline Pyrazol Anilide
β2M	Beta-2-microglobulin
BCR-ABL	Breakpoint Cluster Region-Abelson
BCRP	Breast Cancer Resistance Protein
BSA	Bovine Serum Albumin
Calcein-AM	Calcein Acetoxymethyl Ester

CEBPA	CCAAT/enhancer-binding protein-α
cDNA	Complementary Deoxyribonucleic Acid
Ci	Curie
CLL	Chronic Lymphoid Leukaemia
CML	Chronic Myelogenous Leukaemia
CMV	Cytomegalovirus
CO_2	Carbon Dioxide
ColE1	Colicin E1
CPC	Chromosomal passenger complex
CSA	Cyclosporin A
C-terminus/terminal	Carboxy-(COOH)-Terminus of a Protein
CR	Complete Remission
DAPI	4'-6-Diamidino-2-phenylindole
DMSO	Dimethyl Sulfoxide
DNA	Deoxyribonucleic Acid
DNase	Deoxyribonuclease
DNMT3a	DNA Methyltransferase 3a
DNR	Daunorubicin
dNTPs	Deoxynucleotides
ECACC	European Collection of Animal Cell Cultures
ECL	Enhanced Chemi-Luminescence
EDTA	Ethylenediamine Tetra-Acetic Acid
FAB	French-American-British

FACS	Fluorescence Activated Cell Sorting
FCS	Foetal Calf Serum
FITC	Fluorescein Isothiocyanate
FISH	Fluorescent In Situ Hybridisation
FL	FLT3 Ligand
FLT3	FMS-like tyrosine kinase 3
FLT3-ITD	FMS-like tyrosine kinase 3 Internal Tandem Duplication
FTC	Fumitremorgin C
G-CSF	Granulocyte Colony Stimulating Factor
GM-CSF	Granulocyte-macrophage colony-stimulating factor
GFP	Green fluorescent protein
GO	Gemtuzumab Ozogamicin
HSCs	Haemopoietic stem cells
IgG	Immunoglobulin G
IL-3	Interleukin-3
IL-6	Interleukin-6
INCENP	Inner Centromere Protein
ITD	Internal Tandem Duplication
JAK2/3	Janus Kinase 2/3
LB+AMP	Liquid Broth + Ampicillin
LSCs	Leukaemic stem cells
mAb	Monoclonal Antibody
MDR	Multi-Drug Resistance
MDR1	Multi-Drug Resistance 1 Gene encoding P-glycoprotein

MDS	Myelodysplastic syndromes
MRC	Medical Research Council
$MgCl_2$	Magnesium Chloride
MMLV	Moloney murine leukaemia virus
mRNA	Messenger Ribonucleic Acid
MRP1	Multidrug Resistance-Associated Protein 1
MTD	Maximum Tolerated Dose
NaCl	Sodium Chloride
NaF	Sodium fluoride
NOD/SCID	Non-obese diabetic with severe combined immunodeficiency disease
NK	Normal Karyotype
NPM1 mutation	Nucleophosmin Mutation
N-terminus/terminal	Amino-(NH_2)-Terminus of a Protein
OS	Overall survival
PBS	Phosphate-Buffered Saline
PBSAA	Phosphate-Buffered Saline Albumin Azide
PCR	Polymerase Chain Reaction
PE	PhycoErythrin
Pgp	Permeability-glycoprotein
pHH3	Phosphorylated Histone H3 (Ser10)
PI	Propidium Iodide
PMSF	Phenylmethylsulfonyl Fluoride

pSTAT5	Phosphorylated Signal Transducer and Activator of Transcription factor 5
pFLT3	Phosphorylated FMS-like tyrosine kinase 3
R123	Rhodamine 123
Rb	Retinoblastoma Tumour Suppressor Protein
RPMI	Roswell Park Memorial Institute Medium
RNA	Ribonucleic Acid
RNase	Ribonuclease
RT-PCR	Reverse Transcriptase Polymerase Chain Reaction
SAC	Spindle Assembly Checkpoint
SCF	Stem Cell Factor
SD	Standard Deviation
SDS	Sodium Dodecyl Sulphate
SDS-PAGE	Sodium Dodecyl Sulphate - Polyacrylamide Gel electrophoresis
Ser^{10}	Serine 10
siRNA	Small-Interfering Ribonucleic Acid
SOC medium	Super Optimal Broth with Catabolic Repressor Medium
SP	Side Population
STAT5	Signal Transducer and Activator of Transcription factor 5
STR	Short Tandem Repeats
TBE	Tris Borate EDTA
UV	Ultra-violet
WBC	White blood cell count
WHO	World Health Organisation

WT	Wild-Type

Table of Contents

List of Figures

CHAPTER ONE – INTRODUCTION

CHAPTER TWO – MATERIALS AND METHODS

CHAPTER THREE - VALIDATION OF BIOMARKER AND CHEMOSENSITIVITY OF AML CELLS TO AZD1152-hQPA

CHAPTER FOUR - STABLE TRANSFECTION OF MDR1 INTO THE OCI-AML3 CELL LINE

CHAPTER FIVE - EFFECT OF ATP-BINDING CASSETTE TRANSPORTERS ON AZD1152-hQPA SENSITIVITY

CHAPTER SIX - THE FLT3-ITD MUTATION IS A SECONDARY TARGET OF AZD1152-hQPA IN AML CELLS

CHAPTER SEVEN - EFFECT OF AZD1152-hQPA ON PRIMARY AML CELLS

CHAPTER EIGHT - DISCUSSION

List of Tables

Chapter One
INTRODUCTION

1.1 Background

The global burden of cancer continues to increase largely because of the aging and growth of the world population alongside an increasing adoption of cancer-causing behaviors, particularly smoking, in economically developing countries. In the developed world cancer is considered as one of the leading causes of death, second only to circulatory disorders such as heart disease and strokes, and is therefore a major burden on public health services in these countries. Statistics from Europe in 2008 show there were an estimated 3.2 million new cases of cancer and 1.7 million deaths (Ferlay *et al.*, 2010). The most common cancers were colorectal cancers (436,000 cases, 13.6% of the total), breast cancer (421,000, 13.1%), lung cancer (391,000, 12.2%) and prostate cancer (382,000, 11.9%). The most common causes of death from cancer were lung cancer (342,000 deaths, 19.9% of the total), colorectal cancer (212,000 deaths, 12.3%), breast cancer (129,000, 7.5%) and stomach cancer (117,000, 6.8%) (Ferlay *et al.*, 2010). Cancer is considered an age-dependent disease, with 64% of all cases occurring in patients aged 65 or over and approximately 76% of all cancer mortalities occurring in patients from the same age group (Jemal *et al.*, 2010). The overall risk of an individual developing cancer during their lifetime is one in three. For patients under the age of 50 however, this risk is reduced to 1 in 27 (Ferlay *et al.*, 2010). In the United States in 2010, there are projected to be a total of 1,529,560 new cancer cases, and 569,490 deaths from cancer (Jemal *et al.*, 2010). Leukaemia ranks ninth in the list of most prevalent cancers diagnosed, with 43,050 new cases estimated in 2010, with incidence and mortality greater in males than females (Jemal *et al.*, 2010). Approximately 29%

Table 1.1 – Estimated new leukaemia cases and deaths, United States, 2010. (Data from Jemal et al Ca Cancer J Clin 2010.)

	ESTIMATED NEW CASES			ESTIMATED DEATHS		
	Both Sexes	Male	Female	Both Sexes	Male	Female
Leukaemia	43,050	24,690	18,360	21,840	12,660	9,180
Acute lymphocytic leukaemia	5,330	3,150	2,180	1,420	790	630
Chronic lymphocytic leukaemia	14,990	8,870	6,120	4,390	2,650	1,740
Acute myeloid leukaemia	**12,330**	**6,590**	**5,740**	**8,950**	**5,280**	**3,670**
Chronic myeloid leukaemia	4,870	2,800	2,070	440	190	250
Other leukaemia	5,530	3,280	2,250	6,640	3,750	2,890

of these new cases will be acute myeloid leukaemia (AML) (Table 1.1). In children ages birth to 14, leukaemia, particularly acute lymphocytic leukaemia, is the commonest form of cancer and accounts for nearly one-third of the cases diagnosed (Jemal *et al.*, 2010).

1.2 Leukaemia

The term leukaemia comes from the Greek words for "white" (leukos) and "blood" (haima) and is a broad term covering a spectrum of malignant diseases of the blood and bone marrow. Unlike other cancers, leukaemia does not produce a tumour mass, but results in a clonal, neoplastic over-proliferation of immature cells of the haematopoietic system, which are characterized by aberrant or arrested differentiation. Leukaemia is classified into four main types, acute and chronic leukaemias, which are further subdivided by their lineage into lymphoid or

myeloid. Acute leukaemias are usually aggressive diseases characterized by a rapid accumulation of bone marrow progenitors called blast cells. They are subdivided into AML and acute lymphoblastic leukaemia (ALL) depending on whether the blasts are shown to be myeloblasts or lymphoblasts (Hoffbrand, 2006). Bone marrow failure, caused by accumulation of blast cells, and tissue infiltration are the dominant clinical features of acute leukaemia, which if left untreated is fairly rapidly fatal (Hoffbrand, 2006).

Chronic leukaemias are distinguished from acute leukaemias by their slower progression. Again chronic leukaemia can be subdivided into myeloid (chronic myeloid leukaemia; CML) and lymphoid (chronic lymphoid leukaemia; CLL) groups. Typically taking months or years to progress, they are characterized by the excessive build up of relatively mature, but still abnormal, white blood cells (Hoffbrand, 2006).

1.3 Acute myeloid leukaemia

AML is a heterogeneous clonal disorder of haematopoietic progenitor cells where cells lose the ability to differentiate normally, and to respond to normal regulators of proliferation, resulting in accumulation of non-functional cells termed myeloblasts (Stone *et al.*, 2004). In the absence of treatment this can lead to fatal infection, bleeding, or organ infiltration. AML can be diagnosed and classified using the World Health Organisation (WHO) system, which supersedes the previous French-American-British (FAB) classification (Table 1.2). The FAB

Table 1.2 – Acute myeloid leukaemia and related precursor neoplasms, and acute leukaemias of ambiguous lineage (WHO 2008). (From (Dohner *et al.*, 2010)).

CATEGORIES
Acute myeloid leukaemia with recurrent genetic abnormalities
AML with t(8;21)(q22;q22); RUNX1-RUNX1T1
AML with inv(16)(p13.1q22) or t(16;16)(p13.1;q22); CBFB-MYH11
APL with t(15;17)(q22;q12); PML-RARA
AML with t(9;11)(p22;q23); MLLT3-MLL
AML with t(6;9)(p23;q34); DEK-NUP214
AML with inv(3)(q21q26.2) or t(3;3)(q21;q26.2); RPN1-EVI1
AML (megakaryoblastic) with t(1;22)(p13;q13); RBM15-MKL1
Provisional entity: AML with mutated NPM1
Provisional entity: AML with mutated CEBPA
Acute myeloid leukaemia with myelodysplasia-related changes
Therapy-related myeloid neoplasms
Acute myeloid leukaemia, not otherwise specified (NOS)
Acute myeloid leukaemia with minimal differentiation
Acute myeloid leukaemia without maturation
Acute myeloid leukaemia with maturation
Acute myelomonocytic leukaemia
Acute monoblastic/monocytic leukaemia
Acute erythroid leukaemia
Pure erythroid leukaemia
Erythroleukaemia, erythroid/myeloid
Acute megakaryoblastic leukaemia
Acute basophilic leukaemia
Acute panmyelosis with myelofibrosis (syn.: acute myelofibrosis; acute myelosclerosis)
Myeloid sarcoma (syn.: extramedullary myeloid tumour; granulocytic sarcoma; chloroma)
Myeloid proliferations related to Down syndrome
Transient abnormal myelopoiesis (syn.: transient myeloproliferative disorder)
Myeloid leukaemia associated with Down syndrome
Blastic plasmacytoid dendritic cell neoplasm
Acute leukaemias of ambiguous lineage
Acute undifferentiated leukaemia
Mixed phenotype acute leukaemia with t(9;22)(q34;q11.2); BCR-ABL1
Mixed phenotype acute leukaemia with t(v;11q23); MLL rearranged
Mixed phenotype acute leukaemia, B/myeloid, NOS
Mixed phenotype acute leukaemia, T/myeloid, NOS
Provisional entity: Natural killer–cell lymphoblastic leukaemia/lymphoma

system classified AML by morphology but was relatively poor information in that only a few subtypes, such as acute promyelocytic leukaemia (APL), could be distinguished as having a distinct prognosis. Over the past 20 years, conventional cytogenetic, flow cytometry, fluorescence *in situ* hybdidization, DNA sequencing, and PCR have more precisely defined prognostically important subsets of AML.

The WHO classification reflects the fact that an increasing number of acute leukaemias can be categorized based upon their underlying cytogenetic or molecular genetic abnormalities and recognizing these recurring genetic lesions has prompted development of novel therapies to target them (Dohner *et al.*, 2010). AML is the most common myeloid leukaemia with a prevalence of 3.8 cases per 100,000 rising to 17.9 cases per 100,000 in adults aged 65 years and older. The median age at presentation is about 70 years, and three men are affected for every two women. Risk factors for acquiring AML include exposure to ionizing radiation, benzene (most commonly through smoking) and cytotoxic chemotherapy (Estey, 2006).

In terms of prognosis, there are a number of factors readily identifiable after presentation that can be used to predict the risk of relapse in newly diagnosed patients with AML. The most important are age, karyotype, FMS-like tyrosine kinase (FLT3) status and response to induction chemotherapy. Age is one of the strongest adverse prognostic factors in AML, with investigators defining cutoffs of 60 or 65 years beyond which the outcome is worse (Ravandi *et al.*, 2007). This is partly reflected by the higher proportion of cases with adverse cytogenetics and/or overexpression of the MDR1 gene encoding the drug efflux pump P-glycoprotein which leads to multidrug resistance in elderly patients (Leith *et al.*, 1997). In addition, older patients often do not tolerate chemotherapy and frequently present with intercurrent medical conditions that are exacerbated by standard antileukaemic treatment. Chromosomal abnormalities are detected in approximately 55% of adult AML, and the importance of diagnostic cytogenetics

Table 1.3 – Standardized reporting for correlation of cytogenetic and molecular genetic data. (From Dohner et al Blood 2010, 115:453-474)

GENETIC GROUP	SUBSETS
Favourable	t(8;21)(q22;q22); RUNX1-RUNX1T1
	inv(16)(p13.1q22) or t(16;16)(p13.1;q22); CBFB-MYH11
	Mutated NPM1 without FLT3-ITD (normal karyotype)
	Mutated CEBPA (normal karyotype)
Intermediate-I	Mutated NPM1 and FLT3-ITD (normal karyotype)
	Wild-type NPM1 and FLT3-ITD (normal karyotype)
	Wild-type NPM1 without FLT3-ITD (normal karyotype)
Intermediate-II	t(9;11)(p22;q23); MLLT3-MLL
	Cytogenetic abnormalities not classified as favourable or adverse
Adverse	inv(3)(q21q26.2) or t(3;3)(q21;q26.2); RPN1-EVI1
	t(6;9)(p23;q34); DEK-NUP214
	t(v;11)(v;q23); MLL rearranged
	−5 or del(5q); −7; abnl(17p); complex karyotype

as an independent prognostic factor in AML, was first highlighted by Grimwade et al (Grimwade *et al.*, 1998). They categorized patients into favourable, intermediate, or poor prognostic groups depending on the presence of specific cytogenetic abnormalities (Grimwade *et al.*, 1998). More recently cytogenetic examination at diagnosis has allowed patients to be stratified into four prognostic groups with relapse risks varying from 35% (favourable) to 76% (adverse) (Milligan *et al.*, 2006). Anomalies associated with the favourable prognostic group are more frequent in patients less than 60 years old whilst patients in the poor prognosis group tend to be older and may have a preceding myelodysplastic or myeloproliferative disorder (Dohner *et al.*, 2010). The intermediate prognostic groups encompass 50-60% of patients with AML and include patients with specific chromosomal anomalies, such as trisomy 8 or 21, as well as normal karyotype (NK), characterized by a variety of molecular abnormalities. Along with cytogenetic data these groups have recently been updated to include information from mutation analysis of the FLT3, NPM1, and CEBPA genes (Table 1.3) (Dohner *et al.*, 2010). Internal tandem duplications (ITDs) of FLT3 are present in

25% to 30% of all AML patients (Kottaridis *et al.*, 2001). They predict an increased risk of relapse across all cytogenetic subgroups and will be discussed further in section 1.4. A favourable prognostic factor is the presence of a nucleophosmin (NPM1) mutation which is associated with a higher complete remission (CR) and longer survival. NPM1 gene disruptions are seen in approximately 35% to 50% of patients with AML, particularly those with NK, and have been associated with FLT3 mutations (Cazzaniga *et al.*, 2005; Ravandi *et al.*, 2007). When NPM and FLT3 mutations are co-expressed the negative influence of the FLT3 mutation overcomes the benefit of NPM mutations on survival (Schnittger *et al.*, 2005). Mutations in the transcription factor CCAAT/enhancer-binding protein-α (CEBPA) gene occur in about 15% of NK AML (Ravandi *et al.*, 2007). They are also associated with a favourable prognosis, particularly in patients with double mutations and without a FLT3-ITD (Ravandi *et al.*, 2007). The prognostic effect of FLT3-ITD, NPM1 and CEBPA status on outcome, particularly in NK AML, suggests that screening for these mutations should be done routinely in newly diagnosed AML. The presence of c-kit mutations in AML patients with the favourable risk cytogenetic markers, inv(16) and t(8;21), confers higher relapse and worse overall survival rates (Paschka *et al.*, 2006).

Approximately 85% of patients with NK AML have a mutation although the prognostic significance of some of these is unclear (Marcucci *et al.*, 2011). Adverse outcome has been associated with over-expression of a number of other genes including DNMT3A, IDH1, IDH2, TET2, WT1 and EVI1 (Milligan *et al.*, 2006; Ley *et al.*, 2010; Shen *et al.*, 2011). Mutations in DNA methyltransferase 3a

(DNMT3a) occur in 25-35% of NK AML and are associated with mutations in NPM1 and FLT3-ITD (Thol et al 2011). The clinical significance of mutations in IDH1 and TET2 have been reported to be context dependent with their prognosis depending on association with FLT3-ITD, or NPM1 and CEBPA respectively (Estey, 2012).

1.4 FMS-like tyrosine kinase 3

FLT3 is a class 3 tyrosine kinase membrane bound receptor which is expressed primarily in early haematopoietic progenitors and plays a major role in myeloid differentiation (Gilliland, 2002). It is composed of an immunoglobulin-like extracellular ligand binding domain, a transmembrane domain, a juxtamembrane dimerization domain, and a highly conserved intracellular kinase domain interrupted by a kinase insert (Figure 1.1). Binding of FLT ligand (FL) to FLT3 results in the unfolding of the receptor allowing receptor-receptor dimerization to take place (Meshinchi, 2009). This receptor dimerization results in activation of the tyrosine kinase enzyme leading to phosphorylation of numerous intracellular sites and recruitment of a number of cytoplasmic proteins (Figure1.1).

The ITD mutation of FLT3 is a result of duplication of a fragment within the juxtamembrane coding region encoded by exons 14 and 15 (Nakao *et al.*, 1996). The mutation results in spontaneous dimerization, and enzyme activation, without the need for ligand binding, conferring growth-factor independence to AML cells. Consequently, the ITD mutation constitutionally activates multiple downstream

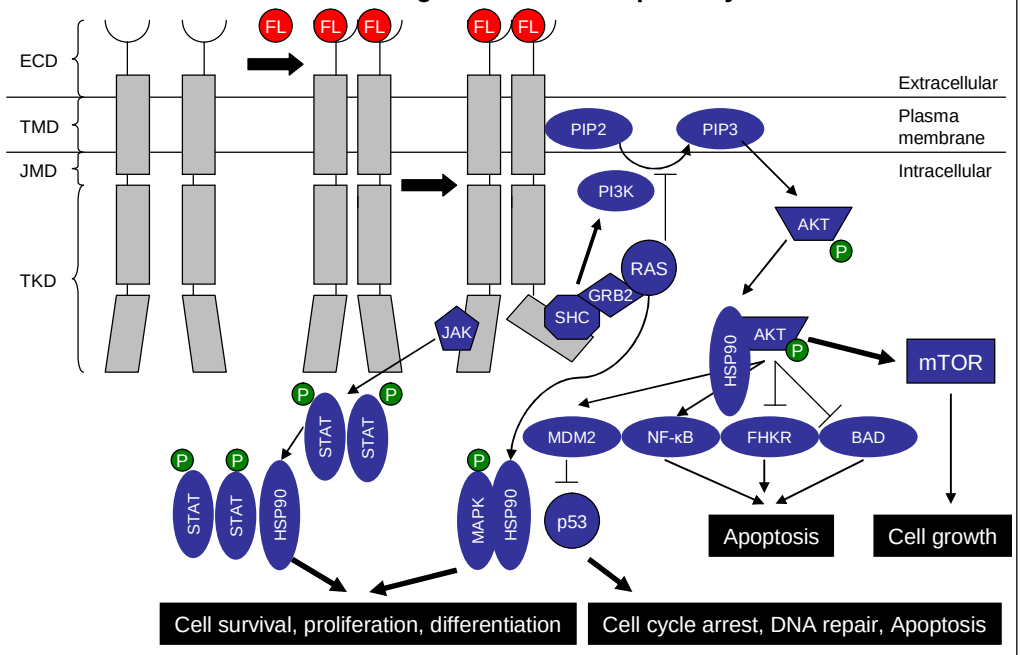

Figure 1.1 FLT3 receptor monomer is composed of an extracellular domain (ECD), a trans-membrane domain (TMD), a juxtamembrane domain (JMD), and a tyrosine kinase domain (TKD). Binding to FLT3 ligand leads to receptor dimerization and activation of the intracellular kinase. Adapted from Meshinchi et al Clin Cancer Res 2009;15(13).

signalling pathways, including PI3K/AKT, MAPK and STAT resulting in leukaemic cell survival and proliferation (Figure 1.1) (Gilliland, 2002; Meshinchi, 2009). In contrast to FLT3-ITD, the FLT3-WT receptor requires FL induced activation to phosphorylate STAT5 during normal haematopoiesis (Zhang *et al.*, 2000; Choudhary *et al.*, 2007). FLT3-ITD mutations are associated with a higher diagnostic white cell count, lower remission rate, higher relapse rate, and worse survival (Kottaridis *et al.*, 2001). The presence of an ITD in conjunction with loss of the second wild-type FLT3 allele confers a particularly poor prognosis (Kottaridis *et al.*, 2001). A study that sorted primary AML samples into stem cell enriched CD34+/CD38- fractions found that FLT3-ITD mutations are present in leukaemia stem cells and that FLT3 inhibitors may have activity against these cells (Levis *et al.*, 2005). Another FLT3 mutation is the FLT3 activation loop mutation

(ALM) (also known as a tyrosine kinase domain point mutation) which occurs in about 7% of AML patients. The majority of ALMs occur in codons 835 with a change of an aspartic acid to tyrosine (Meshinchi, 2009). The presence of FLT-ALMs and FLT3-ITDs are generally mutually exclusive and FLT3-ALMs are not associated with higher diagnostic white cell count or adverse outcome (Meshinchi, 2009). Recent evidence shows that in contrast to FLT3-ALMs, FLT3-ITDs use the Src family kinase SRC to activate STAT5 (Leischner *et al.*, 2012). Therefore, although FLT3-ALMs promote auto-phosphorylation, and FL independent proliferation, similar to FLT3-ITDs, there are different biological responses between the two mutations due to activation of different downstream effectors (Meshinchi, 2009).

1.5 ABC binding cassette transporters

The development of multidrug resistance (MDR) is frequently observed in the treatment of cancer, and is a phenomenon that allows tumour cells that have been exposed to one cytotoxic agent to develop cross resistance to a range of structurally and functionally unrelated compounds. Cells exposed to toxic agents can develop resistance by a number of mechanisms including decreased uptake, accelerated detoxification, defective apoptosis pathways, or increased efflux which lowers the effective drug concentration inside the cell (Gottesman *et al.*, 2002).

ATP-binding cassette (ABC) transporter-mediated active efflux of cytotoxic agents is the most characterized mechanism by which cancer cells develop MDR,

particularly after repeated cycles of chemotherapy (Gottesman *et al.*, 2002). The ABC transporters are an evolutionary extremely well conserved family of transmembrane proteins expressed in most cells and involved in the ATP driven transport of a huge variety of substrates including sugars, peptides, inorganic ions, amino acids, proteins, vitamins and metallic ions (Schinkel, 2003). The family currently consists of 49 members, 13 of which are associated with chemotherapeutical drug transport and drug resistance (De Jonge-Peeters *et al.*, 2007). The genes can be divided into subfamilies based on similarity in gene structure resulting in seven mammalian ABC gene subfamilies (ABCA, B, C, D, E F and G family). The most widely studied members ABCB1 (MDR1/P-glycoprotein), ABCC1 (multidrug resistance-associated protein 1, MRP1) and ABCG2 (breast cancer resistance protein, BCRP) have the ability to export a wide variety of structurally unrelated chemotherapeutic compounds from cancer cells, thereby conferring MDR to these cells (Schinkel, 2003).

Permeability-glycoprotein (Pgp) was the first ABC transporter to be characterized, discovered by Ling and co-workers in multidrug resistant Chinese hamster ovary

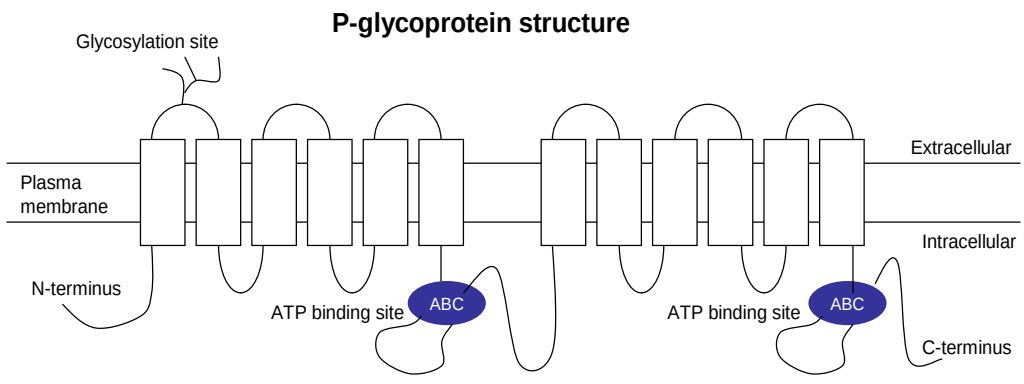

Figure 1.2 The basic structure of P-glycoprotein consisting of two similar six transmembrane spanning regions and two intracellular binding sites.

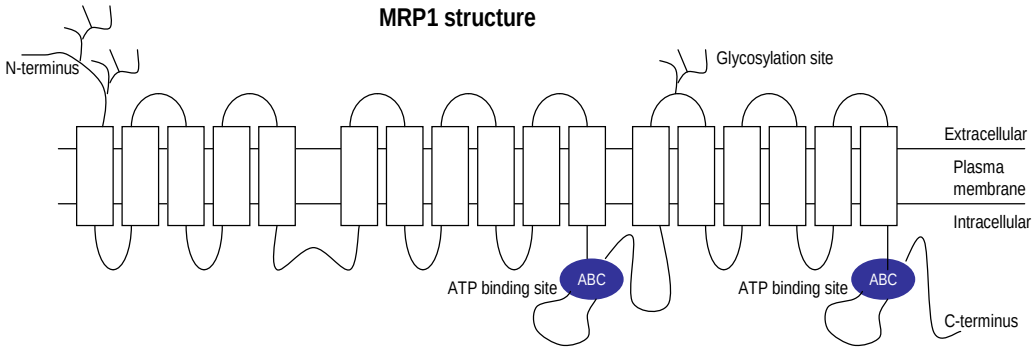

Figure 1.3 The basic structure of multidrug resistance-associated protein 1 (MRP1) consisting of three transmembrane spanning regions and two intracellular binding sites.

cells (Juliano, 1976). Pgp, the product of the MDR1 (ABCB1) gene, is a 170 kDa polypeptide consisting of two very similar halves, each containing 6 transmembrane segments, and an intracellular binding site (Figure 1.2). MRP1 has the same overall architecture as Pgp but has an additional N-terminal extension consisting of 5 transmembrane segments (Figure 1.3). BCRP is considered a half transporter as it consists of only one nucleotide binding domain (NBD) and 6 transmembrane segments (Figure 1.4) (Schinkel, 2003). Also, in contrast to Pgp and MRP1, the NBD of BCRP is at the amino terminal end of the polypeptide (Schinkel, 2003).

Pgp is normally expressed in the intestine, blood-brain barrier, kidney, liver, testes,

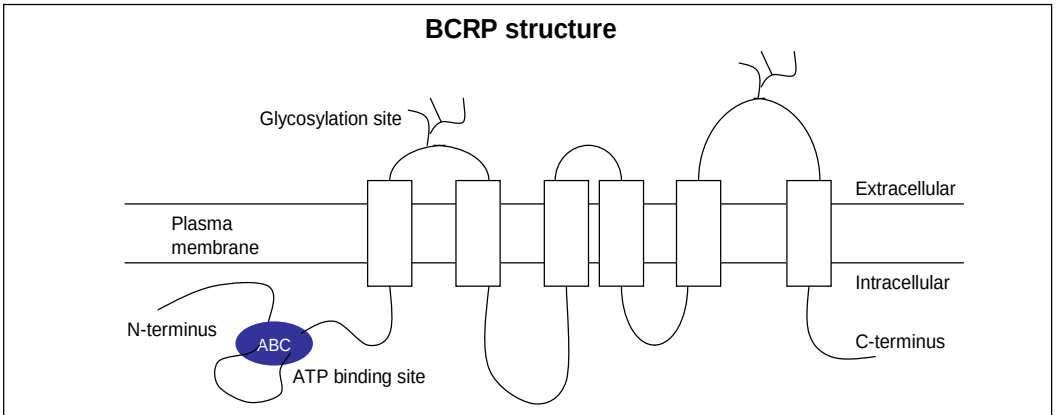

Figure 1.4 The basic structure of breast cancer resistance protein consisting of one six transmembrane spanning region and one intracellular binding site.

placenta and in healthy haematopoietic stem cells (Szakacs *et al.*, 2006). The transmembrane domains of Pgp interact with neutral and positively charged hydrophobic substrates, which are then effluxed by hydrolysis of ATP, thus conferring resistance against a wide spectrum of chemically diverse compounds. These compounds include not only anticancer drugs such as vinca alkaloids, anthracyclines and taxol, but also therapeutic agents such as HIV protease inhibitors and many other exogenous compounds such as rhodamine 123 (R123) (Table 1.4) (Ambudkar *et al.*, 1999). The latter compound has been used extensively in marker assays of Pgp function in normal and cancerous human cells (Pallis, 2005). Also, in addition to drug efflux, Pgp has been reported to play a role in mediating drug independent resistance to apoptosis in AML blasts (Pallis *et al.*, 2002). This resistance is thought to occur due to the physiological role of Pgp as a lipid translocase, which enables it to modulate ceramide mediated apoptotic

Table 1.4 – Selected substrates of P-glycoprotein. (Adapted from (Ambudkar *et al.*, 1999)).

Anticancer Drugs	Vinca Alkaloids (Vincristine, Vinblastine) Anthracyclines (Doxorubicin, Daunorubicin, Epirubicin) Epipodophyllotoxins (Etoposide, Teniposide) Paclitaxel (Taxol) Actinomycin D Topotecan Mylotarg Imatinib
Other cytotoxic agents	Colchicine Ethidium bromide Puromycin
Cyclic and linear peptides	Gramicidin D Valinomycin
HIV protease inhibitors	Ritonavir Idinavir Saquinavir
Other compounds	Rhodamine 123 Hoechst 33342

pathways (Pallis et al., 2002). MRP1 is found on both the plasma membrane and on membranes of intracellular compartments and has very similar substrates to Pgp although its transport activity is dependent on the presence of glutathione (De Jonge-Peeters et al., 2007). BCRP is the more recently discovered ABC transporter that has been shown to play a role in multidrug resistance (Doyle et al., 1998). BCRP is also a drug efflux pump which is associated with mitoxantrone and anthracycline resistance along with substrates including flavopiridol and camptothecin derivatives (Mao, 2005).

In vitro experiments with AML cells were amongst the first to establish the concept of tumour stem cells. In these studies, it was demonstrated that a small proportion of undifferentiated cells were able to reconstitute the tumour when injected into non-obese diabetic with severe combined immunodeficiency disease (NOD/SCID) mice. Along with potent tumour initiation, these cells also showed both self-renewal and differentiation capacity (Bonnet, 1997). A study of 58 AML patients found higher Pgp and MRP functional activities in less mature cells, as defined by immune phenotype, with no consistent up-regulation in relapsed AML (Van Der Kolk et al., 2001). In a smaller study by our group no difference in Pgp protein levels between immature CD34+/CD38- and mature CD34+/CD38+ primary samples was observed (Jawad et al., 2009). A more recent gene expression profiling study in patient samples showed that Pgp and BCRP were preferentially expressed on CD34+/CD38- normal and leukaemic stem cells with subsequent down-regulation upon differentiation to a more mature CD34+/CD38+ phenotype (De Grouw et al., 2006). Also, in contrast to the more mature cells,

leukaemic stem cells with the CD34+/CD38− phenotype possess resistance to the standard chemotherapeutic, and Pgp substrate, daunorubicin (DNR) (Costello et al., 2000). A recent study in CML cell lines reported that the promoter regions of the ABCB1, ABCG2 and ABCC1 genes contain binding sites for the Octamer-4 (Oct-4) transcription factor. Oct-4 is considered a marker of tumour stem cells and their findings suggest that Oct-4 can regulate the expression of these ABC transporters and that this is associated with the MDR phenotype of these cells (Marques et al., 2010).

Normal human haemopoietic stem cells (HSCs) and leukaemic stem cells (LSCs) are characterized by their ability to efflux the fluorescent dyes R123 and Hoechst 33342. Hoechst 33342-dull/R123-dull cells are a highly enriched stem cell fraction called the side population (SP). Although both Pgp and BCRP have the capacity to extrude Hoechst 33342, it has been established that this SP phenotype of HSCs in mice is mainly conferred by the BCRP transporter with Pgp responsible for the extrusion of R123 (Raaijmakers, 2007).

As well as multidrug resistance ABC transporters are known to play an important role in the regulation of cellular cholesterol homeostasis (Gottesman, 2001). AML cells, in contrast to normal mononuclear cells, often do not show efficient feedback repression of cholesterol synthesis when exposed to high sterol media in vitro, a feature that is associated with an increased cell survival (De Jonge-Peeters et al., 2007). Also, indications for an active and dysfunctional cholesterol metabolism have been found at the mRNA level in primitive CD34+ CD38- AML

cells, protecting these cells by this critical cytoprotective lipid signalling pathway (Peeters et al., 2006). It has therefore been suggested that a better understanding of ABC transporter mediated drug resistance and cholesterol metabolism in the primitive leukaemic cell population might lead to new therapeutic approaches and better antileukaemic strategies (De Jonge-Peeters et al., 2007).

1.5.i ABC transporters in AML

Despite improvements accomplished in the last thirty years with the use of a combination of cytarabine and intercalating agents, the overall prognosis of adult AML remains poor (Lowenberg et al., 2003). A major issue in the treatment of AML is MDR to chemotherapeutic drugs (Benderra et al., 2004; Damiani et al., 2006). In patients with AML, MDR can be present intrinsically at diagnosis or can arise during chemotherapy as well as at relapse. One of the most characterized resistance mechanisms in AML is drug extrusion mediated by Pgp. Expression of the MDR1 gene coding for Pgp is high in elderly patients with AML and is associated with worse complete remission rates (Leith et al., 1997). Pgp protein is expressed in 47% of elderly AML cases; (Burnett et al., 2009) compared to 34% in younger patients (Pallis et al., 2011) and is involved in the transport of many drugs used in the treatment of AML, including anthracyclines, etoposide and Mylotarg (Szakacs et al., 2006). A study of 817 patients entered into the National Cancer Research Network AML 14 and 15 trials found that age, low white blood cell (WBC) count, high bcl-2, secondary AML and myelodysplastic syndrome, and

adverse cytogenetics all correlated strongly with high Pgp protein expression (Seedhouse et al., 2007).

BCRP has been shown to be overexpressed in 33% of AML patients with NK and to significantly reduce the duration of CR (Damiani et al., 2006). In a study of 40 AML patients, high ABCG2 mRNA expression was a prognostic factor for poor overall survival (OS) (Uggla et al., 2005). Another study showed BCRP expression to be a poor prognostic factor for CR and OS in 149 AML patients treated with DNR and mitoxantrone but not with idarubicin (Benderra et al., 2004). This group also reported that AML patients co-expressing both Pgp and BCRP had the poorest prognosis. The contribution of MRP1 to MDR in AML is more controversial. One study of 352 younger AML patients found MRP1 to be expressed in 10% of cases but found no relationship between MRP1 expression and clinical outcome (Leith et al., 1999). Another study of 91 AML patients found no association between MRP1 expression and response to chemotherapy or OS (Borg et al., 1998). A further study of 104 AML patients found MRP1 functional expression not to be prognostic in its own right but combined expression of MRP1 and Pgp had a strong negative impact on response and OS (Van Der Kolk et al., 2000). Damiani et al also found that MRP1 expression alone did not influence treatment outcome, but patients over-expressing more than one MDR protein had a lower probability to achieve CR, as if there was an additive effect (Damiani et al., 2007).

Inhibiting Pgp as a way of reversing MDR has been intensively studied for more than 20 years. Many agents that modulate the function of Pgp have been identified, including calcium channel blockers, calmodulin antagonists, steroidal agents, immunosuppressive drugs and antibiotics (Thomas, 2003). However, despite promising theories, treatment results with first generation Pgp inhibitors such as verapamil, cyclosporine A (CSA) and quinidine were poor with only CSA showing any real clinical benefit in AML patients (List et al., 2001). These disappointing results could be attributed to the low binding affinity and therefore the high dosage leading to unacceptable toxicity with these compounds. Also many of these agents are substrates for other transporters and enzyme systems resulting in unpredictable pharmacokinetic interactions in the presence of chemotherapy agents (Qadir et al., 2005).

To overcome these limitations, several novel analogues of the early chemosensitizers were tested and developed, with the aim of finding Pgp modulators with less toxicity and greater potency. These second generation Pgp modulators include valspodar (PSC-833) and biricodar (VX-710) and are more potent and less toxic than their predecessors (Thomas, 2003). PSC-833 is a CSA analogue that does not have the immunosuppressive or nephrotoxic effect of CSA and is 20 times more potent than CSA in increasing DNR retention in MDR cells (Boesch et al., 1991). The cancer and leukaemia group B (CALGB) investigators randomized 120 elderly patients with AML to receive 1 of 2 chemotherapy regimens with PSC-833. Unfortunately the excessive mortality rates in one arm of this trial led to its early closure (Baer et al., 2002). Another study comparing

mitoxantrone, etoposide and cytarabine with or without PSC-833 in poor risk AML patients showed no benefit in using PSC-833 compared to chemotherapy alone (Greenberg et al., 2004). Also, results from the LRF AML14 trial reported no improvement in outcome when combining PSC-833 with DNR in elderly patients with AML and high-risk MDS (Burnett et al., 2009). Although PSC-833 is an efficient Pgp inhibitor, it does have the complication that it is also an inhibitor of cytochrome P450 3A4 (CYP3A4), one of the main drug metabolizing enzymes in the body (Thomas, 2003). Many antileukaemic drugs that are Pgp substrates, such as etoposide and doxorubicin, are also extensively degraded by CYP3A4. Therefore, co-administration with PSC-833 can intensify the toxic side effects of these drugs, necessitating a dose reduction for safe treatment. Third generation molecules that potently and specifically inhibit Pgp and do not affect CYP3A4 have been developed including Elacridar (GF120918), tariquidar (XR9576) and zosuquidar (LY335979) which are being tested in clinical trials (Abraham et al., 2009; Lancet et al., 2009). In a Phase I study, zosuquidar was well tolerated given as a 72-hour intravenous infusion together with induction therapy using cytarabine (Ara-c) and DNR and the recommended dose of this agent for Phase II study was established (Lancet et al., 2009). However a phase II randomized trial of 449 elderly AML or high-risk MDS patients found no benefit of zosuquidar when given in combination with Ara-c and DNR (Cripe et al., 2010). It is hoped that pre-selection of patients with Pgp-positive AML, by phenotyping at diagnosis, would target those who are most likely to benefit from any future modulator trials. Increased toxicity in Pgp negative patients could be masking any positive effects

in Pgp positive patients in the early modulator trials without any pre-selection criteria (Mahadevan, 2004).

More recently, newly developed microarray techniques, have enabled detection of another ABC transporter, ABCA3, as a possible cause for drug resistance in childhood AML (Steinbach et al., 2006). ABCA3 is a novel intracellular transporter that is thought to confer cellular MDR by lysosomal drug sequestration (Chapuy et al., 2008). In another study in adult AML patients, ABCC3 (MRP3) was identified to have a possible role in chemoresistance, particularly in the M5 FAB AML subtype (Benderra et al., 2005). A study of 281 AML patients recently demonstrated that the number of ABC transporters over-expressed had a profound effect on the patient's prognosis (Marzac et al., 2011). In this study complete remission was achieved in 71%, 59%, 54% and 0% of patients over-expressing 0, 1, 2, or 3, ABC genes respectively. This could be a possible explanation as to why only the broad spectrum inhibitor CSA showed any real clinical benefit in AML patients compared to inhibitors such as PSC833 which are tailored against a specific ABC transporter.

1.5.ii Analytical methods for measuring MDR in AML

There are several methods available to measure MDR1/ABCB1 expression in AML samples; although they do not necessarily produce comparable results (Sonneveld, 2001). Generally, bulk methods such as mRNA PCR or Northern blot are not suitable for quantitative differences of MDR1 expression in subpopulations

of AML cells with certain morphologies, and with these assays, it is not possible to correlate MDR1 expression with maturation or differentiation markers (Sonneveld, 2001). Therefore, most investigators prefer to determine MDR1 expression at the protein level (Pgp). Pgp specific antibodies such as C219 and JSB1 have been used in immunocytochemistry, but these assays are not highly reproducible and they are not quantitative (Lizard *et al.*, 1995). Flow cytometry however, can be used to determine Pgp expression in viable cells using monoclonal antibodies such as MRK16 and UIC2, which bind to an extracellular epitope. The reactivity of the UIC2 antibody with Pgp is increased by the addition of Pgp transported compounds and is useful in the identification of Pgp substrates (Mechetner *et al.*, 1997). MRK16 is a monoclonal antibody generated against the human myelogenous leukaemia K-562 cells resistant to adriamycin (K-562/ADM) and this is the antibody of choice for quantifying Pgp in AML cells (Hamada, 1986). Along with allowing the detection of Pgp in different subsets of cells, this technique requires a limited amount of time and cellular material, particularly important as Pgp expression is associated with low cell counts (Pallis *et al.*, 2003b; Seedhouse *et al.*, 2007). This flow cytometric method is established and reproducible within our group using CD45 staining to identify AML blasts (Pallis, 2005; Pallis *et al.*, 2005).

It has been reported that a combination of phenotypic and functional Pgp analysis may predict clinical outcome in AML (Schuurhuis *et al.*, 1995; Broxterman *et al.*, 1996). R123 retention has been comprehensively studied as a method for assessment of Pgp function and good correlation has been shown between R123

efflux and MRK-16 expression (Broxterman *et al.*, 1996). Again, this flow cytometric method is established and reproducible within our group using CSA or PSC-833 as a positive control modulator (Pallis, 2005; Pallis *et al.*, 2005). Using such a functional assay the effect of Pgp inhibition by a drug-resistance modulating agent can also be evaluated.

Functional assays to determine BCRP function have been described using BODIPY-prazosin retention and Fumitremorgin C (FTC) as the positive control modulator (Van Der Kolk *et al.*, 2000; Van Der Pol *et al.*, 2003). We intend to use this flow cytometric method to measure BCRP function in our cell lines. There is some discordance in the literature between BCRP protein expression and function in AML blasts (Suvannasankha *et al.*, 2004). We were not convinced that existing antibodies for BCRP, such as BXP-21 and BXP-34, were sufficiently characterized, and decided to measure BCRP (ABCG2) message by realtime PCR in our patient samples. High ABCG2 mRNA expression has been reported to be a poor prognostic factor for overall OS in AML patients (Uggla *et al.*, 2005).

As described in section 1.5.i the contribution of MRP1 to MDR in AML is more controversial. Functional MRP can be studied by flow cytometry with calcein acetoxymethyl ester (calcein-AM) or carboxyfluorescein diacetate retention with MK-571 as a positive control modulator (Gekeler *et al.*, 1995; Dogan *et al.*, 2004). However, data from such functional studies in AML patients is contradictory. For example, one study found that MRP function correlated with low CR and poor OS (Laupeze *et al.*, 2002), whilst another found MRP function not to be prognostic in

its own right but the combination of MRP and PGP efflux to be highly prognostic (Van Der Kolk *et al.*, 2000). Because of this and the lack of sufficiently characterized antibodies we decided not to measure MRP expression in our patient samples.

1.6 Therapy in AML

Intrinsic resistance or treatment-induced acquired resistance is one of the major obstacles to the effective treatment of patients with AML. Although nearly 80% of younger AML patients may initially achieve complete remission with current therapy most will relapse with resistant disease (Lowenberg *et al.*, 2003). Clinical outcomes in the elderly have been even more modest as these patients do not tend to tolerate intensive chemotherapy regimens and frequently have poor cytogenetics (Leith *et al.*, 1997). Less than 10% of older patients with AML will achieve long-term disease free survival with conventional chemotherapy (Appelbaum *et al.*, 2001). This inability to successfully treat AML patients, particularly the elderly, underlies the continuing need to develop new treatments for AML. During recent years, considerable progress has been made in deciphering the molecular genetic basis of AML in defining new diagnostic and prognostic markers. Such developments prompted an international expert panel to provide recommendations for the diagnosis and management of AML (Dohner *et al.*, 2010). This excludes acute APL whose recommendations are published separately (Sanz *et al.*, 2009). APL is the most curable subtype of AML with a dramatic improvement in survival

with the introduction of all-trans retinoic acid (ATRA) and more recently arsenic trioxide (ATO) into its therapy (Sanz *et al.*, 2009).

Therapy for AML consists of two phases, with the first attempting to produce CR and the second aiming to prolong that CR. The likelihood of relapse declines sharply to less than 10% once a patient has been in remission for 3 years (Estey, 2006). However, current therapeutic strategies for AML, relying on remission induction followed by postremission therapy with additional intensive chemotherapy or stem-cell transplantation, have produced limited survival benefits (Ravandi *et al.*, 2007). Despite multiple clinical trials, examining combinations of cytotoxic agents, remission induction therapy for patients with adult AML has changed little over the past thirty years. Standard therapy for AML consists of a combination of an anthracycline such as DNR and the nucleoside analogue Ara-c (Figure 1.5). The cytotoxic activity of DNR is attributed to the formation of drug-stabilized complexes between DNA and the nuclear enzyme topoisomerase II. Topoisomerase II is essential for the maintenance of DNA integrity and the survival of proliferating cells and topoisomerase II poisons such as DNR, etoposide and doxorubicin, inhibit enzyme-mediated DNA ligation causing the accumulation of double-stranded breaks. Other biological effects include free radical formation, alkylation of DNA and interaction with components of the cell membrane (Come *et al.*, 1999). Nucleoside analogues such as Ara-c are taken into the cell by nucleoside transporters and metabolized by intracellular enzymes, before being incorporated into newly synthesized DNA, leading to chain termination and inhibition of DNA synthesis (Ravandi *et al.*, 2004). The standard

Chemical structure of Daunorubicin and Cytarabine

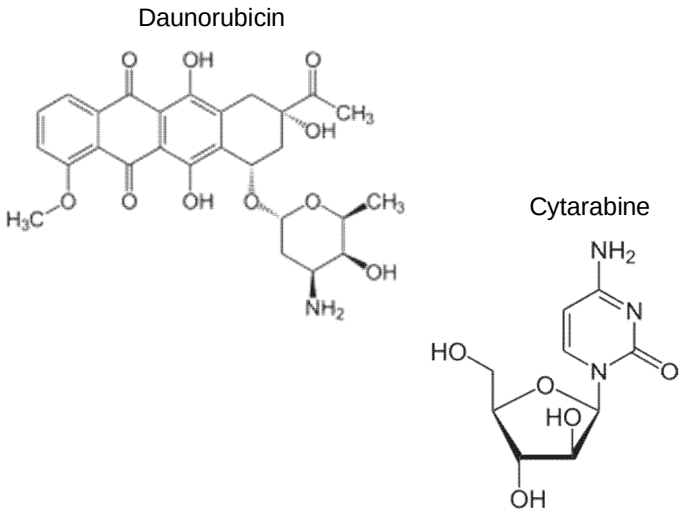

Figure 1.5 The chemical structure of the anthracycline DNR and the nucleoside analogue Ara-c.

induction regimen for newly diagnosed AML consists of three days of an anthracycline (e.g. DNR, at least 60 mg/m^2, idarubicin, 10-12 mg/m^2, or mitoxantrone, 10-12 mg/m^2) intravenously and Ara-c, 100-200 mg/m^2 by continuous infusion for seven days. With such ("3 + 7") regimens 60% to 80% of young adults and 40% to 60% of older adults can achieve CR (Dillman *et al.*, 1991; Zhu *et al.*, 2009). Clinical outcomes in the elderly are more modest as these patients do not tend to tolerate intensive chemotherapy and frequently have cytogenetic abnormalities (as discussed in section 1.3). Less than 10% of older patients with AML will achieve long-term disease free survival with conventional chemotherapy (Appelbaum *et al.*, 2001). The fact that the majority (more than 75%) of newly diagnosed AML patients are 60 years or older, clearly indicates the need for development of less toxic and specific therapies to improve the cure rates in this large patient group (De Jonge-Peeters *et al.*, 2007). New drugs being

Table 1.5 – Examples of novel agents being tested in AML. (Adapted from (Robak, 2009)).

DRUG CLASS	AGENTS	MECHANISM OF ACTION
Tyrosine kinase inhibitors (FLT3 inhibitors)	Lestaurtinib (CEP701) Tandutinib (MLN518) PKC412 AC220 Sorafenib	Inhibition of FLT3 phosphorylation, induction of apoptosis
Newer nucleoside analogues	Clofarabine (Evoltra®) Troxacitabine Troxatyl®) Sapacitabine (CYC682, CS-682)	Inhibition of ribonucleotide reductase and DNA polymerase; induction of apoptosis
Immunotoxins	Gemtuzumab ozogamicin (Mylotarg®)	CD33 binding, toxin internalization, and double strand DNA breaks
Hypomethylating agents	Azacitidine (Vidaza®) Decitabine (Dacogen®)	Inhibition of DNA methylation
Farnesyltransferase inhibitors	Tipifarnib (Zarnestra™) lonafarnib (Sarasar®)	Inhibition of farnesyltransferase, inhibition of angiogenesis, and induction of cellular adhesion
Alkylating agents	Laromustine (Onrigin®)	DNA alkylation and DNA cross-linking
Haematopoietic stem cell mobilizing agent	Plerixafor (AMD3100)	Antagonist of CXCR4 binding to CXCL12

evaluated in clinical studies include FLT3 inhibitors, nucleoside analogues, immunotoxins, hypomethylating agents, farnesyltransferase inhibitors, alkylating agents and haematopoietic stem cell mobilizing agents (Table 1.5). FLT3 inhibitors and the immunotoxin Gemtuzumab ozogamicin will be discussed in the next section.

The newer second-generation purine nucleoside analogue clofarabine has recently been extensively studied in patients with AML and is reviewed by (Tran, 2012). Clofarabine was synthesized to combine the most favourable pharmacokinetic properties of fludarabine and cladribine, and acts by inhibiting ribonucleotide reductase and DNA polymerase, as well as by inducing apoptosis. Clofarabine,

response rates and median OS were higher for clofarabine combined with Ara-c when compared to single agents alone in untreated elderly AML (Tran, 2012). The authors concluded that clofarabine may be a useful alternative in AML patients who may not tolerate standrard therapy with anthracyclines.

Two demethylating agents, the cytosine analogues decitabine and azacitidine are currently in phase III clinical trials and are reviewed by (Garcia-Manero, 2008). DNA methylation is the addition of a methyl group to specific stretches of DNA sequences often located in or near promoter regions. DNA methylation occurs when a methyl group is attached to a cytosine by 1 of the 3 known active DNA methyltransferases (DNMTs). DNA methylation causes loss of gene function induced by epigenetic gene silencing. Such changes may be reversible using DNMT inhibitors and both decitabine and azacitidine have been approved for the treatment of myelodysplastic syndromes (MDS). MDS are clonal disorders of haematopoietic stem cells, characterized by an ineffective haematopoiesis associated with cytopenias, functional abnormalities of bone marrow lineages, and by high incidence of progression to AML. In a trial with high-risk MDS, 2 year overall survival with azacitidine was 50%, compared with 16% with conventional treatment (Fenaux *et al.*, 2010).

Tipifarnib is a farnesyltransferase inhibitor currently under development for the treatment of AML. Farnesyltransferase is an enzyme involved in cell signalling, proliferation, and differentiation. It catalyzes the transfer of the farnesyl moiety to the cysteine terminal residue of a substrate protein on Ras and farnesylated protein

products of the Ras gene family are frequently activated in MDS and AML. Karp et al recently reported the results of a phase II trial where a CR of 25% was achieved in AML patients >70 years receiving tipifarnib and etoposide in combination (Karp *et al.*, 2012). The results of this study are encouraging in that they highlight the therapeutic progress in a population of poor-risk, older AML patients who are very difficult to treat. Another phase I/II study found tipifarnib in combination with idarubicin and Ara-c to cause better CR duration and higher CR rates in AML patients with chromosome 5/7 abnormalities (Jabbour *et al.*, 2011).

1.7 Targeted therapy

Cancer chemotherapy can be limited by a lack of specificity, resulting in damage to normal cells as well as cancer cells. Targeted therapy aims to reduce toxicity in normal tissues and thereby improve quality of life for the cancer patient. AML is a highly heterogeneous disease that lacks efficient markers needed in clinical diagnosis to incorporate more novel risk-adapted therapeutic strategies. However, diagnostic studies, including immunophenotyping, cytogenetic evaluation, and molecular genetic studies, are aiding development of a more targeted approach to treat specific subtypes of AML. Acute promyelocytic leukaemia (APL) became the first subtype of AML to be treated with an agent targeting a specific genetic mutation. High complete remission rates for APL, which is characterized by a t(15:17) translocation resulting in a fusion transcript of promyelocytic leukaemia-retinoic acid receptor α(PML-RARα), are now achievable through treatment with ATRA and ATO (Tallman et al., 2002; Sanz et al., 2009). Further confidence that

small-molecule inhibitors of specific kinases may prove to be highly effective anticancer agents comes from the success of imatinib in the treatment of chronic myelogenous leukaemia (CML). CML is characterized by the presence of a t(9:22) translocation resulting in a constitutively active tyrosine kinase encoded by the breakpoint cluster region-abelson (BCR-ABL) fusion gene. Imatinib is a selective tyrosine kinase inhibitor which competes with ATP binding in the BCR-ABL protein kinase and inhibits tyrosine phosphorylation of the downstream proteins involved in BCR-ABL signal transduction (Crossman, 2004). Whilst imatinib treatment is beneficial in the majority of CML cases it is becoming apparent that some patients are resistant to imatinib and other patients experience relapse after initial success with the drug. Recent evidence demonstrates that Pgp may play a role in this resistance and there is also evidence that imatinib is a BCRP substrate (Burger et al., 2004; Thomas et al., 2004).

Therapeutic targets such as the human epidermal growth factor receptor 2 (HER2) in breast cancer and the KRAS mutation in colon cancer can be used to optimize patient selection for Herceptin and Erbitux treatment respectively (Saijo, 2011). Markers required for stratifying patients with AML according to risk levels and for assigning certain subtypes of this disease to appropriate molecular targeted therapies is complex. However, new targeted molecular approaches in AML are being developed on the basis of the progress made in deciphering the molecular pathogenesis of AML.

FLT3-ITD mutations are among the most frequently detected molecular abnormalities in AML patients and cause constitutive activation of the receptor kinase (Gilliland, 2002). This makes them an attractive target for tyrosine kinase inhibition by small molecule inhibitors and there has been considerable interest in the development of FLT3 inhibitors. A number of these are in phase II/III clinical trials, and include CEP-701 (Lestaurtinib) and PKC-412 (Midostaurin), both of which demonstrate activity in experimental models of FLT3-ITD positive leukaemia (Levis *et al.*, 2002; Weisberg *et al.*, 2002; Smith *et al.*, 2004; Stone *et al.*, 2005; Knapper *et al.*, 2006). CEP701 is part of the international phase 3 AML17 study for young adults with newly diagnosed AML. The use of CEP-701 and PKC-412 as single agents in high risk AML patients has shown only limited benefit with no increase in complete remission observed (Smith *et al.*, 2004; Stone *et al.*, 2005; Knapper *et al.*, 2006). However, studies which combined CEP-701 or PKC-412 with conventional chemotherapy, suggested a possible therapeutic benefit (Fischer *et al.*, 2010; Levis *et al.*, 2011). A study by our research group confirmed that AML samples with a FLT3-ITD are more susceptible to PKC-412 and another FLT3 inhibitor, AG1296, than wild type samples (Hunter *et al.*, 2004). Also, expression of Pgp in the FLT3-ITD cells reduced their sensitivity to AG1296 and the authors concluded that Pgp expression should be assessed in clinical trials of FLT3 inhibitors. Recently, more potent FLT3 inhibitors such as AC220 and sorafenib are being investigated and are reviewed by (Knapper, 2011). They possess the ability to achieve more sustained *in vivo* inhibition of FLT3 and have shown highly promising activity in early clinical studies (Rollig *et al.*, 2011).

AC220 is currently part of the AML18 study in combination with conventional chemotherapy in older patients with AML and high risk MDS.

Gemtuzumab ozogamicin/GO (Mylotarg) is a humanized anti-CD33 antibody chemically linked to the cytotoxic agent calicheamicin that inhibits DNA synthesis and induces apoptosis. CD33 antigen is present on the surface of AML cells in 80% to 90% of patients with AML. Combinations of GO with chemotherapy as induction or post-remission therapy are promising, and phase III trials are ongoing (Stasi *et al.*, 2008). In the medical research council (MRC) AML 15 trial, younger AML patients (under 60 years) with favourable cytogenetics who were treated with GO in combination with induction chemotherapy showed a significant survival benefit, and a trend was also documented for patients with intermediate risk (Burnett *et al.*, 2011b). Results from the MRC AML 16 trial suggest that older patients, including those with intermediate risk cytogenetics, also benefit from the addition of GO to remission induction therapy (Burnett *et al.*, 2011a).

Targeted therapy is a rapidly evolving and expanding topic and recently drugs targeting the aurora kinase family of proteins have come to prominence as being of potential benefit in tumour therapy (Carvajal *et al.*, 2006).

1.8 The aurora kinase family

The mammalian aurora kinases aurora-A, aurora-B and aurora-C comprise a family of serine/threonine kinases that are essential for mitotic progression

(Andrews *et al.,* 2003). Amongst their many functions the auroras act to establish mitotic spindles by regulating the spindle checkpoint, centrosome duplication and separation, as well as microtubule-kinetochore attachment and cytokinesis (Andrews *et al.,* 2003). The expression levels, as well as the kinase activity of all three aurora kinases is cell cycle dependent, with the activity increasing at the S phase, reaching a peak level at the G_2/M phase (Bischoff, 1999). Recently the auroras have been linked to tumourigenesis, and the fact that that they are kinases, amenable to small molecule inhibition, makes them attractive targets for anticancer drug development (Carvajal *et al.,* 2006). The first homologue of the aurora kinase family, Increase-in-ploidy 1 (Ipl1), was identified in budding yeast using a genetic screen for mutants that were defective in chromosome segregation (Chan, 1993). In 1995 the original eukaryotic aurora allele was identified in a screen for Drosophila melanogaster mutants that were defective in spindle-pole behaviour and termed aurora after the phenomenon aurora borealis, of the night skies Polar Regions (Glover *et al.*, 1995). By 1998 three human aurora kinase homologues had been identified and their nomenclature simplified to aurora-A, aurora-B and aurora-C (Carmena, 2003). Interest in the auroras has intensified since the observation that aurora-A over-expression is oncogenic (Bischoff *et al.*, 1998). The aurora kinases are nuclear proteins and although the carboxyl terminus catalytic domains of the auroras are highly conserved (71% between aurora-A and aurora-B), the three members exhibit strikingly different sub-cellular localizations and functions during mitosis interacting with a distinct set of proteins (Carmena, 2003). The auroras play multiple roles during mitotic progression and their distribution correlates strongly with their functions (Carmena, 2003).

Aurora-A is localized primarily on spindle poles and transiently along the spindle microtubules as cells progress through mitosis and is considered orthologous to the initial aurora discovered in Drosophila (Carmena, 2003; Katayama, 2010). The kinase functions primarily in mitotic entry, centrosomal regulation, mitotic spindle formation, alignment of metaphase chromosomes and is also known to phosphorylate numerous centrosomal proteins (Carmena, 2003). Loss of aurora-A function leads to monopolar mitotic spindles, cell cycle arrest, accumulation of cells in the G2/M phase and apoptosis (Carmena, 2003).

Aurora-B is a chromosomal passenger protein whose kinase activity peaks during mitosis. Chromosomal passenger proteins are characterized by their unique property of translocation from the chromosomal inner centromeric region to the central mitotic spindle and cell cortex during mitotic progression (Carmena, 2003). As such aurora-B undergoes dynamic localization, associating first to the kinetochores from prophase to metaphase, and then to the spindle midzone and midbody during late anaphase, telophase and cytokinesis (Andrews *et al.*, 2003; Fu *et al.*, 2007). This kinase was first associated with cancer in 1998 when it was found to be overexpressed in colon tumours (Bischoff *et al.*, 1998). Inhibition of aurora-B results in abnormal cell division, polyploidy and apoptosis (Ditchfield *et al.*, 2003).

Aurora-C is the least studied of the aurora family and its expression was originally thought to be restricted to the testis where it has a specific role in the regulation of chromosome segregation during male meiosis (Hu *et al.*, 2000). More recently,

aurora-C has been identified at low levels in sixteen other tissues including bone marrow, with studies suggesting that it has a similar intracellular distribution and complementary role to aurora-B along with survivin as a chromosomal passenger protein (Sasai *et al.*, 2004; Yan *et al.*, 2005).

Aurora-B is the catalytic component of the chromosomal passenger complex (CPC), which is composed of three additional non-catalytic subunits that direct its activity: survivin, inner centromere protein (INCENP) and borealin. Survivin and INCENP have both regulatory and targeting functions and are phosphorylated by aurora-B *in vitro* whilst borealin is thought to target aurora-B to centromeres (Gassmann *et al.*, 2004). The CPC orchestrates the spindle checkpoint and ensures the accurate segregation of chromatids and correct microtubule/kinetochore attachment during mitosis and cytokinesis (Andrews *et al.*, 2003). Aurora-B is required for cleavage furrow ingression (Fuller *et al.*, 2008), and inhibition of aurora-B function results in premature exit from mitosis without undergoing chromosome segregation and cytokinesis, and continued re-entry into the cell cycle (a process referred to as endoreduplication), resulting in multi-nucleated cells and ultimately cell death (Ditchfield *et al.*, 2003). This increase-in-ploidy phenotype makes aurora-B orthologous to Ipl1 in budding yeast (Carmena, 2003) where it is required for spindle checkpoint function in response to a lack of tension across attached kinetochores (Lampson, 2010). In higher eukaryotic cells, catalytic activity of aurora-B is required for recruitment of checkpoint protein BubR1 to kinetochores and sustained mitotic arrest in the absence of tension (Ditchfield *et al.*, 2003). In mitotic chromosomes, kinetochore-microtubule attachments can be

found in many states; monotelic (one kinetochore attached to a microtubule from only one pole), syntelic (each kinetochore attached to microtubules emanating from one pole), merotelic (both kinetochores attached to microtubules derived from both poles) and amphitelic (bi-polar bi-oriented attachment). Aurora-B is essential for the generation of the correct amphitelic attachment state required for accurate chromosome segregation (Figure 1.6) (Andrews *et al.*, 2003). Aurora-B is also known to phosphorylate Histone H3 (pHH3) at the serine 10 (Ser^{10}) position during mitosis (Hsu *et al.*, 2000; Giet, 2001; Bhaumik *et al.*, 2007). Inhibition of pHH3 reflects aurora-B inhibition and as such can be considered a biomarker for aurora-B activity. There is some confusion about the actual definition of what a biomarker is and what its characteristics are. However, the most widely accepted definition of a biomarker is "a characteristic that is objectively measured and

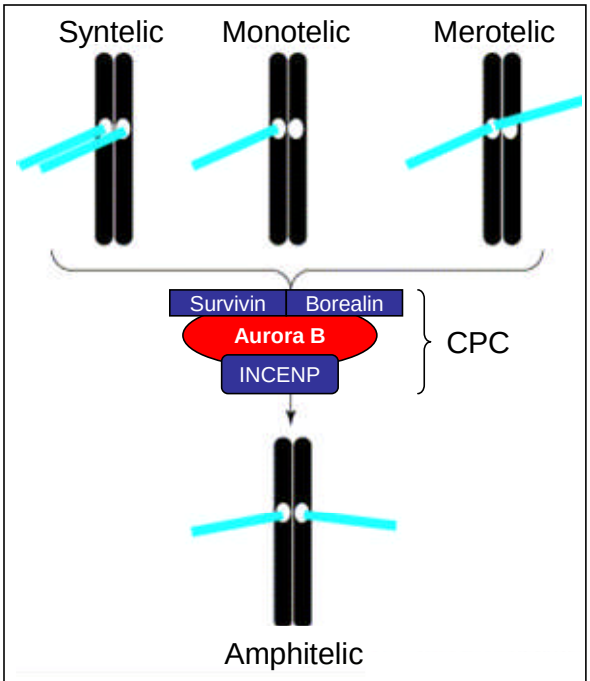

Figure 1.6 Functions of the CPC in kinetochore–microtubule attachment. Adapted from Andrews et al Curr Opin Cell Biol 2003.

evaluated as an indicator of normal biological processes, pathogenic processes, or pharmacological responses to a therapeutic intervention" (Atkinson *et al.*, 2001). Inhibition of Histone H3 phosphorylation has been reported to prevent initiation of chromosome condensation and entry into mitosis (Van Hooser *et al.*, 1998). Aurora-B has also been reported to directly phosphorylate the retinoblastoma tumour suppressor protein (Rb), a function which regulates the postmitotic checkpoint to prevent endoreduplication after aberrant mitosis (Nair *et al.*, 2009). Both Aurora-A and B have been shown to be over-expressed in a wide variety of tumour types (Katayama *et al.*, 1999; Han *et al.*, 2002; Tong *et al.*, 2004; Chieffi *et al.*, 2006) including those of haematological origin (Ikezoe *et al.*, 2007; Yang *et al.*, 2007; Careta *et al.*, 2012) and are therefore thought to represent promising targets for anticancer drug development.

1.9 Aurora kinase inhibitors

Anti-mitotic drugs such as the taxanes (e.g. paclitaxel, docetaxel) and the vinca alkaloids (e.g. vincristine, vinblastine) block tumour cell division and are used routinely in the clinic to treat cancer (Jordan, 2004). A major drawback of these drugs is the collateral damage caused to non-dividing cells, including clinical neuropathy, caused by the inhibition of microtubule dependent processes in axons and glial cells. The common feature of the anti-mitotic drugs is that they all bind tubulin, leading to the suppression of microtubule dynamics, inhibition of spindle assembly and activation of the spindle assembly checkpoint (SAC). SAC activation induces mitotic arrest and tumour cells typically die directly in mitosis

or following mitotic exit. This mechanism of action is distinct to that seen with aurora-B inhibition which results in inactivation of the SAC, leading to aborted cell division without mitotic arrest. Continued suppression of aurora-B activity leads to further rounds of genome replication without division, a process referred to as endoreduplication, which ultimately results in tumour cell death (Ditchfield *et al.*, 2003). Therefore, compounds that inhibit aurora-B and prevent spindle assembly without affecting micotubules in non dividing cells should in principle have anti-tumour activity without the neuropathies associated with the classical antimitotic drugs.

Success of agents such as imatinib in the treatment of CML has increased confidence that small-molecule inhibitors of specific kinases may prove to be highly effective anticancer agents (Crossman, 2004). The implication of the auroras in tumourigenesis and the fact that that they are kinases, amenable to small molecule inhibition, makes them attractive targets for anticancer drug development. In particular, both aurora-A and aurora-B have been shown to be aberrantly expressed in freshly isolated leukaemia cells from individuals with AML, compared with bone marrow mononuclear cells from healthy volunteers (Ikezoe *et al.*, 2007). A growing number of aurora kinase inhibitors have been described that show anti-tumour activity *in vivo*. Whether aurora-A or aurora-B is the better anticancer drug target is a matter of debate. One study compared the effects of aurora-A and aurora-B antisense oligonucleotides in pancreatic cells and found that aurora-A targeted therapy may be preferable to aurora-B (Warner *et al.*, 2006). However, most of the evidence points to aurora-B as the target of choice.

Three non-specific aurora kinase inhibitors ZM447439, Hesperadin and VX-680 all induce similar phenotypes when tested in cell based assays (Ditchfield *et al.*, 2003; Hauf *et al.*, 2003; Harrington *et al.*, 2004). Specifically, all three inhibit phosphorylation of Histone H3 on Ser^{10} and induce DNA endoreduplication in the absence of cytokinesis, results that suggest that their cellular effects are largely due to the inhibition of aurora-B (Keen, 2004). Another study compared the effects of RNA interference and small molecules targeting aurora-A versus aurora-B in colon cancer cells and found that the cells tested were extremely sensitive to aurora-B inhibition (Girdler *et al.*, 2006). Recently a group using RNA interference experiments showed that inactivation of aurora-B bypasses the requirement for aurora-A leading to polyploidy, indicating that aurora-B is responsible for mitotic arrest in the absence of aurora-A (Yang *et al.*, 2005). More recently a study of 297 ALL and 237 newly diagnosed paediatric AML patient samples reported an increase in expression of both aurora-A and aurora-B proteins when compared to normal bone marrow samples (Segers *et al.*, 2011). The group used a short hairpin RNA system to silence aurora-A and aurora-B in both ALL and AML cell lines and found that only silencing of aurora-B resulted in proliferation arrest and apoptosis. With this in mind more specific inhibitors for aurora-B are being developed, one of which is AZD1152, and is discussed later.

1.10 Aurora kinase inhibitors in AML

There are pre-clinical data on several aurora kinase inhibitors with promising results in AML cells. ZM447439 was the first aurora kinase inhibitor to be

developed (Ditchfield *et al.*, 2003). It is an inhibitor of both aurora-A and aurora-B that causes growth inhibition in colony forming assays and apoptosis in AML cells (Ditchfield *et al.*, 2003; Ikezoe *et al.*, 2007). Importantly, ZM447439 did not inhibit clonogenic growth of myeloid stem cells from healthy donors (Ikezoe *et al.*, 2007). PHA-680632 is a potent inhibitor of all three aurora kinases that has shown tumour growth inhibition in nude mice bearing a human leukaemia (HL-60) xenograft (Soncini *et al.*, 2006). VX-680 is another selective inhibitor of all three aurora kinases which inhibits Histone H3 phosphorylation and demonstrates anti-tumour activity in mouse xenograft models (Gizatullin *et al.*, 2006). When VX-680 was delivered to nude mice bearing a human leukaemia (HL-60) xenograft it resulted in a 98% reduction in tumour volume compared with controls. Interestingly, VX-680 also exhibits cross-inhibitory activity against the receptor tyrosine kinase FLT3 and ablated colony formation in primary AML cells with FLT3-ITD (Harrington *et al.*, 2004; Carvajal *et al.*, 2006). The non-specific aurora kinase inhibitor AS703569 is also a potent inhibitor of FLT3 and has shown anti-tumour activity in AML cell lines and primary blasts (Sarno *et al.*, 2007). VX-680 has also been shown to increase Bax/Bcl-2 expression ratio in primary AML cells, a favourable proapoptotic predictor for drug response and survival in AML, and to enhance the cytotoxic effect of the chemotherapeutic agent etoposide on AML cells (Huang *et al.*, 2008).

1.11 AZD1152-hQPA (Barasertib-hQPA)

AZD1152 is a novel pyrazoloquinazoline prodrug developed by AstraZeneca that has good solubility, making it suitable for parenteral administration, which is then converted rapidly to the active drug AZD1152 hydroxy-QPA (AZD1152-hQPA) in human plasma (Figure 1.7) (Mortlock *et al.*, 2007). It is the more active AZD1152-hQPA that has been supplied by AstraZeneca for the purpose of this study. AZD1152-hQPA is a highly potent sub-micromolar selective inhibitor of aurora-B (Ki, 0.36nM/L) compared with aurora-A (1369nM/L) and aurora-C (17nM/L) and has a high specificity versus a panel of 50 other serine/threonine and tyrosine kinases (Keen *et al.*, 2005). A study investigating the activity of AZD1152 in AML cells found anti-proliferative and apoptotic activity in cell lines

Chemical structure of AZD1152 prodrug and de-phosphorylated AZD1152-hQPA

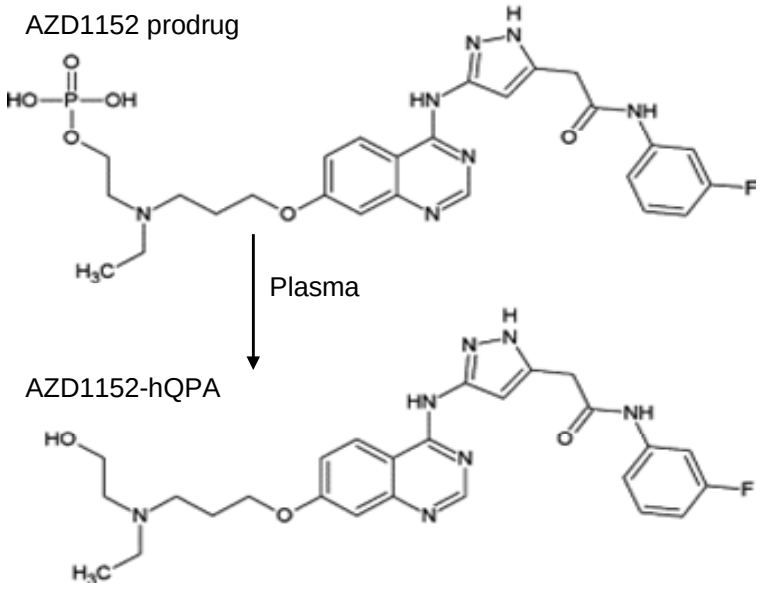

Figure 1.7 The chemical structure of AZD1152 prodrug and the active moiety AZD1152-hQPA ($C^{26}H^{30}FN^{7}O^{3}$, m.w. 507.57) after de-phosphoryation in plasma. (Adapted from D.Pluim et al. J. Chromatogr 2009)

and primary cells at concentrations associated with changes in the phosphorylation status of the aurora-B substrate Histone H3 (Joel *et al.*, 2005). AZD1152-hQPA has also been shown to significantly inhibit the growth of human colon, lung and haematologic tumour xenografts in immunodeficient mice, with phenotypes indicative of aurora-B inhibition such as, chromosome misalignment, loss of cell division, suppression of Histone H3 phosphorylation and subsequent apoptosis (Mortlock *et al.*, 2007; Wilkinson *et al.*, 2007).

AZD1152 has also shown tumouricidal activity against a panel of tumour cell lines including those of AML origin (Joel *et al.*, 2005; Walsby *et al.*, 2005; Oke *et al.*, 2009). Recently AZD1152 has been reported to reduce aurora-B protein stability in breast cancer cell lines by enhancing proteasome mediated polyubiquitination and degradation (Gully *et al.*, 2010). Therefore AZD1152 is the first aurora kinase inhibitor shown to be negatively regulating both activity and stability of the protein. A study on the potential of AZD1152 as a new treatment for multiple myeloma found high levels of aurora-B kinase mRNA and protein expression in a panel of human myeloma cell lines and primary myeloma cells (Evans *et al.*, 2008). AZD1152 induced apoptotic death in myeloma cell lines at nanomolar concentrations and combination of AZD1152 with dexamethasone showed increased anti-myeloma activity compared with the use of either agent alone. Another study, investigating the effects of AZD1152 administration on human leukaemic cell lines has recently been reported (Yang *et al.*, 2007). The compound inhibited the proliferation of AML, Acute lymphocytic leukaemia (ALL), and CML cell lines with an IC_{50} ranging from 3nM to 40nM. The cells all had 4N/8N

DNA content followed by apoptosis. Of note, AZD1152 synergistically enhanced the anti-proliferative activity of vincristine, a tubulin depolymerizing agent, and DNR, a topoisomerase II inhibitor. The authors concluded that AZD1152 is a promising new agent for the treatment of individuals with leukaemia and that the combined administration of AZD1152 with conventional chemotherapeutic agents warrants further investigation.

Data on results from the first phase I clinical trial in advanced pretreated solid malignancies has been reported (Boss *et al.,* 2006). AZD1152 was well tolerated when administered as a 2 hour intravenous infusion at doses up to 300mg. Neutropenia was the dose limiting toxicity at 450mg with no other clinically significant toxicities reported. They reported significant disease stabilization suggesting a promising clinical future development for the drug. More recently another phase I/II clinical trial provided information on the safety and efficacy of AZD1152 in patients with advanced AML showing that the drug had an acceptable tolerability profile in patients with AML (Lowenberg *et al.*, 2009).

AZD1152 is currently being tested in phase II clinical trials as a single agent or in combination with low dose Ara-c for the treatment of elderly patients with AML who are unsuitable for standard induction treatment.

1.12 Project objective

This study investigates the efficacy of the novel aurora-B kinase inhibitor AZD1152-hQPA in a panel of AML cell lines and primary samples. Down-regulation of phosphorylation of Histone H3 on Ser^{10} (pHH3) can be used to measure aurora-B inhibition and will be used as a biomarker for AZD1152-hQPA activity. Initially it was planned to investigate the specificity of AZD1152-hQPA in AML cell lines and primary samples in relation to their ABC transporter status. In response to some of the initial observations further work was undertaken including biomarker assay optimisation, development of a new MDR cell line and investigation of FLT3-ITD as possible secondary target of AZD1152-hQPA.

Chapter Two MATERIALS AND METHODS

2.1 Materials

Materials were from Sigma (Poole, Dorset UK) unless otherwise stated. AZD1152-hQPA (active drug) was supplied by AstraZeneca in powdered form. A 10mM stock solution was prepared in DMSO, aliquoted and then frozen. Further dilutions were made in cell culture/assay medium. Radio-labelled [^{14}C]-AZD1152-hQPA was also supplied by AstraZeneca for use in the drug accumulation assays.

2.2 Cell lines and cell culture

OCI-AML3, MOLM-13 and M-07e myeloid leukaemia cell lines were obtained from the German Collection of Microorganisms and Cell Cultures (DSMZ, Braunschweig, Germany). U937 and KG-1a cell lines were from the European Collection of Animal Cell Cultures (Salisbury, UK). MV4-11 cell line was obtained from the American Type Culture Collection (Manassas, VA, USA). HL-60 cells were a gift from Dawn Bradbury (Nottingham University Hospitals, UK), OCI-AML6.2 cells a gift from Dr. Jo Mountford (University of Glasgow, UK) and HL-60ADR (Krishnamachary *et al.*, 1994) cells a gift from Mark Center (Kansas State University, USA). HL-60, U937, OCI-AML3, OCI-AML6.2, MOLM-13 and MV4-11 cell lines were maintained in RPMI 1640 medium with 10% foetal calf serum (FCS; First Link, Birmingham, UK), 2mM L-glutamine, 100 U/ml penicillin and 10µg/ml streptomycin. The KG-1a and M-07e cell lines were maintained as above with 20% FCS and the M-07e having the addition of 10ng/ml GM-CSF (Novartis, Basel, Switzerland).

Table 2.1 – Human leukaemic cell line panel used in the study. (Information taken from<URL:http://www.dsmz.de/human_and_animal_cell_lines/cell_line_index.php)

CELL LINE	CELL TYPE	ORIGIN
OCI-AML3	Human acute myeloid leukaemia	Established from the peripheral blood of a 57-year-old man with acute myeloid leukaemia (AML FAB M4) at diagnosis
OCI-AML6.2	Human acute myeloid leukaemia	Derived within the St Jude Children's Research Hospital, Memphis, USA (Abbott *et al*., 2002).
MOLM-13	Human acute myeloid leukaemia	Established from the peripheral blood of a 20-year-old man with acute myeloid leukaemia AML FAB M5a at relapse after initial MDS
MV4-11	Human acute monocytic leukaemia	Established from a 10-year-old boy with acute monocytic leukaemia (AML FAB M5) at diagnosis
M-07e	Human acute megakaryoblastic leukaemia	Established from the peripheral blood of a 6-month-old girl with acute megakaryoblastic leukaemia (AML M7) at diagnosis; Subline of the growth factor-independent M-07
HL-60	Human acute myeloid leukaemia	Established from the peripheral blood of a 35-year-old woman with acute myeloid leukaemia (AML FAB M2)
HL-60ADR	Human acute myeloid leukaemia	Derived within Kansas State University, USA by isolating HL-60 cells resistant to adriamycin.
U937	Human histiocytic lymphoma	Established from the pleural effusion of a 37-year-old man with generalized diffuse histiocytic lymphoma; Cells were described to express markers and properties of monocytes
KG-1a	Human acute myeloid leukaemia (derivative of KG-1)	Established from the bone marrow of a 59-year-old man with erythroleukaemia that developed into AML; KG-1a is a subclone of the AML cell line KG-1

All cultures were kept at 37°C in 5% CO_2 and all experiments were performed with cell lines in log phase. The leukaemic cell lines that were used are shown in table 2.1. Continued testing to authenticate these cell lines was initially performed using a panel of monoclonal antibodies and later by STR fingerprinting (2.4). Cell line FLT3-ITD status was confirmed using the protocol described in 2.16.

2.3 Cell line validation and mycoplasma testing

2.3.i Cell line validation using monoclonal antibodies

Continued testing to authenticate these cell lines was performed using a panel of monoclonal antibodies and FLT3 mutational analysis towards the final passage of each batch thawed. CD38 FITC, CD33 PE, CD34 Percp (BD Biosciences), CD13 FITC (Dako) and CD42 PE (Pharmingen) mouse monoclonal antibodies along with their isotype control were used to validate the cell line phenotype. $2x10^5$ cells were incubated with 2.5µl normal mouse serum and 2.5µl monoclonal antibody or the isotype control followed by washing in PBSAA (PBS; Oxoid, Basingstoke, UK/1% bovine serum albumin/0.5% sodium azide) and analysis by flow cytometry. Cell line FLT3-ITD status was confirmed using the protocol described in 2.16. The phenotypes and FLT3 status of the cell lines used in the study are

Table 2.2 – Cell line panel phenotype and FLT3 status.

CELL LINE	CD13	CD33	CD38	CD34	CD42	FLT3
OCI-AML3	Positive	Positive	Positive	Negative	Negative	WT
OCI-AML6.2	Positive	Positive	Positive	Negative	Negative	WT
OCI-AMLDNR	Positive	Positive	Positive	Negative	Negative	WT
MOLM-13	Negative	Positive	Positive	Negative	Negative	ITD
MV4-11	Negative	Positive	Positive	Negative	Negative	ITD
M-07e	Positive	Positive	Positive	Negative	Positive	WT
HL60	Positive	Positive	Negative	Negative	Negative	WT
U937	Positive	Positive	Positive	Negative	Negative	WT
KG-1a	Positve	Negative	Negative	Positive	Negative	WT

shown in table 2.2.

2.3.ii OCI-AML3/OCI-AML6.2 genetic analysis

DNA was prepared using a QIAamp DNA blood mini kit (Qiagen, Crawley, UK) and 5ng DNA was amplified using the Powerplex 16 System (Promega, Southampton, UK) to assess short tandem repeats (STR). The products were run on a 3130 Genetic Analyzer and the data analyzed using GeneMapper ID v3.2 software. The STR analysis of the OCI-AML6.2 cell line was shown to be identical to the parent OCI-AML3 cell line indicating that there were no significant genetic changes.

2.3.iii Mycoplasma testing

Mycoplasma testing was carried out at a similar time to cell phenotyping using a mycoalert mycoplasma detection kit (Lonza, Rockland, USA) and following the manufacturer's instructions. Briefly, cells were centrifuged and 100µl of supernatant removed to a 96 well luminescent plate (Costar) and mixed with 100µl mycoalert reagent. After 5 minutes incubation, luminescence was read on a POLARstar Optima plate reader (BMG Labtech, UK) (Reading A) followed by a further 10 minute incubation with 100µl mycoalert substrate. A second luminescence reading was then taken (Reading B) and the ratio of Reading B/Reading A calculated. A ratio of >1.0 indicated the presence of mycoplasma. Positive and negative controls were supplied for validation.

2.4 Primary patient samples

Multi-centre presentation peripheral blood (PB) or bone marrow (BM) samples were obtained at diagnosis from patients with AML (excluding M3 subtype) and taken into preservative-free heparin or into EDTA tubes. All samples were pre-treatment and only samples received within 48 hours of being removed from the patient were analyzed. Use of these samples was approved by the Nottingham 1 Research Ethics Committee (reference number 06/Q2403/16).

2.5 Isolation of mononuclear cells from peripheral blood and bone marrow

Peripheral blood or bone marrow was diluted 1 in 2 in RPMI before being layered onto an equal volume of Histopaque and centrifuged at 600g for 20 minutes (Fig. 2.1). Using a sterile pipette the mononuclear cells were carefully removed from the plasma-histopaque interface and placed into RPMI before being centrifuged at 600g for 10 minutes. At this stage any contaminating red blood cells were removed by the addition of 6mls ice cold 0.89% Ammonium chloride (For 500ml: 4.495g NH_4Cl, 18.5mg EDTA, 0.5g $KHCO_3$ + 500ml dH_2o) and incubation on ice for 10 minutes. Cells were then centrifuged at 400g for 10 minutes, re-suspended in fresh RPMI and then centrifuged at 200g for a final 10 minutes before counting.

2.6 Cryopreservation and thawing of cell lines and patient cells

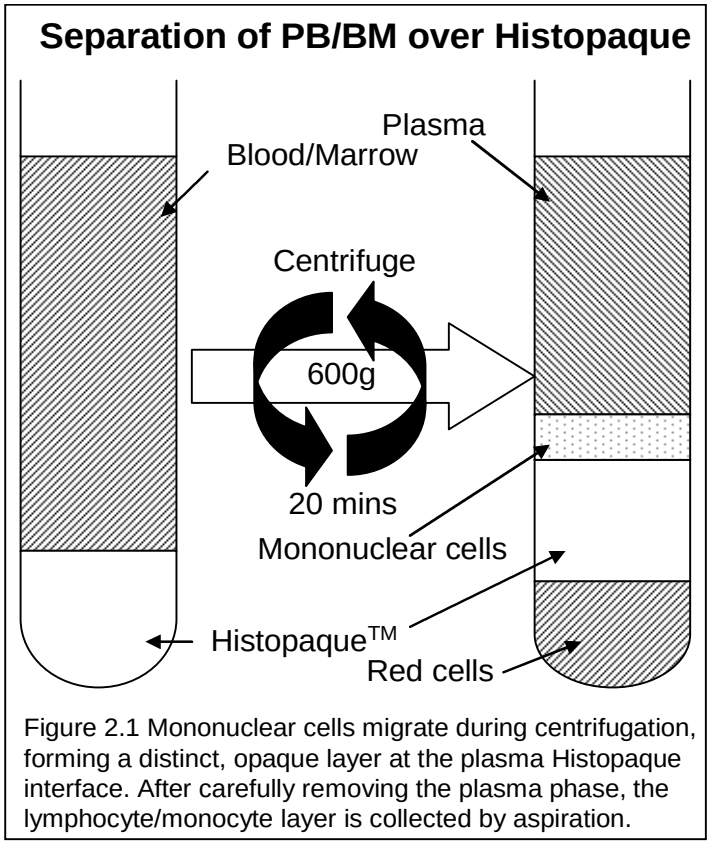

Figure 2.1 Mononuclear cells migrate during centrifugation, forming a distinct, opaque layer at the plasma Histopaque interface. After carefully removing the plasma phase, the lymphocyte/monocyte layer is collected by aspiration.

For cryopreservation, cells were counted and re-suspended at $1x10^7$/100µl ($1x10^6$/100µl for cell lines) in cold RPMI. Cryovials were labelled with sample code, cell concentration, and date and placed on ice before the addition of 700µl freeze solution (For 35ml: 5ml DMSO (Origen Biomedical, Sweden), 10ml FCS + 20ml RPMI). 300µl cells were added to each cryovial (the final concentration in each vial is 10% DMSO and 20% FCS) before being placed in a freezing chamber and frozen at -80°c for at least 2 hours followed by transfer to liquid nitrogen for long term storage. To thaw, samples were removed from liquid nitrogen, placed into a water bath at 37°C for about 2 minutes and then transferred drop wise to cold thaw solution (RPMI containing 10% FCS and 1% heparin (Hospital pharmacy) – heparin only used when thawing patient samples). Cell lines were re-suspended in the appropriate media, placed into flasks and incubated directly at

37°C/5% $C0_2$. Patient cells were then centrifuged at 250g for 5 minutes and re-suspended in rest medium (RPMI containing 20% FCS and 1% L-glutamine) for 90 minutes at 37°C/5% $C0_2$. Thawed and rested samples were then subjected to viability analysis using trypan blue exclusion and only samples with > 85% post-rest viability were used.

2.7 Suspension culture of primary patient samples

Primary AML samples were cultured at $1x10^6$/ml in RPMI 1640 with 10% FCS, 2mM L-glutamine, supplemented with 20ng/ml interleukin (IL)-3 (gift from Novartis, Surrey, UK), 20ng/ml stem cell factor (SCF) (R+D Systems, Abingdon, UK), 20ng/ml IL-6 (R+D Systems) + 25ng/ml granulocyte colony-stimulating factor (G-CSF) (R+D Systems) + 0.07µl/ml beta-mercaptoethanol.

2.8 Cell viability assays

2.8.i Preparation of fixed stained cells

Peripheral blood mononuclear cells from healthy volunteers were prepared by a standard density gradient technique. Cells in PBSAA were incubated with CD45 FITC antibody for 20 minutes, washed twice, and resuspended in fresh 2% Paraformaldehyde (VWR International). The final cell concentration was determined using a haemocytometer and trypan blue exclusion.

2.8.ii 7-AAD/fixed stained cell viability assay

This was done by a previously published in-house method which allows rapid evaluation of viable cells by flow cytometric counting (Pallis *et al.*, 1999a). 100µl cells were cultured at $2x10^5$ml in 96-well plates in triplicate. 7-Amino-actinomycin D (7-AAD), which detects dead cells, was diluted in PBS as a 50µg/ml stock solution and mixed with harvested AZD1152-hQPA treated or control cells to give a final concentration of 12.5µg/ml. Samples were incubated in the dark for 20 minutes before being analyzed by flow cytometry. The number of viable cells remaining was quantified by excluding dead cells and calculating a ratio with reference to an internal standard of fixed, pre-labelled cells.

2.9 Histone H3 phosphorylation status and cell cycle analysis by intracellular flow cytometry

Cells were harvested by centrifugation washed in PBSAA and $3x10^5$ cells treated with fixation medium (Abd Serotec, Oxford, UK) at room temperature (RT) for 15 minutes. Ice cold methanol was added and after 10 minutes incubation on ice, cells were washed in PBSAA, re-suspended in permeabilization medium (Abd Serotec) and 5µg/ml of anti-phospho-histone H3 (Ser 10) mouse monoclonal antibody (Upstate; now part of Millipore, Livingstone, UK) or mouse isotype control (Dako, Ely, UK) was added. After 2 hours incubation at RT, cells were washed twice in PBSAA, re-suspended with 3µl of secondary antibody (goat anti-mouse IgG FITC $F(ab`)_2$; Dako), and incubated for 1 hour in the dark. Cells were then washed twice in PBSAA and re-suspended in 25µg/ml 7-AAD for 20 minutes in the dark. Samples were collected using a FACScalibur. Isotype controls were used for

cytometer set up and doublets were gated out before fluorescence data were collected. Data were analyzed using Cellquest software with phosphorylation status expressed as percentage of total cells gated.

2.10 Immunofluorescence analysis of Histone H3 phosphorylation status

Cells were treated identically as for Histone H3 flow cytometric analysis up until the final wash step. Cells were then manually placed onto glass slides, mounted in VECTASHIELD mounting medium containing DAPI (Vector laboratories, Inc), and visualized with a fluorescent microscope (Olympus, UK).

2.11 Determination of Pgp and BCRP function

Functional Pgp expression was determined by modulation of rhodamine 123 (R123) efflux. Cells were re-suspended at $1x10^6$/ml in culture medium and incubated (75 minutes, 37°C) with R123 (200ng/ml) with or without 2.5µg/ml cyclosporine A (CSA; hospital pharmacy) or diluent control. Control tubes containing R123 were placed on ice to halt the reaction. Functional BCRP expression was measured similarly and was determined by modulation of BODIPY-prazosin (BODIPY; Invitrogen) efflux. Cells were re-suspended at $1x10^6$/ml in culture medium and incubated (75 minutes, 37°C) with BODIPY (25nM) with or without 10µM FTC (Calbiochem) or diluent control. Control tubes containing BODIPY were placed on ice. All tests were carried out in duplicate. Patient samples had the added step of the addition of 5µl CD45 PerCP to identify

the blast population before cells were washed twice in PBSAA at 4°c, collected using a FACScalibur (Becton Dickson, UK) and analyzed using Cellquest software. Mean fluorescence intensity (MFI) of each sample in the FL1 channel was measured, since this corresponds to R123/BODIPY retention. The modulation ratio is calculated as: (MFI with modulator – cold control MFI)/(MFI with diluent control – cold control MFI). The average of the duplicate experiments was calculated.

2.12 Pgp protein expression – MRK16 mAb

For Pgp protein expression cells were harvested, washed in PBSAA, and $2x10^5$ cells incubated with 1µg MRK16 anti-Pgp antibody (Kamiya Biomedical) or IgG2a isotype control (Dako) for 30 minutes at RT. Cells were washed x3 in PBSAA and blocked in 80µl 20% normal rabbit serum for 30 minutes on ice. 5µl FITC-conjugated rabbit anti-mouse secondary antibody (Dako) was added and cells incubated for 30 minutes on ice. Cells were washed twice in PBSAA and cell line data collected using a FACScalibur. Patient samples had the added step of the addition of 5µl CD45 PerCP (Becton Dickinson) and 5µl Normal Mouse serum before being washed twice in PBSAA and collected using a FACScalibur. Labelling the patient samples with CD45 PerCP allowed the leukaemic blast (CD45 low/side scatter low) cells to be gated.

2.13 Apoptosis assays

2.13.i Detection of apoptosis with Annexin V-FITC

Detection of apoptosis was determined using the Annexin V-FITC apoptosis detection kit according to the manufacturer's instructions. Briefly, following treatment for 48 hours with AZD1152-hQPA the cells were washed in PBS and re-suspended in the supplied binding buffer containing calcium chloride and incubated with annexin V-fluoroscein-isothiocyanate (FITC) and propidium iodide for 10 minutes in the dark. Data on the annexin V positivity of the cells were collected on a FACScalibur and analyzed using Cellquest software.

2.13.ii Detection of apoptosis with active Caspase-3 and Apop2.7 (7A6) antibodies

Active caspase-3 and 7A6 expression was determined in U937 cells treated for 48 hours with 0-300nM AZD1152-hQPA. To measure active caspase-3 expression, treated cells were harvested by centrifugation, washed in PBSAA and $5x10^5$ cells treated with fixation medium (Abd Serotec) at RT for 15 minutes. Cells were then washed in PBSAA and re-suspended in permeabilization solution (Abd Serotec) with 20% Normal Rabbit serum. After 15 minutes at RT, 20µl PE-conjugated polyclonal Rabbit anti-active caspase-3 (BD Pharmingen) was added and cells incubated for 1 hour at RT. Cells were washed and data collected on a FACScalibur using Cellquest software for analysis. Cells for 7A6 analysis were counted and washed in PBSAA before re-suspending in 25µg/ml Digitonin and incubation on ice for 20 minutes. The cells were then pelleted and either 20µl of Anti-APO2.7-PE (Beckman Coulter) or Mouse IgG1 PE isotype control (BD Pharmingen) was added before incubation for 20 minutes at RT. Cells were

washed in PBSAA before collection on a FACScalibur and analysis using Cellquest software.

2.13.iii H2A.X phosphorylation

Measurement of DNA double strand breaks, characteristic of apoptosis, was determined using the H2A.X phosphorylation kit (Upstate) according to the manufacturer's instructions. Briefly, after 24 hours treatment with AZD1152-hQPA the cells were washed in PBSAA and re-suspended in the supplied fixation buffer. After further washes cells were permeabilized and incubated with either anti-phospho-H2A.X (Ser139) FITC or IgG FITC control antibody. Following further washes in saponin containing buffer, cells were re-suspended in 10µg/ml 7-AAD and data collected using a FACScalibur.

2.14 p53 Sequencing

Cell line cDNA was prepared using QIAamp blood isolation kits (Qiagen, Crawley, UK) according to manufacturer's instructions. Exons 2-11 of p53 were amplified using 4 over-lapping sets of primers p53; 1F-gacacgcttccctggat tggc, 1R-gcaaaacatcttgttgagggca, 2F-gtttccg tctgggcttcttgca, 2R-ggtacagtcagagccaacctc, 3F-tggcccctcctcagcatctta, 3R-caaggcctcattcagctctc, 4F-cggcgcacagaggaagagaatc, 4R-cgcacacctattgcaa gcaaggg. Approximately 50ng of cDNA was used as template in each of the PCR amplifications. The 50µl reaction also included 150µM of each dNTP (Amersham Biosciences, Buckinghamshire, UK), 1µM of each primer, 1.0mM $MgCl_2$ for fragments 1 and 2 or 1.5mM $MgCl_2$ for fragments 3 and 4, and

2 units of Amplitaq Gold (Applied Biosystems) in the manufacturer's buffer. Following an initial heat activation step at 95°C for 10 minutes amplification was performed in a PTC-100TM Programmemable Thermal Controller (MJ Research) using the following conditions; denaturation at 95°C for 1 minute, annealing for 1 minute at 55°C for fragments 1 and 2 or 60°C for fragments 3 and 4, extension at 72°C for 1 minute for a total of 35 cycles ending with a final extension at 72°C for 10 minutes. PCR products were purified using a QIAquick PCR purification kit (Qiagen) prior to sequencing. Sequencing reactions were set up with approximately 200ng of purified PCR product and 3.2pM primer using BigDye® Terminator v3.1 Cycle Sequencing Kit (Applied Biosystems). The primers used for sequencing were the same as those used for the PCR amplifications. The reactions were electrophoresed using an ABI 3130 Genetic Analyzer (Applied Biosystems) and results analyzed using the Sequencing Analysis 5.2 software (Applied Biosystems).

2.15 Cloning assays

2.15.i Bacterial electroporation

The MDR1 gene cloned into the pCMV6-Neo vector (RSPD001-Neo) was supplied by Origene (Rockville, USA). To amplify stocks RSPD001-Neo or pCMV6-Neo control was transformed into ElectroTen-Blue electroporation competent bacteria (XL1-Blue MRF´ strain) (Stratagene, Stockport, UK), following the manufacturer's instructions. Briefly, 1µl of RSPD001-Neo plasmid was gently added to 30µl of bacteria in a pre-chilled eppendorf tube and then

transferred to a chilled cuvette which was then incubated on ice for 1 minute. An electroporation control was included using the pUC18 control plasmid (Stratagene). Samples were placed into a chilled electroporation chamber and pulsed once with 2500 applied volts. Immediately following electroporation, 250µl of SOC (Super optimal broth with catabolic repressor) medium was added to the cell suspension, before transfer to a 15ml Falcon polypropylene round-bottom tube. The tubes were then incubated at 37°C for 60 minutes while shaking at 225rpm to allow expression of the antibiotic genes. Agar plates were prepared by melting powdered LB agar at 35g/L into 200ml distilled water by heating in a microwave for approximately 4 minutes on medium (with occasional agitation), until the agar was molten. The agar was cooled slightly, before addition of 100µg/ml ampicillin and then divided between 10-12 sterile Petri dishes and left to set. 200µl of neat and a 1:10 dilution of the RSPD001-Neo or pCMV6-Neo vector transformations and pUC18 electroporation control were spread over the agar plates, before being incubated overnight at 37ºC. If the transformation experiment was successful, bacterial colonies would be present. Two bacterial colonies were selected from each agar plate and grown up overnight at 37ºC in LB Broth (20g/L in ddH_20) medium containing 100µg/ml ampicillin (LB+AMP) with constant agitation.

2.15.ii Plasmid preparation

Qiagen plasmid mini and midi kits (Qiagen) were used for plasmid preparation. Briefly, 3ml (mini) or 25ml (midi) bacteria from the overnight culture were

centrifuged at 6,000g for 15 minutes and re-suspended in 0.3ml or 4ml 'buffer P1'. The remaining culture was stored at 4°C for making glycerol stocks if digests proved to be successful. 0.3ml or 4ml 'buffer P2' was added, thoroughly mixed, and incubated at room temperature for 5 minutes before addition of 0.3ml or 4ml 'buffer P3' and incubation on ice for 5 or 15 minutes. Cells were centrifuged at 13,000g for 10 or 30 minutes at 4°C. The cleared lysate was then transferred to a Qiagen-tip which had been equilibrated with 1ml or 4ml 'buffer QBT' and then washed twice with 2ml or 10ml 'buffer QC'. The DNA was eluted with 0.8ml or 5ml 'buffer QF' before precipitation by addition of 6µl or 350µl 3mM NaAC (pH5.2) and 1.4ml or 12.5ml ethanol followed by incubation at -70°C for 30 minutes and centrifuging at 8,500 for 30 minutes at 4°C. The DNA pellet was washed with 1ml or 2ml 70% ethanol, centrifuged at 15,000 for 10 minutes and then air-dried for 10 minutes before re-suspension in Tris-EDTA (10mM Tris, pH 7.5, 1 mM EDTA) buffer and stored at -20ºC until required.

2.15.iii Restriction digestions

A 20µl digestion reaction volume contained 1µl NotI or 1µl EcoRI (for pUC18 samples), 2µl 10x buffer D (Pomega), 2µl 10x BSA (Promega), 4µl plasmid and 11µl DNase/RNase-free distilled water. The restriction enzyme targets specific sequences in the DNA and is listed in Table 2.3. The DNA was digested overnight, at 37ºC, with the resulting products run out on a 0.7% agarose gel.

Table 2.3 – Specification of the NotI restriction endonuclease (cleaved at the points *).

RESTRICTION ENZYME	TARGET SEQUENCE IN DNA
NotI (Promega)	5'-GC*GGCC GC-3' 3'-CG CCGG*CG-5'

2.15.iv Agarose gel purification

A 0.7% agarose gel was prepared by melting 2.1g agarose into 300ml 1x TBE (Tris Borate EDTA) buffer, which was diluted from a 10x stock. The buffer was heated in a microwave for approximately 5 minutes, with regular agitation, until the agarose was molten. The agarose was allowed to cool slightly and 0.5µg/ml ethidium bromide was added. The agarose gel was then poured into the gel electrophoresis casting containing a 16-well gel comb and left to set. Once set, the agarose gel was placed into an electrophoresis tank, filled with 1x TBE buffer. 10µl of DNA was loaded per well, after being diluted 5:1 with 6x Gel loading solution (Fisher Scientific, Loughborough, UK). The gel was also loaded with 10µl of a 1 kb DNA ladder (New England Biolabs, Hitchin, UK), which provided an accurate molecular weight scale, to aid with DNA size quantification. The gel was run at 150V for approximately 60minutes. The DNA molecules ran towards the cathode, being separated according to their molecular weight. The mutagen ethidium bromide intercalated itself into the double-stranded DNA, allowing it to be visualised under ultra-violet (UV) light, either via the Syngene ChemiGenius BioImaging system, or a UV lamp. The DNA was purified from the agarose gel using the Wizard® SV Gel Clean-Up System (Promega). Briefly, using a clean

scalpel, the larger (5838bp) pCMV6-Neo DNA fragments were excised from the gel into a 1.5ml microcentrifuge tube and weighed. The gel slices were dissolved at 60ºC in 10µl membrane binding solution per 10mg of gel. The DNA samples were incubated on minicolumns for 1 minute and then collected onto the filter by centrifugation at 16,000g for 1 minute. The DNA was then washed by adding 700µl membrane wash solution and centrifuging the samples at 16,000g for 1 minute followed by 500µl membrane wash solution and centrifuging at 16,000g for 5 minutes. The DNA was eluted into a clean 1.5ml microcentrifuge tube by addition of 50µl nuclease-free H_2O and centrifuging at 16,000g for 1 minute and its concentration was determined using the CE 7200 spectrophotometer (Cecil instrument Ltd, Cambridge, UK) according to the manufacturer's instructions. The DNA was stored at -20ºC until required.

2.15.v Ligations

A 10µl ligation reaction volume contained 1µl 10x buffer, and T4 DNA ligase enzyme (Promega), 4µl pCMV6-Neo, with the difference made up using nuclease-free H_2O. A second ligation reaction was set up, which contained 8µl pCMV6-Neo for comparison. The two ligations were incubated overnight at 15ºC, to allow for the compatible ends of the pCMV6-Neo vector to combine. Prior to transfection modifying enzymes were removed from the ligation reactions by addition of 5µl StrataClean resin (Stratagene) and centrifuging at 2,000g for 1 minute. 10µl of supernatant was removed to a fresh microcentrifuge tube before repeating the process.

2.15.vi Plasmid sequencing reactions

The reactions used the forward sequencing primers VP1.5 (5`GGACTTTCCAAAATGTCG-3`) and reverse primers XL39 (5`-ATTAGGACAAGGCTGGTGGG-3`) as recommended by Origene. Sequencing reactions were set up using BigDye® Terminator v3.1 Cycle Sequencing Kit (Applied Biosystems) according to manufacturer's instructions. The sequencing reaction consisted of 5µl buffer, 3µl sequencing mix, 1µl plasmid clone, 1µl (3.2pM) primer and 10µl distilled H20, which was run on the Biometra T gradient PCR machine (Biometra, Goettingen, Germany) using the following programme; 96ºC for 1 minute followed by 25 cycles of 96ºC for 10secs (denaturing stage), 50ºC for 5secs (annealing stage) and 60ºC for 4 minutes (extension stage). The sequencing reaction was then added to 2µl sodium acetate/EDTA followed by 66µl absolute ethanol and incubation on ice for 15 minutes. After centrifuging at 13,000g for 20 minutes the supernatant was removed and 250µl 70% ethanol was added before centrifuging at 13,000g for 5 minutes and air drying for 20 minutes. Samples were re-suspended in HiDi buffer and then electrophoresed using an ABI 3130 Genetic Analyzer (Applied Biosystems) and results analyzed using the Sequencing Analysis 5.2 software (Applied Biosystems).

2.16 UIC2 shift assay

The reactivity of the UIC2 antibody with Pgp is increased by the addition of Pgp transported compounds and has been described by Park (Park *et al.*, 2003). Briefly, cells were re-suspended at $5x10^5$/ml in culture medium and incubated for 10

minutes at 37°C, 5% $C0_2$. 1µM AZD1152-hQPA or 5µM of the known Pgp substrate vinblastine, or both were added to cells in duplicate and incubated at 37°C, 5% $C0_2$ for 4 hours. 10µg/ml etoposide +/- vinblastine was also included as a negative control. Either 0.1µg/ml UIC2 monoclonal antibody (Immunotech) or IgG2a isotype control (Dako) was added to paired samples and incubated for a further 15 minutes. Cells were washed twice in PBSAA, re-suspended in 20% Rabbit serum, and placed on ice for 30 minutes. 5µl FITC-conjugated rabbit anti-mouse secondary antibody (Dako) was then added to cells, and following 30 minutes incubation on ice, cells were washed twice and analyzed by flow cytometry. An increase in FL1 fluorescence compared to a drug free control is taken to indicate the presence of a Pgp substrate.

2.17 Radio-labelled drug accumulation assay

OCI-AML3, OCI-AML3DNR and OCI-AML6.2 cell lines were plated in duplicate onto 12 well plates and pre-incubated for 30 minutes with or without the Pgp modulators CSA (Hospital pharmacy) at 2.5µg/ml or PSC833 (Sandoz pharmaceuticals) at 2µM/ml or the BCRP modulator FTC at 10µM/ml or diluent control. Medium containing 0.017µCi radio-labelled [^{14}C]-AZD1152-hQPA (Astra Zeneca; Figure 2.2) was then added to give a final drug concentration of 300nM. The cultures were incubated for 1 hour at 37°C with agitation after 30 minutes. The radioactive medium was then aspirated and cells washed twice with ice cold PBS before permeabilization with 1% sodium dodecylsulphate. Cell extracts were then added to scintillation fluid (Perkin Elmer)

Chemical structure of radiolabelled AZD1152-hQPA

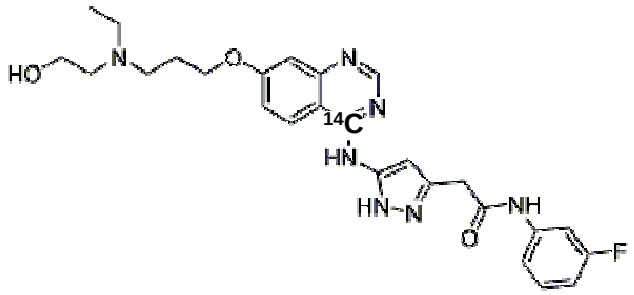

Figure 2.2 The chemical structure of radiolabelled AZD1152-HQPA.

and radioactivity, recorded as counts per minute (CPM), measured using a TRI-CARB 2100TR liquid scintillation analyzes (Packard).

2.18 FLT3 mutation analysis

Genomic DNA was extracted from samples using a QIAamp blood DNA isolation kit (Qiagen, Crawley, UK) according to the manufacturer's protocol. Approximately 100ng of genomic DNA was used as template in fluorescent PCR amplification (24 cycles) to amplify exons 14 and 15 and the intervening intron of the FLT3 gene using previously described primers with the FOR primer FAM-labelled (Kiyoi *et al.*, 1999). Analysis was performed on a 3130 Genetic Analyzer using the GeneMapper ID software v3.2 (Applied Biosystems), this allowed for determination of length of FLT3-ITD and proportion of DNA containing the length mutation.

2.19 Detection of pFLT3 – Immunoprecipitation and immunoblotting

Cell lines were washed in ice cold PBS and resuspended in lysis buffer (50nM Tris[pH 7.4], 150mM NaCL [Fisher Scientific, Loughborough, UK], 1% NP-40 [BDH Laboratory supplies, Lutterworth, UK], 0.25% Na-deoxycholate, 1mM EDTA, 2µg/ml leupeptin, 5µg/ml aprotinin, 1µg/ml pepstatin, 20mM NaF, 1mM PMSF and 3mM sodium orthovanadate) for 30 minutes. Samples were then sonicated before addition of 200mM PMSF and incubation for 30 minutes on ice. The samples were clarified by centrifugation at 100,000g and the supernatant was assayed for protein content using Bio-Rad dye reagent. Rabbit polyclonal FLT3 (Santa Cruz, CA, USA) was added to the extract and incubated overnight with mixing. Protein A agarose beads (Upstate) were added for an additional 2 hours. After sodium dodecyl sulphate-polyacrylamide gel electrophoresis (SDS-PAGE) and transfer to nitrocellulose membranes, immunoblotting was performed with mouse monoclonal anti-phosphotyrosine antibody (Upstate) to detect phosphorylated FLT3 and then the blots were stripped and re-probed with rabbit polyclonal Flt-3/Flk-2 (Santa Cruz) antibody to measure total FLT3. Proteins were visualized using chemiluminescence (Hyperfilm ECL; Amersham), scanned using a Syngene densitometer and analyzed using GeneSnap software (Syngene, Cambridge, UK).

2.20 Phosphorylated signal transducer and activator of transcription factor 5 (pSTAT5) analysis

Cells treated with AZD1152-hQPA or control cells were harvested, washed in PBSAA, and $5x10^5$ cells treated with fixation medium at RT for 15 minutes. Ice

cold methanol was added and after 10 minutes incubation on ice, cells were washed in PBSAA, re-suspended in permeabilization medium and 5µg of Mouse anti-phosphoSTAT5 (Zymed) or mouse isotype control (Dako) was added. After 30 minutes incubation at RT, cells were washed twice in PBSAA, re-suspended in 20% Normal rabbit serum and incubated for 30 minutes on ice. 5µl of secondary antibody (Rabbit anti-mouse IgG F(ab)2 FITC; Dako), was added and cells incubated on ice for 30 minutes before washing twice in PBSAA and addition of 5µl CD45 PerCP (Becton Dickinson) and 5µl Normal Mouse serum. Samples were then washed twice in PBSAA and collected using a FACScalibur.

2.21 Blast cell proliferation assay – ^{3}H-Tdr uptake

To measure stimulated proliferation rate, blast cells were cultured as previously described in section 2.7. Cells were plated onto 96-microwell plates at a concentration of $1x10^{6}$/ml. After 48 hours of culture, cells were exposed to tritiated thymidine ([^{3}H]-Tdr, 5µCi/well; Amersham) for 6 hours. Cells were harvested onto a 96 well filter plate using a Mash harvester and left overnight to dry. Incorporation of [^{3}H]-Tdr was then evaluated by β-scintillation counting. Basal proliferation was measured similarly without the 48 hours cytokine incubation.

2.22 Real-time PCR for ABCG2 and Aurora kinase B mRNA message levels

Thawed and rested AML blasts were depleted of $CD2^+$ cells using Dynabeads (to deplete NK and T cells some of which express ABCG2 mRNA (Scharenberg *et al.*, 2002). RNA from CD2 depleted AML blasts, the ABCG2 positive OCI-AML6.2 and MV4-11 cell lines was prepared using QIAamp RNA kits with DNase treatment according to the manufacturer's instructions (Qiagen). Up to 2µg of RNA was used in a reverse transcription reaction with Moloney murine leukaemia virus (MMLV) reverse transcriptase (Invitrogen) and random hexamers (Amersham Pharmacia). Quantitative PCR was performed on an ABI prism 7700 (Applied Biosystems, Warrington, UK) using Excite Real Time Mastermix with sybr green (Biogene). Each reaction consisted of 1x Excite mastermix, sybr green (1:60,000 final concentration), 40nM of both forward and reverse primers (for ABCG2 reactions) or 2µl of aurora kinase B forward and reverse primer mix (Qiagen: QT00067403), 1.6µl cell line or blast cDNA (or H_2O for template control) and H_2O to a final volume of 20µl. Thermal cycler conditions included an incubation at 95^{o}C for 10 minutes followed by 40 cycles of 95^{o}C for 15secs and 60^{o}C for 1 minute. Following the 40 cycles, the products were heated from 60^{o}C to 95^{o}C over 20 minutes during which a melting curve analysis was performed. This allowed the specificity of the products to be determined (indicated by the presence of a single melting peak) and confirmed the absence of product generated by primer-dimer association. To enable the levels of transcripts to be quantified standard curves were generated using serial dilutions of OCI-AML6.2 or MV4-11

Table 2.4 – Oligonucleotide primer pairs used during real-time RT-PCR for ABCG2 mRNA.

PRIMER:	SEQUENCE:
ABCG2	Forward: TGCAACATGTACTGGCGAAGA Reverse: TCTTCCACAAGCCCCAGG
β2M	Forward: GAGTATGCCTGCCGTGTG Reverse: AATCCAAATGCGGCATCT

cDNA. The housekeeping gene beta-2-microglobulin (β2M) was used to standardize the samples and the relative expression levels of ABCG2 or aurora kinase B transcripts were therefore calculated as the ratio between the level of ABCG2 or aurora kinase B and the level of β2M. Both sets of real time primers used for ABCG2 message levels have been previously published (Pallisgaard *et al.*, 1999; Abbott *et al.*, 2002) and are shown in table 2.4. Negative controls (no template) were included in each experiment and all reactions were run in triplicate.

2.23 Primary cell colony formation assay

Freshly isolated mononuclear cells were washed, resuspended in methylcellulose based medium H4534 (Stem Cell Technologies) containing 0-30nM AZD1152-hQPA or diluent control (Astra Zeneca, Alderley Edge, UK) and plated in triplicates onto 96 well plates (100µl containing $2x10^4$ cells). The plates were incubated for 14 days at 37°C in 5% CO_2 and the number of colonies formed then counted under the microscope. Colonies were defined as >20 cells and growth defined as >12 colonies present in untreated wells.

2.24 Statistical analysis

Statistical analysis was carried out using the Statistical Package for Social Sciences, version 16 (SPSS, Chicago, IL, USA). P values of ≤ 0.05 were considered to represent significance.

Chapter Three BIOMARKER VALIDATION AND CHEMOSENSITIVITY OF AML CELLS TO AZD1152-hQPA

3.1 Background

AZD1152-hQPA is a highly potent and selective inhibitor of aurora-B. It is known that aurora-B phosphorylates Histone H3 at Ser^{10} during mitosis (Hsu *et al.*, 2000) a process thought to be required for correct chromosome condensation (Wei *et al.*, 1999). We therefore intended to use Histone H3-Ser^{10} phosphorylation as a biomarker for AZD1152-hQPA activity in our assays.

3.2 Does AZD1152-hQPA reach its target? Measurement of pHH3/DNA content and protocol validation

The effects of AZD1152-hQPA were examined in logarithmically growing KG-1a, U937, M-07e, OCI-AML3, OCI-AML6.2, MV4-11 and MOLM-13 leukaemic cell lines. This panel of cell lines was selected to represent the heterogeneous nature of AML. The KG1-a cell line is drug naïve, but positive for Pgp, as are many cases of untreated AML. There is no known drug naïve BCRP positive AML cell line in existence, so the BCRP-transfected OCI-AML6.2 cell line was used. The FLT3-ITD expressing MV4-11 and MOLM-13 cell lines were included as the FLT3 gene is one of the most commonly mutated genes in AML and is associated with poor prognosis (Gilliland, 2002). All of the previously mentioned cell lines are cytokine independent so the cytokine dependent M-07e cell line was included for comparison (Brizzi *et al.*, 1990).

An in house flow cytometry protocol for measuring phosphorylated proteins was used to measure pHH3 expression and the fixation and permeabilization technique

previously developed by our group for measuring phosphorylated STAT5 was employed (Pallis *et al.*, 2003a). The pHH3 antibody stained with extreme brightness in the FITC (Fluorescein isothiocyanate) channel (Figure $3.1_{(A)}$). Because previous work with aurora kinase inhibitors had shown an increase in ploidy of treated cells (Ditchfield *et al.*, 2003) we wanted to be able to counter stain with propidium iodide (PI) to measure cellular DNA content. However, because of spectral overlap between PI in the PE (PhycoErythrin) channel and the FITC channel, compensation was impossible to set with any confidence. It was decided to change the counter-stain to 7-AAD which has minimal spectral overlap with FITC (Rabinovitch *et al.*, 1986) (Figure $3.1_{(B)}$). Back gating solely on the pHH3 positive population (Figure $3.1_{(C)}$) showed pHH3 expression only in the G2/M phase of the cell cycle as determined by 7-AAD staining. To confirm that pHH3 was only seen in mitotic cells it was decided to visualize the cells using immunofluorescence. Cells were treated identically as for Histone H3 flow cytometric analysis up until the final wash step. Cells were then manually placed

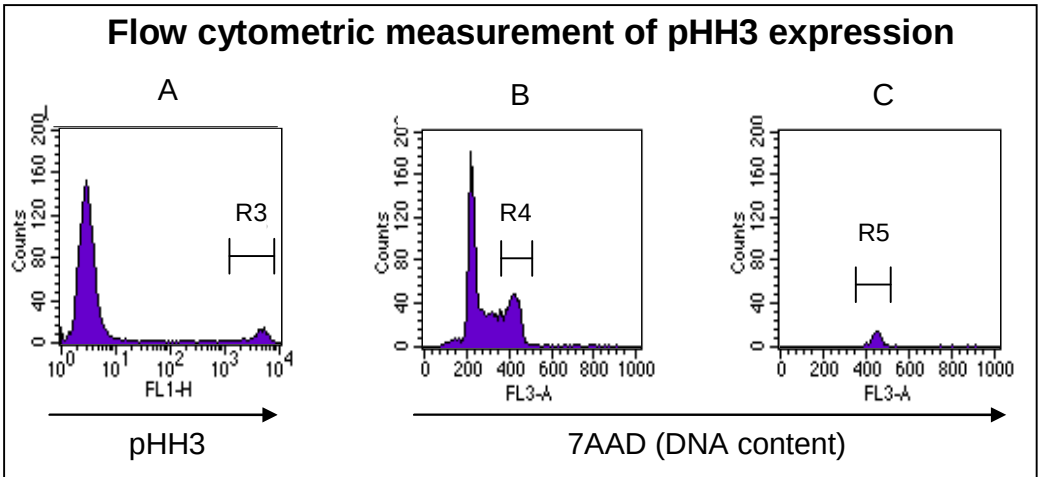

Figure 3.1 Flow cytometric measurement of pHH3 expression (FL1-H) and 7-AAD (DNA) content (FL3-A) in log phase U937 cell line (A and B). The histogram in plot (C) is gated solely on the pHH3-positive population (R3) and confirms 7AAD content/pHH3 expression only in the G_2-M phase of the cell cycle. Representation of three separate experiments.

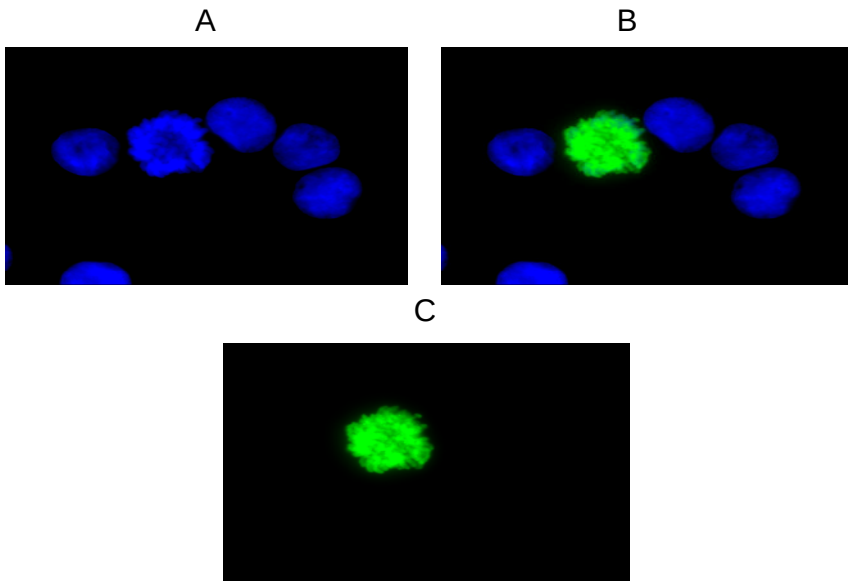

Figure 3.2 pHH3 (FITC) labelled U937 cells counterstained with DAPI measured on the FISH microscope with (A) DAPI, (B) DAPI/FITC and (C) FITC fluorescence. Cells with mitotic DNA are clearly distinguished with DAPI and the pHH3 stained cells were all mitotic.

onto glass slides, mounted in VECTASHIELD mounting medium containing DAPI, and visualized with a fluorescent microscope. Immunofluorescence confirmed that pHH3 was only present in mitotic cells (Figure 3.2).

To be able to use pHH3 as a biomarker for AZD1152-hQPA activity we needed to demonstrate its inhibition by the drug. U937 cells treated with AZD1152-hQPA at relatively low concentrations and time periods showed significant inhibition of percent of total cells expressing pHH3 (Figure 3.3). U937 cells treated with 300nM AZD1152-hQPA for 60 minutes showed almost complete loss of pHH3 (Figure 3.3).

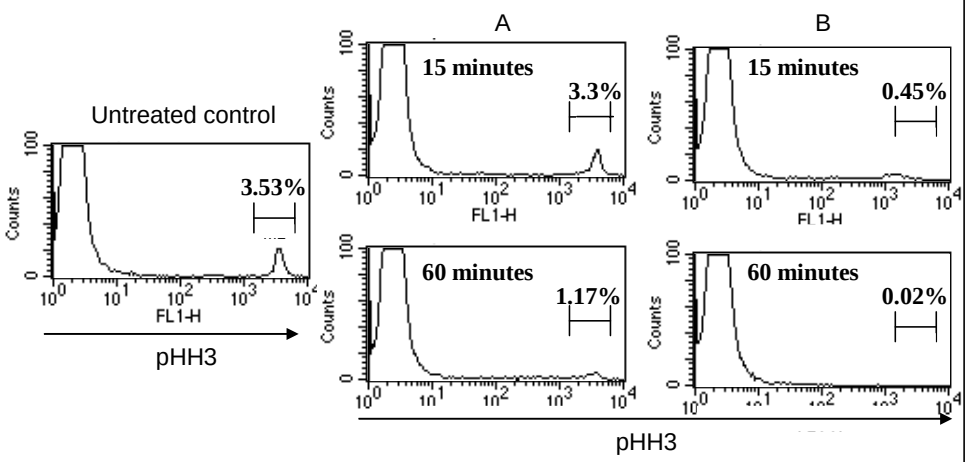

Figure 3.3 Inhibition of pHH3 expression by AZD1152-hQPA in U937 cells. pHH3 (FITC/FL1-H) labelled U937 cells treated with 30nM AZD1152-hQPA (A) or 300nM AZD1152-hQPA (B) for 15 or 60 minutes. Percentages are % of total cells expressing pHH3. Representation of three separate experiments.

3.3 Chemosensitivity of AML cell lines to AZD1152-hQPA

Inhibition of aurora-B activity by AZD1152-hQPA was indicated by a decrease in the phosphorylation of Histone H3 on Ser10 (Figure 3.3). The basal range of pHH3 expression in the cell lines was 2.5-4.8% of total cells (Figure 3.4). At concentrations of 0-1000nM after 24 hours, inhibition of pHH3 was achieved in all but one of the seven cell lines with complete inhibition achieved at 300nM in all but two of the lines (Figure 3.4). Seventy-two hours incubation with AZD1152-hQPA caused loss of viability to a varying degree in the cell lines, with an IC_{50} of <60nM achieved in all but two cell lines (Figure 3.5).

The Pgp expressing KG-1a cell line showed high resistance to pHH3 down-regulation and cell death compared to the Pgp null U937 cell line (Figure $3.4_{(A)}$ and $3.5_{(A)}$). Almost complete loss of pHH3 was achieved at a concentration of 30nM in U937 cells (p=0.001) with KG-1a resistant at concentrations up to

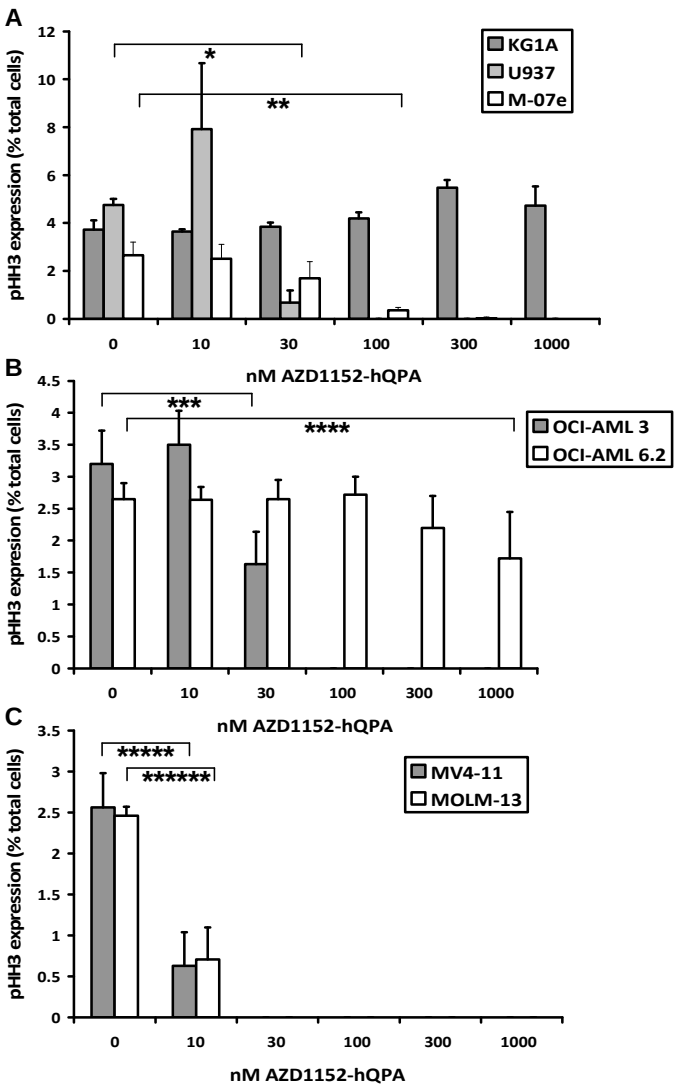

Figure 3.4 Flow cytometric measurement of pHH3 expression in AML cell lines after 24 hours of AZD1152-hQPA exposure (*p=0.001/**p=0.019/***p=0.003/****p=0.207/*****p=0.035/****** p=0.013, (analyzed using paired samples t-test), +95% confidence interval). Columns, mean of three experiments; bars, SD.

1000nM. Although the KG-1a cells are resistant to 24 hour pHH3 down-regulation with 1000nM AZD1152-hQPA, the same concentration of drug induced an 80% loss of viability after 72 hours (Figure $3.5_{(A)}$). The p53 wildtype cell line M-07e was sensitive to AZD1152-hQPA with a significant loss of pHH3 at 100nM

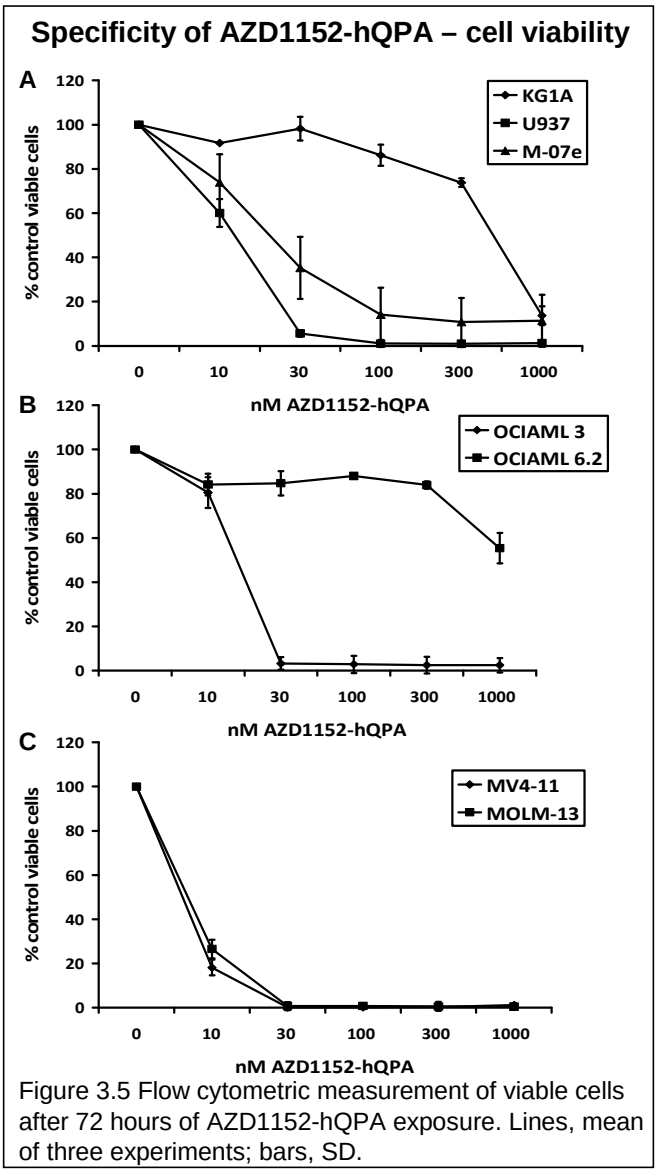

Figure 3.5 Flow cytometric measurement of viable cells after 72 hours of AZD1152-hQPA exposure. Lines, mean of three experiments; bars, SD.

(p=0.019) and 300nM inducing complete loss with subsequent loss of viability at 72 hours (Figure $3.4_{(A)}$ and $3.5_{(A)}$).

The BCRP transfected OCI-AML6.2 cell line also showed a high degree of resistance compared to the parental cell line OCI-AML3 (Figure $3.4_{(B)}$ and $3.5_{(B)}$). There was significant inhibition of pHH3 in the OCI-AML3 (p=0.003) cells at 30nM AZD1152-hQPA before complete inhibition at 100nM. The decrease in pHH3 seen at 300nM and 1000nM AZD1152-hQPA in the OCI-AML6.2 cells was

not statistically significant (p=0.408/0.207). In terms of viability OCI-AML6.2 cells were the most resistant with no IC_{50} achieved after 72 hours of high dose AZD1152-hQPA (Figure $3.4_{(B)}$).

Interestingly, the most sensitive of the cell lines tested were the FLT3-ITD expressing MV4-11 and MOLM-13 cell lines. Both lines showed significant pHH3 inhibition at 10nM AZD1152-hQPA, p=0.035 and p=0.013 respectively (Figure $3.4_{(C)}$), before complete inhibition at 30nM and a 72 hour viability IC_{50} of <10nM (Figure $3.5_{(C)}$).

3.4 AZD1152-hQPA sensitive cells develop a polyploid DNA content

Cell lines treated with AZD1152-hQPA for 24 hours were dual stained with pHH3 antibody along with 7-AAD to measure cellular DNA content (Figure 3.6A). Cell lines sensitive to pHH3 inhibition consistently failed to divide and developed a polyploid (8N) DNA content after treatment with AZD1152-hQPA. U937 cells exhibit an 8N population after 10nM treatment with the majority of cells having a polyploid DNA content after 30nM treatment (Figure 3.6A). Likewise, OCI-AML3 and M-07e cells show >4N DNA content after 24 hour incubation with low concentrations of AZD1152-hQPA. No polyploid populations were seen in the KG-1a or OCI-AML6.2 cell lines following 100nM AZD1152-hQPA treatment for 24 hours.

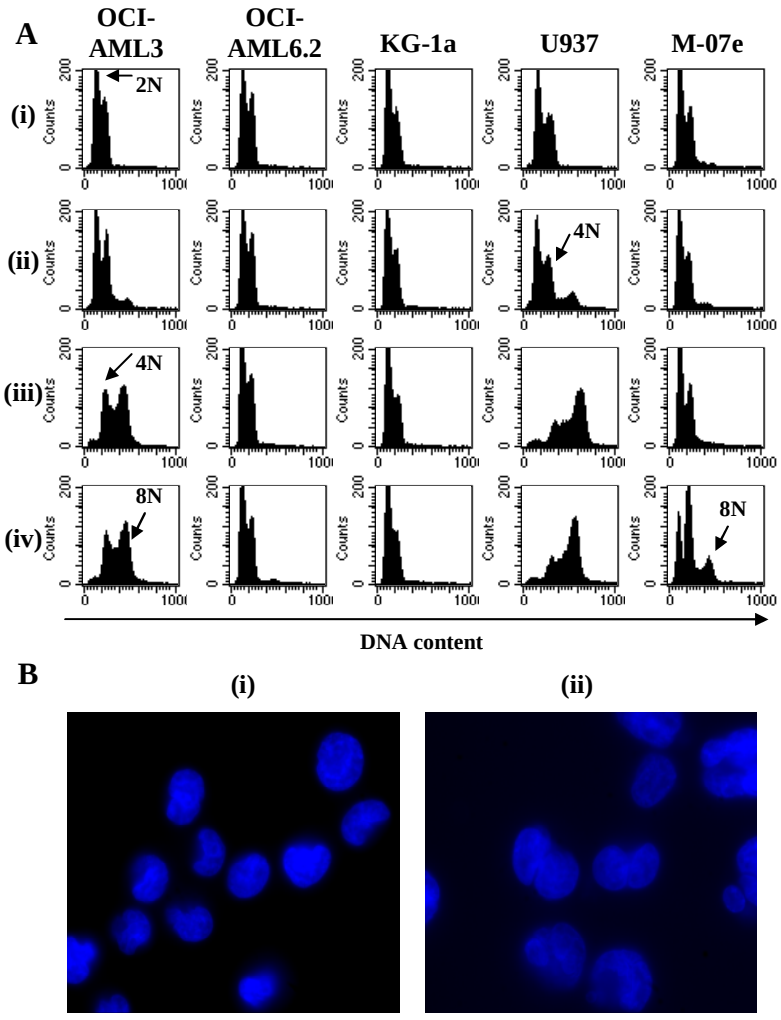

Figure 3.6 Flow cytometric DNA (7-AAD) content histograms of AML cell lines exposed to 0nM (i), 10nM (ii), 30nM (iii) and 100nM (iv) AZD1152-hQPA for 24 hours (A). OCI-AML3 cells exposed to 0nM (i) and 30nM (ii) AZD1152-hQPA for 24 hours stained with DAPI and viewed on the FISH microscope. Cells with polyploid DNA (ii) are clearly distinguished with DAPI stain.

To confirm whether the AZD1152-hQPA sensitive cells were becoming polyploid and we were not just seeing a shift in fluorescence in the flow histograms, OCI-AML3 control (Figure 3.6$A_{(i)}$) and 24 hour 30nM AZD1152-hQPA treated cells (Figure 3.6$A_{(iii)}$ were stained with DAPI and visualized on the FISH microscope (Figure 3.6B). Cells with polyploid DNA can clearly be distinguished in the AZD1152-hQPA treated cells (Figure 3.6$B_{(ii)}$).

3.5 Chemosensitivity of AML cell lines to AZD1152-hQPA compared to conventional therapy

The standard induction regimen for newly diagnosed AML consists of three days of an anthracycline (e.g. DNR, at least 60 mg/m^2, idarubicin, 10-12 mg/m^2, or the anthracenidione mitoxantrone, 10-12 mg/m^2) intravenously and cytarabine (Ara-c), 100-200 mg/m^2 by continuous infusion for seven days. With such ("3 + 7") regimens 60% to 80% of young adults and 40% to 60% of older adults can achieve CR (Zhu *et al.*, 2009). Any novel drug for potential use in the treatment of AML should compare favourably with these standard treatments as a single agent and possibly enhance their effects when used in combination.

Seven leukaemic cell lines were cultured for 72 hours with either 0-1000nM of AZD1152-hQPA, DNR or Ara-c (Figure 3.7). 72 hour viability was measured using 7-AAD and IC_{50} calculated for each cell line. In terms of concentration of drug used AZD1152-hQPA compares better than DNR and Ara-c in achieving 72 hour IC_{50} in all but the KG-1a cell line. Interestingly, the specificity of AZD1152-hQPA is extremely similar to that seen with DNR ($p=<0.0001$), with the KG-1a cell line standing out as the most resistant to the two agents (Figure $3.7_{(A)}$ and $_{(B)}$). The specificity profile of AZD1152-hQPA is significantly different to that of Ara-c ($p=0.533$) (Figure $3.7_{(A)}$ and $_{(C)}$). To study the effects of AZD1152-hQPA when used in combination with DNR and Ara-c an IC_{50} concentration for 72 hour viability for each drug was selected for MOLM-13 cells (Figure 3.7). MOLM-13 cells were then treated with IC_{50}, ½IC_{50} and ¼IC_{50} for each drug alone or a

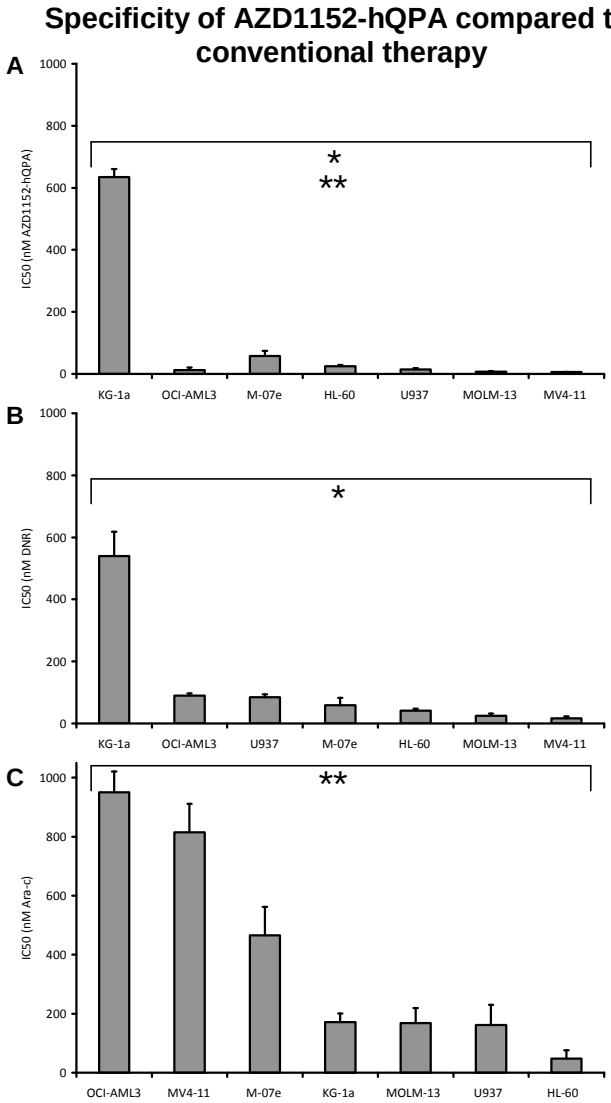

Figure 3.7 Flow cytometric IC_{50} values of leukaemic cell lines treated for 72 hours with AZD1152-hQPA (A) compared to DNR (B) or Ara-c (C) (*p<0.0001/**p=0.533, analyzed using Pearson's correlation). Columns, mean of three experiments; bars, SD.

combination of AZD1152-hQPA plus DNR or Ara-c (Figure $3.8_{(A) \text{ and } (B)}$) for 72 hours and resulting viability data fed into CalcuSyn software. CalcuSyn is a dose effect analyzes programme for single and multiple drugs (Chang, 2000). It quantifies the effects of drug combinations to determine whether they give greater effects together (synergism) than that expected from their individual effects. The programmeme automatically plots the data and produces reports of summary

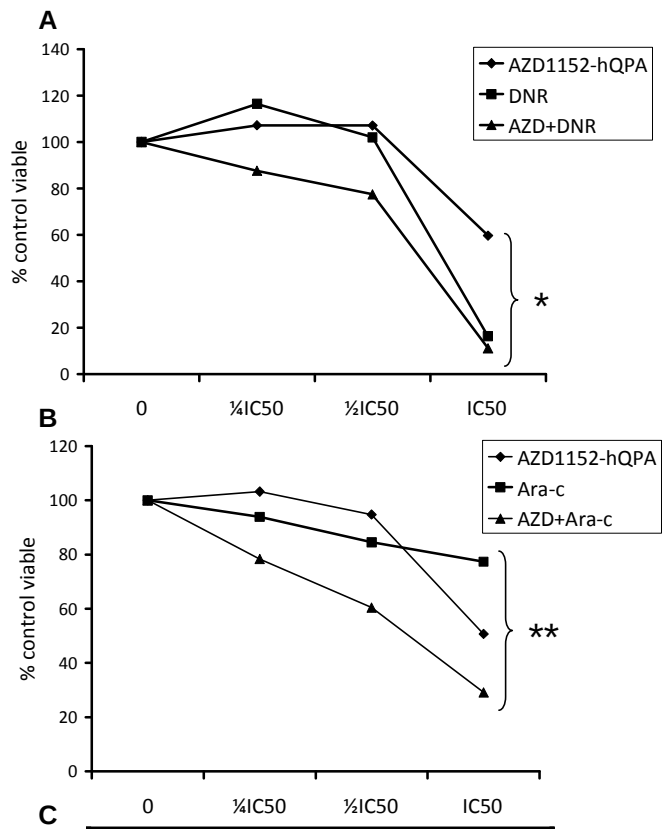

C

Range of CI	Description
<0.1	Very strong synergism
0.1-0.3	Strong synergism
0.3-0.7	Synergism **
0.7-0.85	Moderate synergism
0.85-0.9	Slight synergism
0.9-1.1	Nearly additive
1.1-1.2	Slight antagonism
1.2-1.45	Modrate antagonism *
1.45-3.3	Antagonism

Figure 3.8 Flow cytometric measurement of viable MOLM-13 cells after 72 hours exposure of AZD1152-hQPA, DNR or a combination of both (A) and AZD1152-hQPA, Ara-c or both (B). Lines, mean of three Experiments. CalcuSyn gives an IC_{50} CI value of 1.24 (*) and 0.55 (**). Combination index (CI) table (C).

statistics for all drugs and detailed analysis of drug interactions including the Combination Index (CI) (Figure $3.8_{(C)}$). CalcuSyn gave an IC_{50} CI value of 1.24 for the combination of AZD1152-hQPA and DNR which is in the "moderate

antagonism" range. However, an IC_{50} CI value of 0.55 was obtained for the combination of AZD1152-hQPA and Ara-c which is in the "synergism" range.

3.6 Mechanism of cell death following AZD1152-hQPA treatment

3.6.i Detection of apoptosis with the Annexin V-FITC assay

Apoptosis, or programmemed cell death, is an essential mechanism used by multi-cellular organisms to negatively select cells that are deemed deleterious to the host. Typical apoptosis is distinguished from necrosis as the former involves the activation of specific pathways that result in characteristic morphological features including DNA fragmentation, chromatin condensation and formation of apoptotic bodies. Many stimuli can trigger various pathways to apoptosis, but all these pathways converge to a common process involving the activation of a cascade of caspases that specifically cleave substrates at aspartic acid residues. One of the distinct cellular changes during apoptosis is the loss of phospholipid asymmetry, where during early apoptosis phosphatidylserine is translocated from the internal to the external portion of the cellular membrane.

Annexin V-FITC is a fluorescent probe which detects early apoptosis by binding to externalized phosphatidylserine in the presence of calcium using flow cytometry (Pepper *et al.*, 1998). Dual staining of cellular DNA with propidium iodide (PI) allows detection of cells where the membrane has been totally compromised. Cells which are early apoptotic will stain with the Annexin V-FITC alone. Live cells

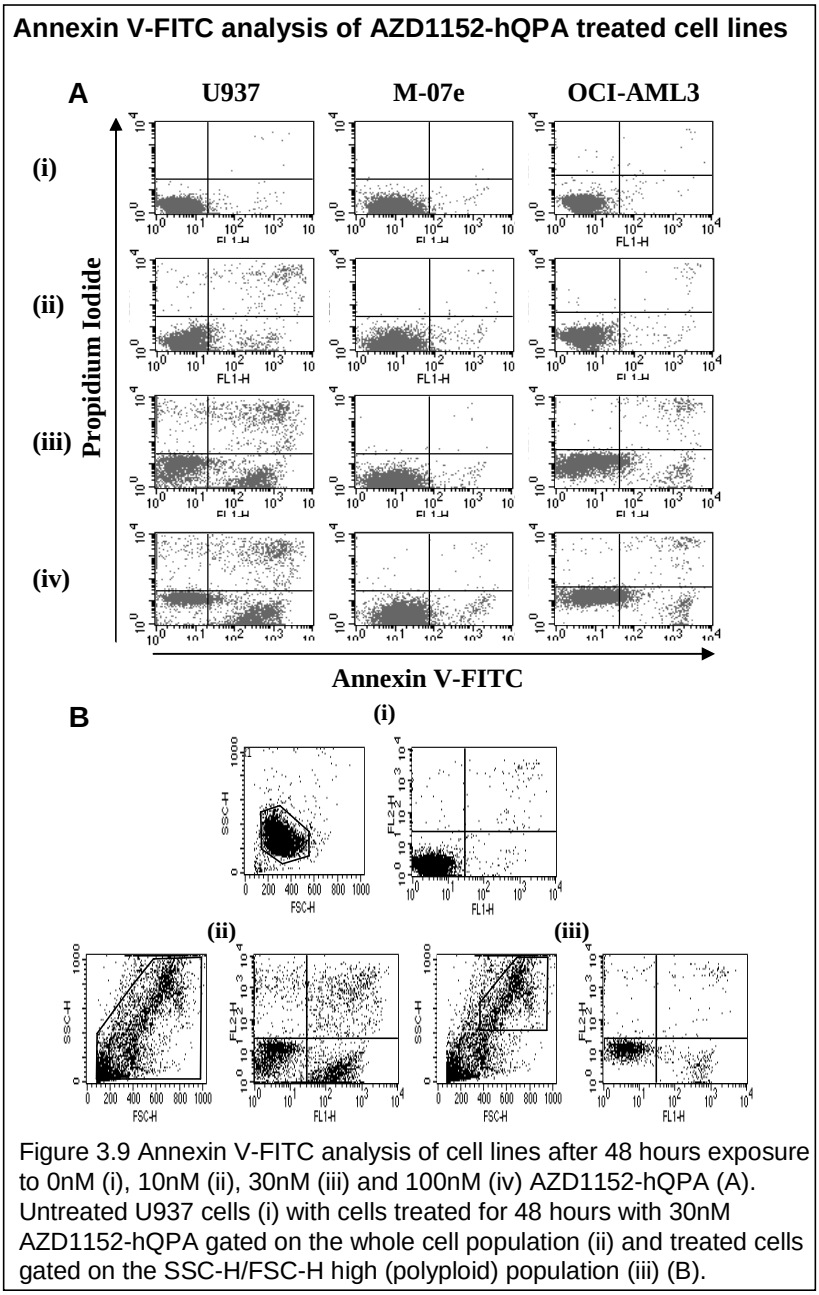

Figure 3.9 Annexin V-FITC analysis of cell lines after 48 hours exposure to 0nM (i), 10nM (ii), 30nM (iii) and 100nM (iv) AZD1152-hQPA (A). Untreated U937 cells (i) with cells treated for 48 hours with 30nM AZD1152-hQPA gated on the whole cell population (ii) and treated cells gated on the SSC-H/FSC-H high (polyploid) population (iii) (B).

show no staining with either Annexin V-FITC or PI while necrotic cells are stained by both Annexin V-FITC and PI. Annexin staining of AZD1152-hQPA treated cell lines demonstrates that cell death is by apoptosis (Figure 3.9A). The FSC-H/SSC-H histogram plot in Figure 3.9B is a measure of cell size (FSC-H) and granularity (SSC-H) and allows us to distinguish the polyploid (FSC-H/SSC-H high) population of cells. Gating on the treated cells whole population

(Figure3.9B$_{(ii)}$) demonstrates a clear apoptotic (FL1 high/FL2 low) and necrotic (FL1 high/FL2 high) population. By back-gating on the polyploid population (Figure 3.9B$_{(iii)}$) it can be seen that this population contains apoptotic cells. This agrees with previous findings that treatment with aurora-B inhibitors results in the accumulation of polyploid cells and subsequent apoptosis (Wilkinson *et al.*, 2007; Yang *et al.*, 2007).

3.6.ii Detection of apoptosis with active Caspase-3 and Apop2.7 (7A6) antibodies

Annexin staining of AZD1152-hQPA treated cells demonstrates that cell death is by apoptosis (Figure 3.9). To investigate this further two more markers of apoptosis were used, namely active caspase-3 and 7A6 antigen.

Caspase-3 is a key protease that is activated in the early stages of apoptosis (Belloc *et al.*, 2000). It is synthesized as an inactive pro-enzyme, and is mainly located in the cytoplasm of cells. During apoptosis, caspase-3 is cleaved and activated by upstream caspases, and is translocated into the nucleus to cleave its nuclear substrates, resulting in characteristic apoptotic nuclear changes such as DNA fragmentation, chromatin condensation and nuclear disruption (Belloc *et al.*, 2000).

7A6 is a 38 kDa mitochondrial membrane protein also expressed in early apoptosis which is recognized by the Apop2.7 antibody (Nagahara *et al.*, 2007). Active

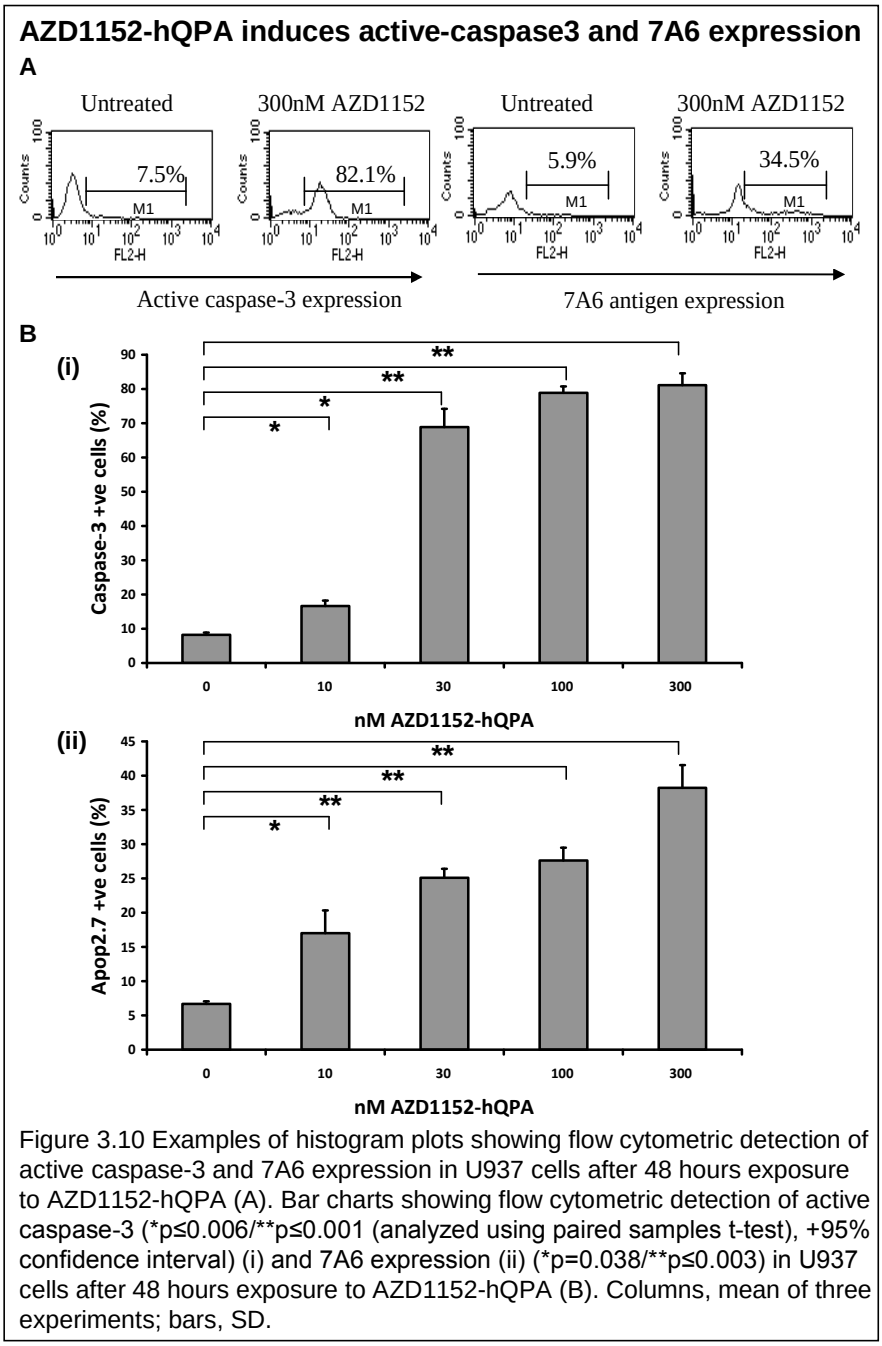

Figure 3.10 Examples of histogram plots showing flow cytometric detection of active caspase-3 and 7A6 expression in U937 cells after 48 hours exposure to AZD1152-hQPA (A). Bar charts showing flow cytometric detection of active caspase-3 (*p≤0.006/**p≤0.001 (analyzed using paired samples t-test), +95% confidence interval) (i) and 7A6 expression (ii) (*p=0.038/**p≤0.003) in U937 cells after 48 hours exposure to AZD1152-hQPA (B). Columns, mean of three experiments; bars, SD.

caspase-3 and 7A6 expression was measured by flow cytometry in U937 cells after 48 hours culture with 0-300nM AZD1152-hQPA (Figure 3.10A). Both apoptotic markers were increased in a dose dependent manner to AZD1152-hQPA ($p<0.05$ for all conditions when compared to untreated controls for both markers) (Figure

AZD1152-hQPA induces active-caspase3 from the polyploid population of cells

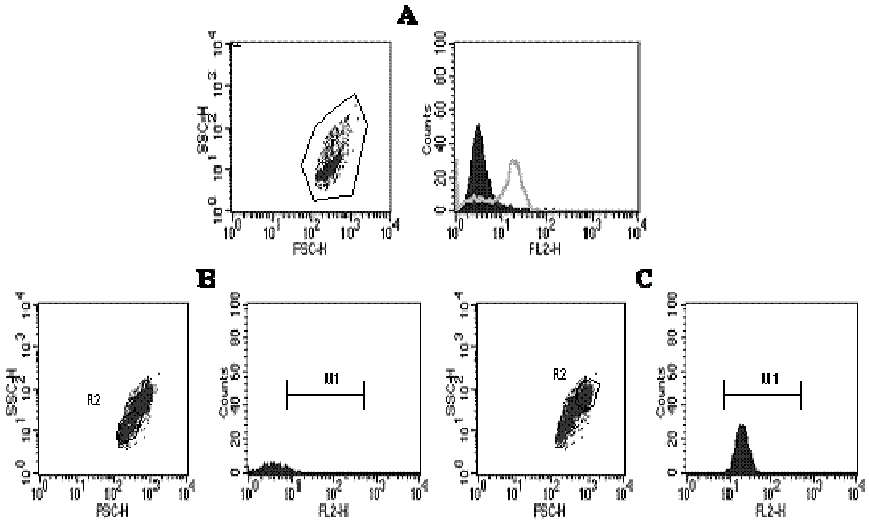

Figure 3.11 Flow cytometric detection of active Caspase-3 (FL2-H) in U937 cells after 48 hours culture (A). The solid line is the untreated control and the hollow grey line shows cells treated with 100nM AZD1152-hQPA. Plots B and C are cells treated with 100nM AZD1152-hQPA with plot B gated on FSC/SSC low cells and plot C gated on the FSC/SSC high (polyploid) cells.

3.10B). Back-gating on the polyploid population of cells showed that active caspase-3 is only expressed in this population (Figure 3.11). This again supports the argument that treatment with AZD1152-hQPA results in the accumulation of polyploid cells that subsequently apoptose.

3.6.iii H2A.X phosphorylation

In the eukaryotic nucleus, the genome is organized into chromatin. Two molecules each of the core histones (H2A, H2B, H3 and H4) form a single histone octamer, around which 146 base pairs of DNA are wrapped in repeating units, called nucleosomes, forming the basic subunit of chromatin (Kornberg, 1974). Nucleosomes wrap DNA into chromatin, allowing for the compaction and storage of genetic material. DNA accessibility is regulated via a complex set of post-

translational modifications of histones, which are of great importance to their function as governors of genome access, as they mediate rapid and reversible responses to changing cellular signals. Histones therefore play a central role in transcription regulation, DNA repair, DNA replication and chromosomal stability (Ismail, 2008). Agents that cause DNA damage and double-stranded DNA breaks (DSBs) include ionizing radiation, topoisomerase inhibitors, or DNA binding drugs. One of the principal responses to DSBs is the activation of the ATM-initiated signalling cascade to arrest cell division until repairs can be made. A major substrate of the kinases in this cascade is H2A.X which becomes phosphorylated on serine 139 and is subsequently termed γH2A.X (Rogakou *et al.*, 2000). These phosphorylation events are important for recruitment and maintenance of the DNA repair machinery to the site of the break. When the DNA damage is severe enough, the cell will undergo apoptosis, which involves processing of the genome into small fragments and creating more DSBs. Thus H2A.X phosphorylation at serine 139 can be used as an early marker for apoptosis.

Anti-phospho-H2A.X and 7-AAD staining was used to assess whether cells treated with AZD1152-hQPA undergo DNA double strand breaks, characteristic of early apoptosis, and at which point in the cell cycle these breaks occur. MOLM-13, OCI-AML3 and U937 cells treated with AZD1152-hQPA for 24 hours all express DNA double strand breaks shown by positive H2A.X staining (Figure 3.12). Furthermore, all the cell lines exhibit double strand breaks in pre-polyploid cells (R6 and R7 gates in H2A.X plots, Figure 3.12) as well as in cells with 8N DNA content (R8 gates in H2A.X plots, Figure 3.12).

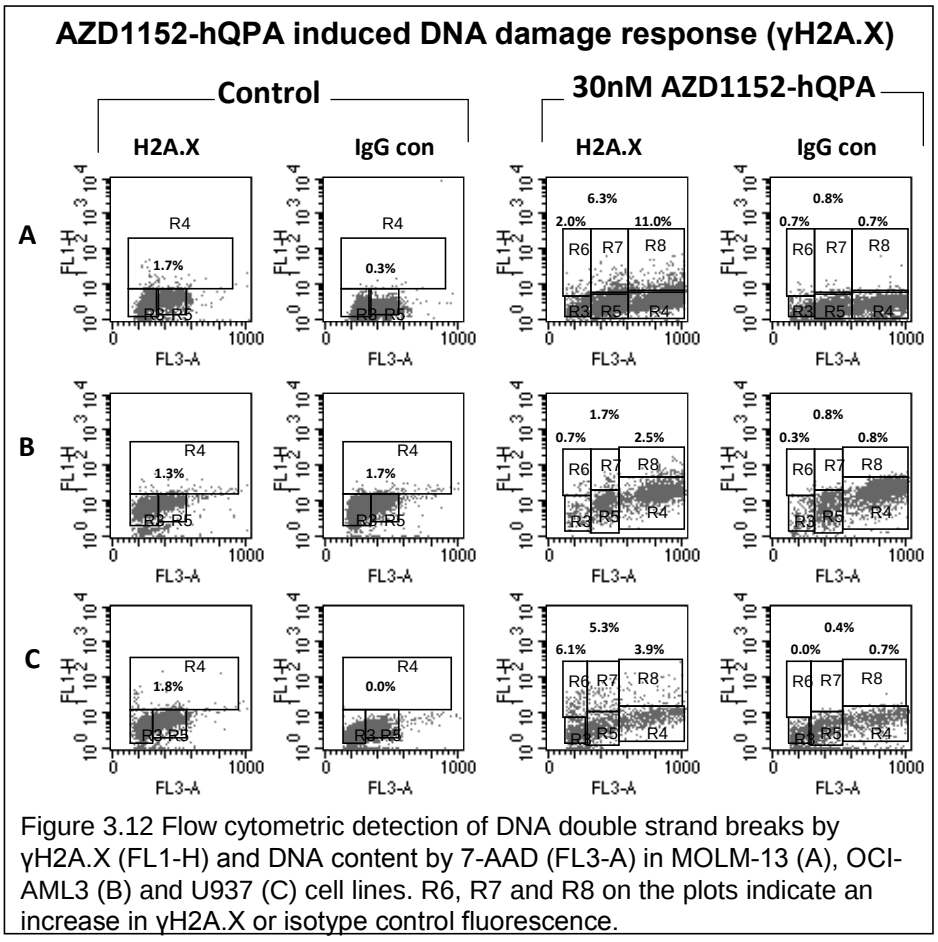

Figure 3.12 Flow cytometric detection of DNA double strand breaks by γH2A.X (FL1-H) and DNA content by 7-AAD (FL3-A) in MOLM-13 (A), OCI-AML3 (B) and U937 (C) cell lines. R6, R7 and R8 on the plots indicate an increase in γH2A.X or isotype control fluorescence.

AZD1152-hQPA therefore appears to induce a damage response in all phases of the cell cycle with the phase affected more dependent on variability between AML cell types than on drug.

3.7 Does cellular p53 status affect response to AZD1152-hQPA?

A research group has recently published data suggesting that p53 is critical for aurora-B kinase inhibitor mediated apoptosis in AML cells (Ikezoe *et al.*, 2009). Also, VX-680 is an aurora kinase inhibitor that is selective for aurora-A, B and C and has been shown to preferentially induce endoreduplication in cells with

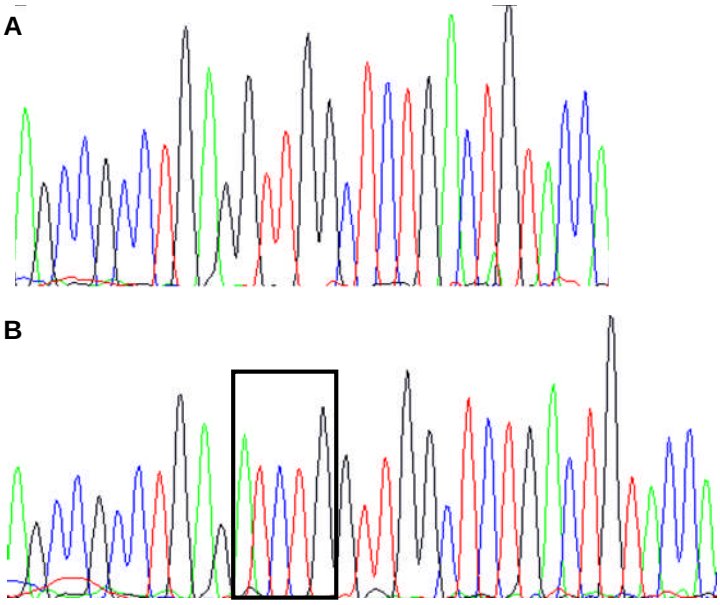

Figure 3.13 Example of a wild-type p53 sequence in OCI-AML3 (A) and a mutation in KG-1a (B) cell lines. The black box in B highlights a 5 base pair insertion (ATCTG) between codons 224 and 225 in the KG-1a cell line.

compromised p53 (Gizatullin *et al.*, 2006).

With this in mind it was decided to sequence our cell lines for p53 status (Figure 3.13 and Table 3.1). By measuring cellular DNA content, the effect of p53 status on the cell lines response to AZD1152-hQPA, was then investigated (Figure 3.14A). p53 compromised HL60 and U937 cells acquired 8N DNA 24 hours after AZD1152-hQPA treatment and continued DNA synthesis to a point where, at 48 hours, 8N peaks are not detected. The p53wt cell lines also acquire 8N at 24 hours at which point DNA synthesis appears to be partially checked because the 8N peaks remain visible for up to 72 hours. This seems to agree with results seen with VX-680 where differences in cellular DNA content after AZD1152-hQPA treatment depends on p53 status (Gizatullin *et al.*, 2006). However if we look at

Table 3.1 – Cell line p53 status.

CELL LINE	P53 STATUS
OCI-AML3	WT
MOLM-13	WT
MV4-11	WT
M-07e	WT
HL-60	Null
U937	Mut (46 bp deletion)
KG-1a	Mut (5 bp insertion)

the same AZD1152-hQPA treated p53wt MOLM-13, M-07e and OCI-AML3 cells and analyze by flow cytometry with decreased voltage in the FL-2 channel a further 16N peak can be detected (Figure 3.14B).

So although the p53wt cells are checked in comparison to p53 compromised cells, p53 is not saving them from massive endoreduplication and subsequent loss of viability. A 16N peak was not detected in the p53 compromised HL60 and U937 cells lines after decreasing the FL2 voltage (Figure 3.14B) indicating that these cells apoptose before reaching this ploidy. Also, by revisiting figure 3.12 with regard to cellular p53 status it should be noted that it is the p53 compromised U937 cells which display more DNA damage (6.1%) in the G_1/S phase of the cell cycle (R6 gate in H2A.X plots, Figure 3.12) when compared to the p53wt MV4-11 (2.0%) and OCI-AML3 (0.7%) cells.

AZD1152-hQPA induced endoreduplication is paused but not stopped in p53wt cell lines

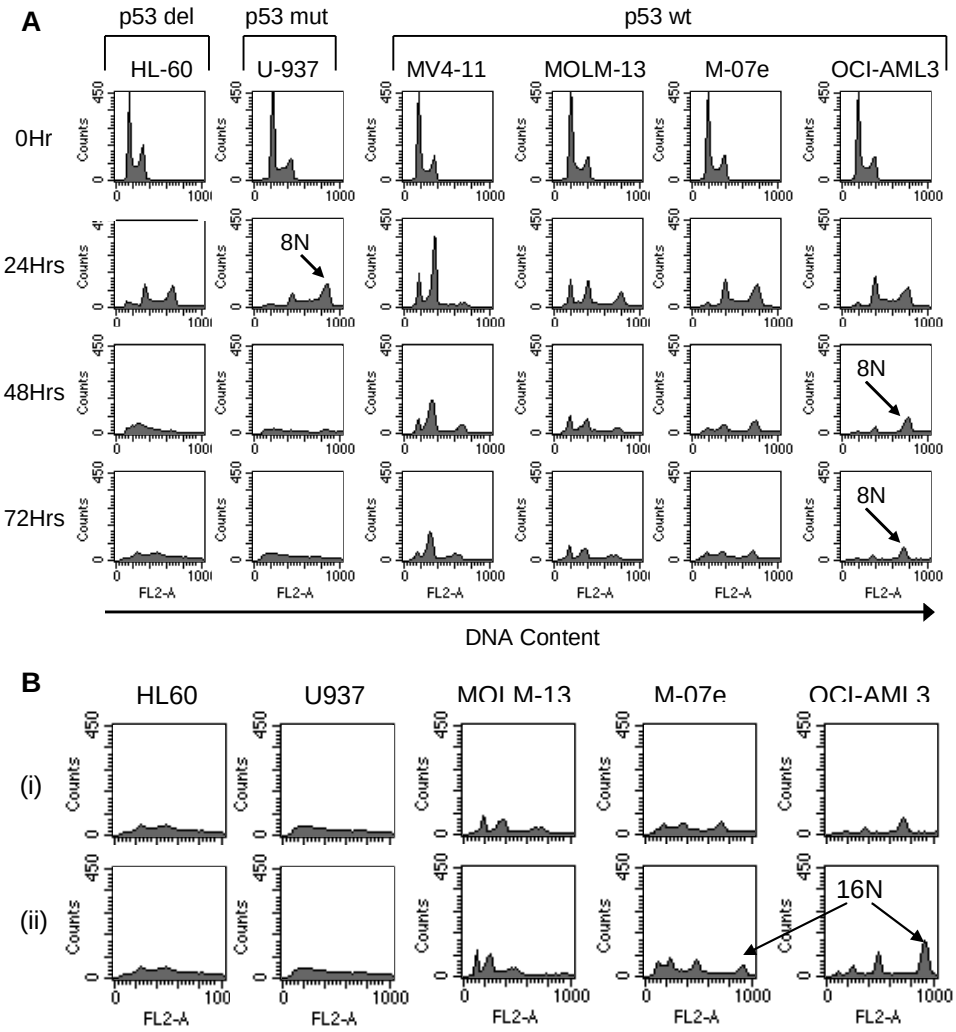

Figure 3.14 Flow cytometric DNA content histograms (measured using 7-AAD) after treatment with 30nM AZD1152-hQPA (A). Cell line DNA content after 72 hours treatment with 30nM AZD1152-hQPA (B). In plot B(ii), the cells were acquired at a lower voltage in the FL-2 channel, which allows us to see a further 16N peak in p53 wt cells compared with the plots in B(i).

Chapter Four GENERATION OF A PGP POSITIVE VARIANT OF THE OCI-AML3 CELL LINE

4.1 Background

The effects of AZD1152-hQPA were examined in logarithmically growing OCI-AML3, OCI-AML6.2, KG-1a, U937, M-07e, MOLM-13 and MV4-11 leukaemic cell lines. The ABCG2 transfected OCI-AML6.2 along with the Pgp expressing KG-1a cells, were the most resistant cell lines to both pHH3 inhibition and loss of viability (Figure 4.1). Elevated expressions of Pgp and BCRP have both been associated with poor prognosis and worse complete remission rates in AML (Leith *et al.*, 1997; Damiani *et al.*, 2007). Because of this it was decided to measure Pgp and BCRP transporter status in all of our cell lines and compare it to sensitivity to AZD1152-hQPA.

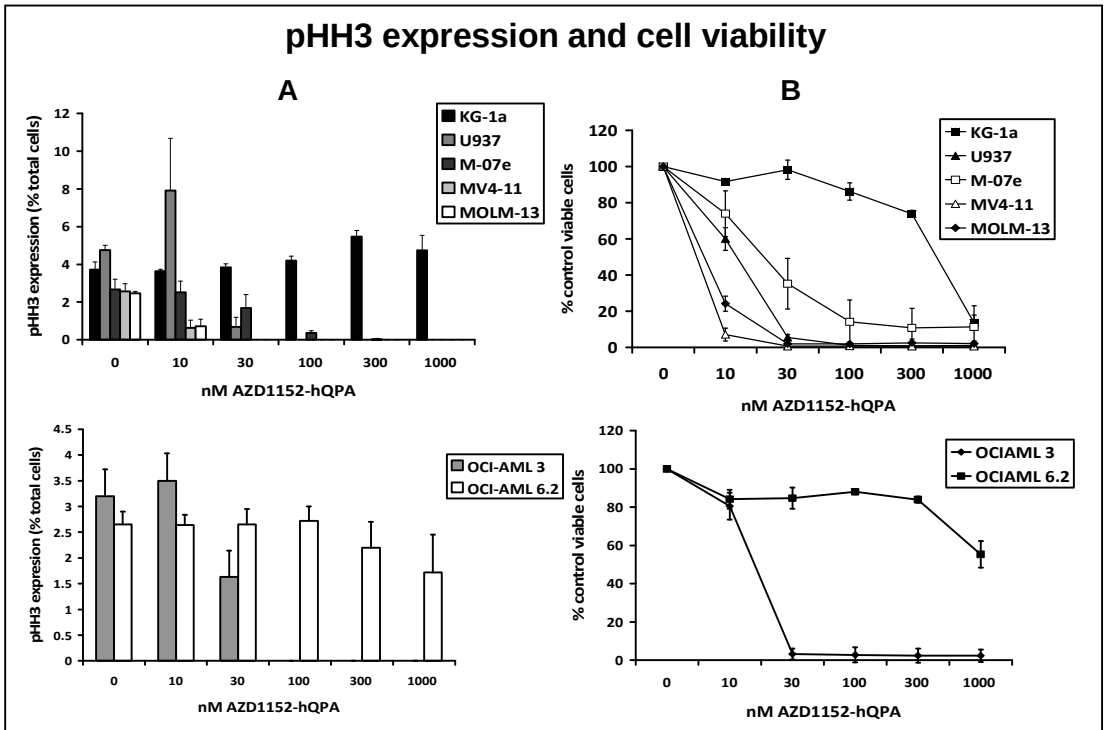

Figure 4.1 Flow cytometric measurement of pHH3 expression in AML cell lines after 24 hours of AZD1152-hQPA exposure (A) and flow cytometric measurement of viable cells after 72 hours of AZD1152-hQPA exposure (B). Columns/lines, mean of three experiments; bars, SD.

4.2 Cell line Pgp and BCRP transporter status

Functional Pgp was determined using R123 retention and the known Pgp modulator CSA as a positive control modulator (Pallis, 2005; Pallis *et al.*, 2005). The KG-1a cell line showed more than eleven times as much functional Pgp expression compared to the other cell lines (p=0.002) (Figure 4.2). Functional BCRP was measured using BODIPY retention and FTC as a modulator (Rabindran *et al.*, 2000). The OCI-AML6.2 cell line was the only one to show any functional BCRP activity; more than six times that of their parent OCI-AML3 cells (p=0.015) (Figure 4.2). High KG-1a Pgp levels (p=0.006) were also observed when Pgp protein was measured using the MRK-16 monoclonal antibody (Figure $4.3_{(A)}$). High BCRP expression in the OCI-AML6.2 cell line was confirmed using real-time PCR to measure ABCG2 message levels (Figure $4.3_{(B)}$). Clearly then, the

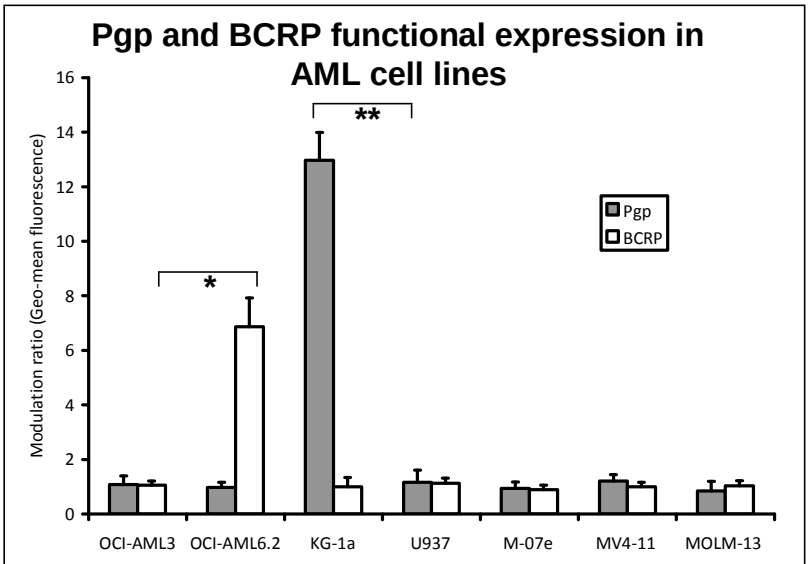

Figure 4.2 Flow cytometric measurement of Pgp and BCRP function in AML cell lines. Pgp function was measured using R123 accumulation and CSA as a positive control modulator. BCRP was measured similarly with BODIPY-prazosin accumulation and FTC as the modulator (*p=0.015/**p=0.002 (analyzed using paired samples t-test), +95% confidence interval).

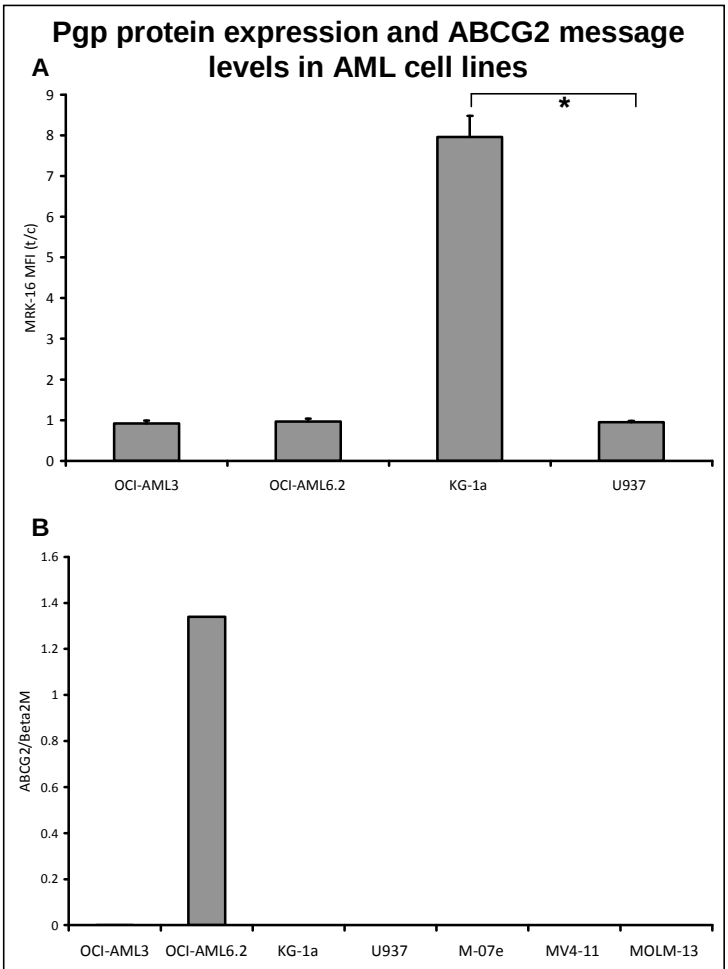

Figure 4.3 Pgp protein expression and ABCG2 message levels in AML cell lines. Pgp protein expression was determined flow cytometrically using the MRK-16 monoclonal antibody (*p=0.006 (analyzed using paired samples t-test), +95% confidence interval) (A). Columns, mean of three experiments; bars, SD. ABCG2 message levels were determined by real-time PCR (B).

only two cell lines which have elevated ABC transporter levels are the cell lines which are most resistant to AZD1152-hQPA, both at the level of the biomarker and cell viability.

An “isogenic” model for BCRP expression in our cell lines was available in our lab, with the stably transfected OCI-AML6.2, and the parent OCI-AML3 cells. To create a similar model for Pgp expression it was decided to stably transfect the

MDR1 gene, coding for Pgp, into the OCI-AML3 cell line. It has been reported that leukaemia and lymphoma cells are resistant to most non-viral gene transfer methods (Schakowski *et al.*, 2004). A novel electroporation based technique called nucleofection has recently become available. This technique uses a combination of special electrical parameters and cell type specific solutions to deliver the DNA directly to the cell nucleus under mild conditions thus giving high efficiency and low cell death rates (Schakowski *et al.*, 2004).

4.3 Stable transfection of MDR1 into the OCI-AML3 cell line

4.3.i Optimization of cell viability and GFP expression

Initially the nucleofection protocol needed to be optimized for the OCI-AML3 cell line. Logarithmically growing OCI-AML3 cells cultured for one week without penicillin/streptomycin and with low passage number were used for transfection experiments. Nucleofector solution was prepared by mixing nucleofector supplement and nucleofector solution T (Amaxa Biosystems, Cologne, Germany) (1:4.5). Cells were then counted, centrifuged for 10 minutes and re-suspended in 100µl pre-warmed nucleofector solution before addition of 2µg of pmaxGFP (green fluorescent protein) in a 2mm nucleofection cuvette (Amaxa) and nucleofection using programme X-001. Use of solution T and programme X-001 was recommended by Amaxa Biosystems for optimal transfection efficiency and viability in OCI-AML3 cells. Immediately after nucleofection, 500µl of pre-warmed RPMI containing 10% FCS was added to the nucleofection mixture, and the cells were transferred to six-well plates containing RPMI supplemented with

Table 4.1 – OCI-AML3 nucleofection conditions.

CELL CONC	SOL. T	GFP	PROGRAMME	GFP (% GATED)	VIABILITY (%)
$1x10^6$	-	-	-	0.75	99.34
$1x10^6$	+	+	-	0.94	99.3
$1x10^6$	+	-	X-001	2.59	78.06
$1x10^6$	+	+	X-001	**60.4**	**70.4**
$2x10^6$	+	+	X-001	56.2	69.7
$3x10^6$	+	+	X-001	54.2	68.4
$4x10^6$	+	+	X-001	57.8	70.2
$5x10^6$	+	+	X-001	53.2	67.1

10% FCS and 2mM L-glutamine. Cells were cultured for 24 hours, harvested and counted, before addition of 50µg/ml 7-AAD for 15 minutes. Cell viability and GFP expression (a measure of transfection efficiency) were determined flow cytometrically. Controls consisted of cells alone and cells processed through the nucleofection procedure +/- DNA or +/- programme X-001 (Table 4.1). A cell concentration of $1x10^6$ was deemed to be optimal giving a transfection efficiency of 60.4% and a viability of 70.4%.

4.3.ii Expression vector for MDR1

The pCMV6-Neo vector contains a cytomegalovirus (CMV) immediate-early promoter sequence (suitable for protein over-expression), a simian virus (SV)-40 and colicin E1 (ColE1) replication site and genes for neomycin and ampicillin

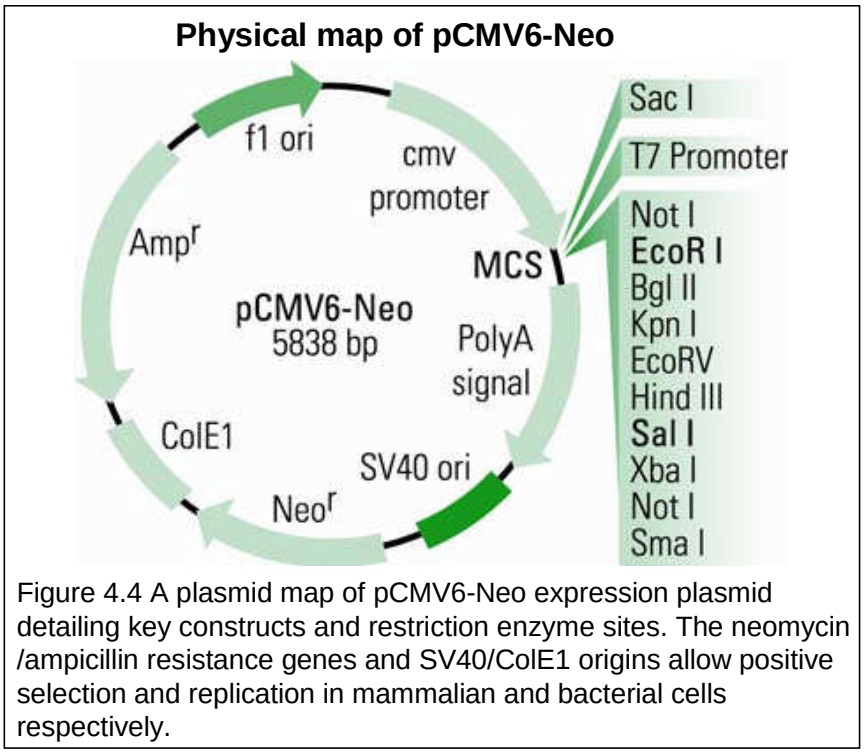

Figure 4.4 A plasmid map of pCMV6-Neo expression plasmid detailing key constructs and restriction enzyme sites. The neomycin /ampicillin resistance genes and SV40/ColE1 origins allow positive selection and replication in mammalian and bacterial cells respectively.

resistance along with restriction sites for subcloning genes of interest (Figure 4.4). Neomycin is a natural product that binds to ribosomal subunits inhibiting protein synthesis and elongation resulting in cell death. G418 is a synthetic analogue that mimics this inhibition, but whose action on mammalian cells is blocked by the presence of the neomycin resistance gene product. Culturing transfected cells in the presence of G418 effectively permits only those containing the pCMV6-Neo gene construct to survive. Continued growth under antibiotic pressure allows clonal selection of stable cell lines perpetually over-expressing the protein of interest at 100% transfection efficiency. The MDR1 gene cloned into the pCMV6-Neo vector (RSPD001-Neo) was supplied by Origene.

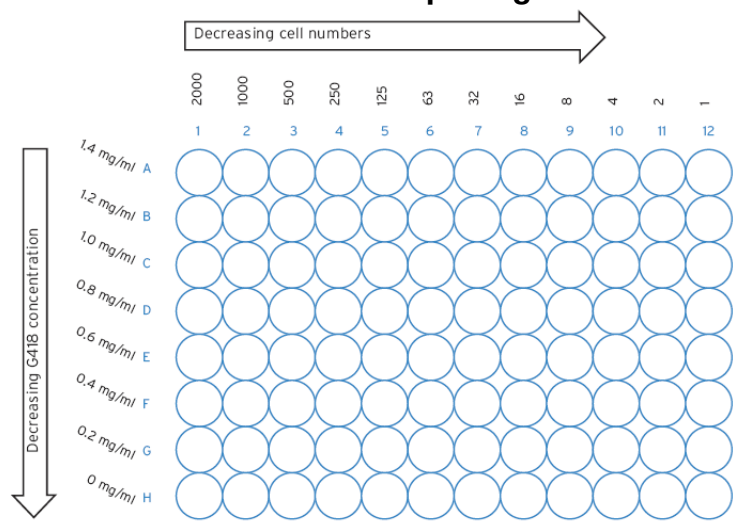

Figure 4.5 Plate set up for limiting dilution assay to determination G418 and plating concentrations for OCI-AML3 cells.

4.3.iii Limiting dilution of cells and G418 dosing

Optimization of the G418 concentration with the OCI-AML3 cell line was first established before attempting positive selection. A limiting dilution procedure to assess whether OCI-AML3 cells were able to produce colonies from isolated cells also needed to be performed as some cell lines only grow if they have contact with one another. Logarithmically growing OCI-AML3 cells cultured for one week without penicillin/streptomycin and with low passage number were counted and re-suspended in RPMI supplemented with 10% FCS and 2mM L-glutamine at a concentration of $4x10^4$/ml. 100µl media was added to each well of a 96wp followed by 100µl cell suspension to the first column of the well. After mixing, 100µl was carried over to the next and subsequent columns, discarding 100µl from the last column. 100µl G418 containing media at 2.8mg/ml was then added to row A followed by decreasing concentrations in the subsequent rows (Figure 4.5). After 10 days cell growth was observed in wells without G418 and initially less

than 4 cells so it was assumed that the OCI-AML3 cells could grow from isolation. Complete cell death measured by trypan blue exclusion was observed in row F (0.4mg/ml G418) after 10 days culture so a concentration of 0.6mg/ml G418 was chosen for later positive selection experiments.

4.3.iv Preparation of control plasmid

To create a negative control for our nucleofection assays a plasmid without the MDR1 gene insert needed to be prepared. To amplify stocks RSPD001-Neo was transformed into ElectroTen-Blue electroporation competent bacteria as described in the methods. Initially, the DNA plasmids were prepared using the Promega PureYield plasmid miniprep and midiprep systems (Promega, Southampton, UK). However, although DNA was obtained with these systems, when the NotI digestions were run (as described later) we did not see the expected bands. We thought the problem could be the amount of residual ethanol that was consistently left-over in the binding column after processing with the Promega midiprep system and that this was interfering with the digest. Because of this it was decided to switch to Qiagen plasmid mini and midi kits (Qiagen) for plasmid preparation.

Prior to ligation and bacterial transformation, the DNA was digested using a sequence-specific restriction enzyme. The object of the digestion was to cut out the MDR1 insert from the RSPD001-Neo plasmid to produce pCMV6-Neo DNA molecules with compatible ends for ligation. RSPD001-Neo plasmid was digested

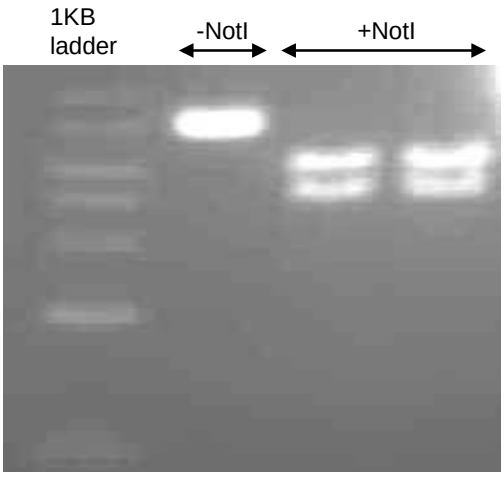

Figure 4.6 An agarose gel image of RSPD001-Neo NotI digestion. The larger (5838bp) pCMV6-Neo plasmid can be distinguished from the smaller (4700bp) MDR1 plasmid. A reaction without NotI was included as a digestion control.

using NotI restriction enzyme. Two bands (at 4700bp and 5838bp) of the correct size were present in the RSPD001-Neo digest (Figure 4.6) and the larger band was then gel purified as described in the methods. Following ligation, the pCMV6-Neo vector was then transformed into ElectroTen-Blue electroporation competent bacteria as previously described to amplify stocks. The ligation reactions were added to the bacteria and two different concentrations of each transformation were plated onto agar in an attempt to obtain colonies. A control transformation containing pUC18 was included to act as an electroporation control. Two bacterial colonies were selected from each agar plate and grown up overnight. DNA plasmids were prepared using the Qiagen plasmid miniprep kit and NotI digestions performed as previously described before running on a 0.7% agarose gel. Two bands (at 4700bp and 5838bp) were present in the RSPD001-Neo digest and just one band (at 5838bp) in the pCMV6-Neo digest (Figure 4.7). 500µl of RSPD001-Neo and pCMV6-Neo cultures were then taken to 19.5ml LB+AMP and grown up

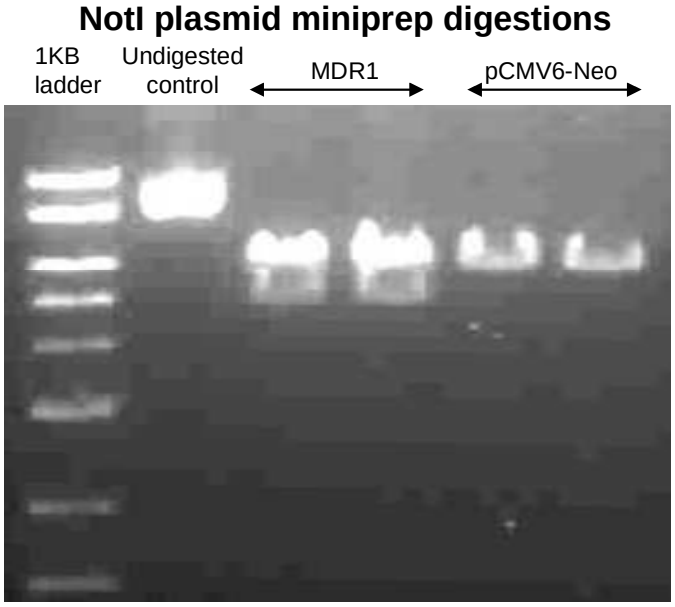

Figure 4.7 An agarose gel image of RSPD001-Neo (MDR1) and pCMV6-Neo NotI midiprep digestions. A digestion without NotI was included as an enzyme control.

overnight at 37ºC. Cultures were then centrifuged at 6,000g for 10 minutes and re-suspended in 1ml 15% glycerol in LB before storage at -80°C. To amplify DNA for transfection a small amount of each glycerol stock was transferred in to 10ml LB+AMP and incubated overnight. Plasmids were prepared with Qiagen plasmid midiprep kits as previously described before digestion and running on a 0.7%agarose gel to confirm bands.

Sequencing reactions were electrophoresed using an ABI 3130 Genetic Analyzer and results analyzed using the Sequencing Analysis 5.2 software as described in the methods. The MDR1 and control pCMV6-Neo sequences matched those in the literature and the control vector did not contain the MDR1 insert (NCBI Reference Sequence: NM_000927.4 and www.origene.com).

4.3.v Nucleofection and phenotyping for Pgp expression

Logarithmically growing OCI-AML3 cells cultured for one week without penicillin/streptomycin and with low passage number were used for transfection experiments. Nucleofector solution was prepared as previously described and $1x10^6$ cells were then counted, centrifuged for 10 minutes, and re-suspended in 100µl pre-warmed nucleofector solution before addition of either 2µg MDR1 (RSPD001-Neo) or pCMV6-Neo in a 2mm electroporation cuvette and electroporation using programme X-001. A nucleofection control condition was included with no DNA. Immediately after electroporation, 500µl of pre-warmed RPMI containing 10% FCS was added to the electroporation mixture, and the cells were transferred to six-well plates containing RPMI supplemented with 10% FCS and 2mM L-glutamine. Six hours post nucleofection an additional 1ml of growth medium was added to each well to avoid overcrowding of cells. Cells were then allowed to express the protein for G418 resistance under non-selective conditions for 48 hours before being transferred to $25cm^2$ culture flasks and the addition of 0.6mg/ml G418. Cells were incubated for 72 hours, counted by trypan blue exclusion, and plated out in three 96wps per condition at $4x10^4$/ml. After 9 days cells were fed with fresh growth medium containing 0.6mg/ml G418. At day 16 cellular outgrowths were seen in the RSPD001-Neo and pCMV6-Neo plates whilst all of the control cells were dead. Cells were then expanded further before another round of serial dilution (as previously described) under G418 selection to assure that cell populations represented clones from a single cell. After further expansion, 13 RSPD001-Neo clones were present, where outgrowth appeared to be from a

Table 4.2 – Pgp protein expression and function in RSPD001-Neo and pCMV6-Neo clones.

CLONE/CELL LINE	MRK-16 MFI (T/C)	R123 MODULATION RATIO
RSPD001-Neo (1)	1.01	0.97
RSPD001-Neo (2)	1.0	-
RSPD001-Neo (3)	1.02	1.01
RSPD001-Neo (4)	1.03	1.02
RSPD001-Neo (5)	1.06	0.97
RSPD001-Neo (6)	0.96	-
RSPD001-Neo (7)	1.03	1.06
RSPD001-Neo (8)	1.03	1.04
RSPD001-Neo (9)	0.98	-
RSPD001-Neo (10)	0.99	-
RSPD001-Neo (11)	0.98	-
RSPD001-Neo (12)	0.97	-
RSPD001-Neo (13)	0.96	0.95
KG-1a	6.65	14.99
OCI-AML3	0.97	0.91
pCMV6-Neo	0.94	0.98

single cell. Pgp protein expression was measured in all 13 clones using the MRK-16 monoclonal antibody with KG-1a and OCI-AML3 cells included for positive and negative controls along with the pCMV6-Neo clone (Table 4.2). Pgp function was determined by modulation of R123 efflux by the Pgp modulator PSC833 in 7 of the clones (Table 4.2). Pgp protein level was recorded as positive when the MRK-16 test/control value was ≥1.1 (based on data gathered during the AML14

and AML15 trials carried out in our lab). Pgp was recorded as functional when the PSC833/R123 modulation ratio was ≥1.7 based on a previous study (Pallis *et al.*, 1999b). None of the G418 resistant RSPD001-Neo clones were positive for Pgp expression or function.

4.4 Selection of Daunorubicin resistant OCI-AML3 cells

Because the RSPD001-Neo clones failed to show any increase in Pgp it was decided to try and select for Pgp expression in the OCI-AML3 cell line using the known Pgp substrate DNR (Legrand *et al.*, 1999; Borg *et al.*, 2000) and a method adapted from (Randle *et al.*, 2007). OCI-AML3 cells were initially exposed to DNR at a concentration of 10nM, which represented the IC_{50} concentration. Cells were seeded at $5x10^5$/ml in 50ml of complete medium containing 10nM DNR. At days 3, 10 and 14, 50ml of fresh culture medium without DNR was added. At day 18 cells were pelleted and re-suspended in 160ml medium containing 10nM DNR. From day 26 to day 35 the DNR containing medium was changed once per week. At day 35 there were very few remaining viable cells, so cells were separated over histopaque to exclude dead cells and cell debris. The remaining cells were re-suspended in 10ml of medium containing 10nM DNR up until day 45 when cell growth was seen. Cells were maintained at this drug concentration until their growth rate approached that of untreated OCI-AML3 cells.

Over the next 10 weeks cells were exposed to gradually increasing concentrations of DNR up to a final concentration of 15nM. By using the R123 accumulation

assay these cells were confirmed to have increased levels of Pgp function and were subsequently cloned by limiting dilution. Cells were serially diluted in 96 well plates down to a concentration of 1 cell/well in medium containing 15nM DNR. Any cells showing outgrowth were then gradually cultured in medium containing 15nM DNR up to sufficient numbers to be able to assay for Pgp protein and function. One clone, which was named OCI-AML3DNR, showed an increase in both Pgp expression and function. These cells were then cryo-preserved for future use.

4.4.i OCI-AML3/OCI-AML3DNR genetic analysis

DNA was prepared using a QIAamp DNA blood mini kit (Qiagen, Crawley, UK) and 5ng DNA was amplified using the Powerplex 16 System (Promega, Southampton, UK) to assess short tandem repeats (STR). The products were run on a 3130 Genetic Analyzer and the data analyzed using GeneMapper ID v3.2 software. The STR analysis of the OCI-AML3DNR cell line was shown to be identical to the parent OCI-AML3 cell line indicating that there were no significant genetic changes.

4.4.ii OCI-AML3 DNR cell line validation using monoclonal antibodies and FLT3 analysis

Continued testing to authenticate the OCI-AML3DNR cell line was performed using a panel of monoclonal antibodies and FLT3 mutational analysis towards the final passage of each batch thawed. CD38 FITC, CD33 PE, CD34 Percp (BD

Table 4.3 – OCI-AML3 cell line family: phenotype and FLT3 status.

Cell line	CD13	CD33	CD38	CD34	CD42	FLT3
OCI-AML3	Positive	Positive	Positive	Negative	Negative	WT
OCI-AML6.2	Positive	Positive	Positive	Negative	Negative	WT
OCI-AML3DNR	Positive	Positive	Positive	Negative	Negative	WT

Biosciences), CD13 FITC (Dako) and CD42 PE (Pharmingen) mouse monoclonal antibodies along with their isotype control were used to validate the cell lines phenotype. $2x10^5$ cells were incubated with 2.5µl normal mouse serum and 2.5µl monoclonal antibody or the isotype control followed by washing in PBSAA and analysis by flow cytometry. Cell line FLT3-ITD status was confirmed using the protocol described in 2.16. The phenotype and FLT3 status of the OCI-AML3DNR cell line is consistent with that of the parent OCI-AML3 and OCI-AML6.2 cell lines as shown in table 4.3.

4.5 ABC transporter status of the OCI-AML3DNR cell line

Experiments were carried out on logarithmically growing OCI-AML3DNR cells cultured with 15nM DNR until seven days before the assay. Pgp expression was determined by modulation of R123 efflux by PSC833. Functional BCRP was measured using BODIPY-prazosin retention and the BCRP modulator FTC (Rabindran *et al.*, 2000). A six fold increase in Pgp functional activity (p=0.039) was seen in the OCI-AML3DNR cells compared to the OCI-AML3 parent cell line (Figure $4.8_{(A)}$). No increase in BCRP function was seen in the OCI-AML3DNR

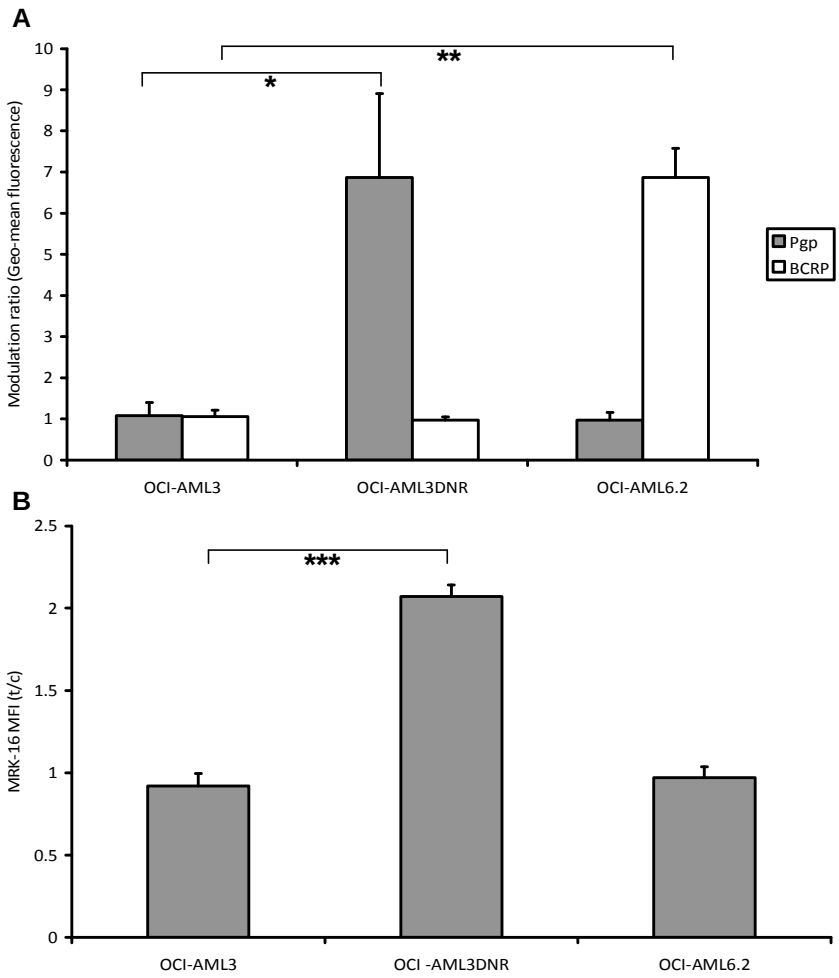

Figure 4.8 Pgp function was measured using R123 accumulation and PSC833 as a positive control modulator. BCRP was measured similarly with BODIPY-prazosin accumulation and FTC as the modulator (*p=0.039/**p=0.015 (analyzed using paired samples t-test), +95% confidence interval) (A). Pgp protein expression was determined using the MRK-16 monoclonal antibody (***p=0.003) (B). Columns, mean of three experiments; bars, SD.

cells (Figure $4.8_{(A)}$). More than twice as much Pgp protein (p=0.003) was observed in the OCI-AMLDNR cells compared to the OCI-AML3 cells (Figure $4.8_{(B)}$).

MRP1 has been associated with efflux and in vitro resistance to DNR in AML cells (Legrand *et al.*, 1999; Borg *et al.*, 2000). To determine whether MRP1 expression had also been elevated in our DNR selected cell line a calcein-AM

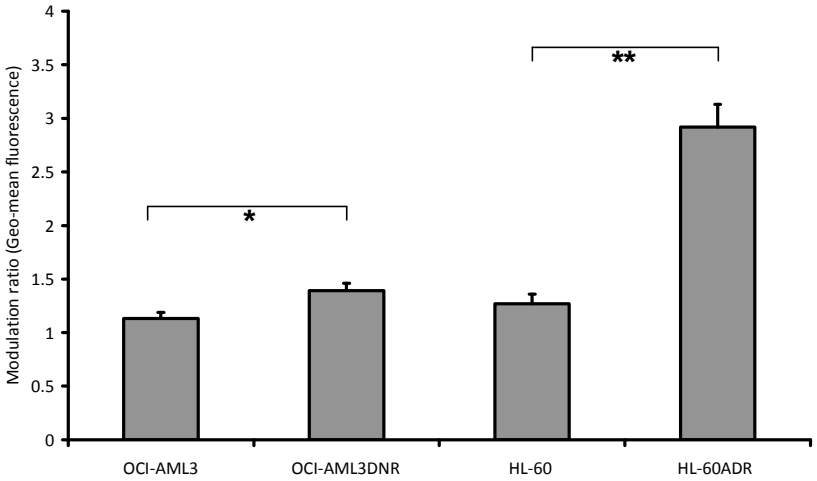

Functional MRP1 expression measured using Calcein-AM accumulation and MK-571 as a modulator (*p=0.358/**p=0.004 (analyzed using paired samples t-test), +95% confidence interval). Columns, mean of three experiments; bars, SD.

retention assay was used with the MRP1 modulator MK-571 (Gekeler *et al.*, 1995; Dogan *et al.*, 2004) and MRP function was compared to the adriamycin selected, MRP1 positive, HL-60ADR cell line (Krishnamachary *et al.*, 1994) (Figure 4.9). No significant increase in MRP1 function was detected in the OCI-AML3DNR cells (p=0.358) in contrast to that seen in the HL-60ADR cells (p=0.004) whencompared to the parent cell lines.

Chapter Five EFFECT OF ATP-BINDING CASSETTE TRANSPORTERS ON AZD1152-hQPA SENSITIVITY

5.1 Background

We have previously shown that the ABCG2 transfected OCI-AML6.2 along with the Pgp expressing KG-1a cells, were the most resistant cell lines to both pHH3 inhibition and loss of viability (Figure 4.1). By selecting the OCI-AML3 cell line for resistance to DNR, a cell line which expressed elevated Pgp protein and function was created, with no increase in BCRP or MRP expression (Figure 4.7 and 4.8). We now had two cell lines, OCI-AML3DNR and OCI-AML6.2, with respective elevated Pgp and BCRP levels compared to the parent OCI-AML3 cells. We intended to investigate the effect of ABC transporter status on the specificity of AZD1152-hQPA in these cell lines.

5.2 Specificity of AZD1152-hQPA in OCI-AML3DNR cells

Initially, it was decided to measure the specificity of AZD1152-hQPA in our new model for elevated Pgp expression, the OCI-AML3DNR cell line. The OCI-AML3DNR cells were much more resistant to pHH3 inhibition by AZD1152-hQPA compared to the OCI-AML3 parent cell line, with no inhibition at 1000nM AZD1152-hQPA (Figure 5.1). The OCI-AML3DNR cell line was also much more resistant to seventy-two hour AZD1152-hQPA induced loss of viability compared to the parent cell line (Figure 5.1). There was a significant ($p=0.001$) loss of viability at 30nM AZD1152-hQPA in the OCI-AML3 cells whilst there was only significant ($p=0.011$) loss of viability at 1000nM in the OCI-AML3DNR cells.

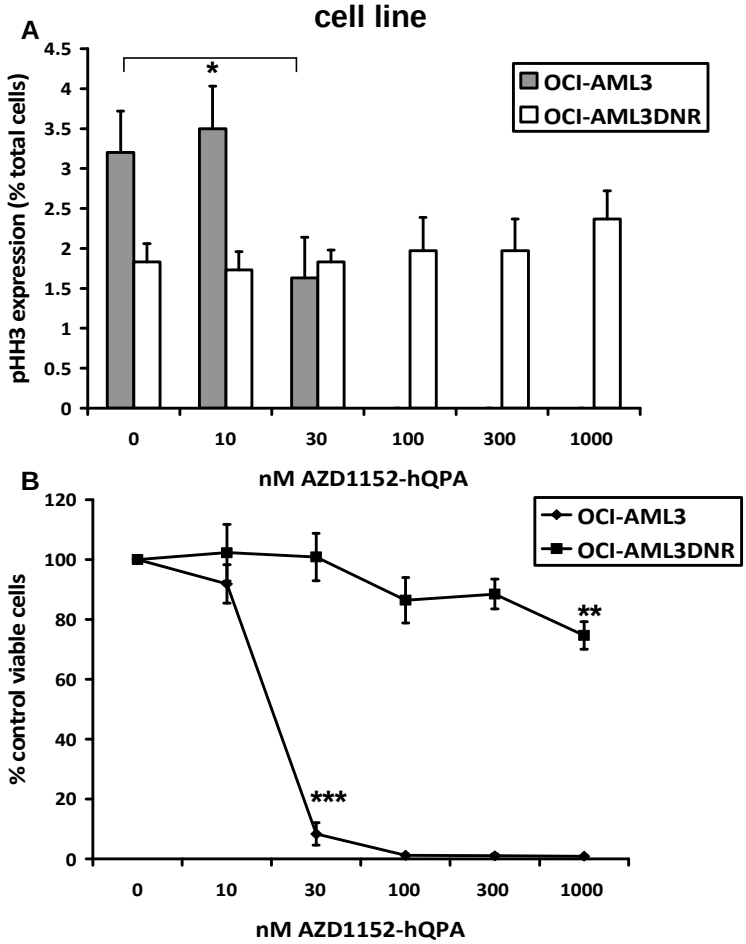

Figure 5.1 Flow cytometric measurement of pHH3 expression in AML cell lines after 24 hours AZD1152-hQPA exposure (A) (*p=0.003 (analyzed using paired samples t-test), +95% confidence interval) and flow cytometric measurement of viable cells after 72 hours AZD1152-hQPA exposure (**p=0.011/***p=0.001) (B). Columns/lines, mean of three experiments; bars, SD.

5.3 Is AZD1152-hQPA a substrate or modulator of drug efflux molecules in AML cells?

5.3.i UIC2 shift assay

An indirect way of measuring unlabelled Pgp substrates has recently become available due to the development of the UIC2 shift assay (Park *et al.*, 2003). The

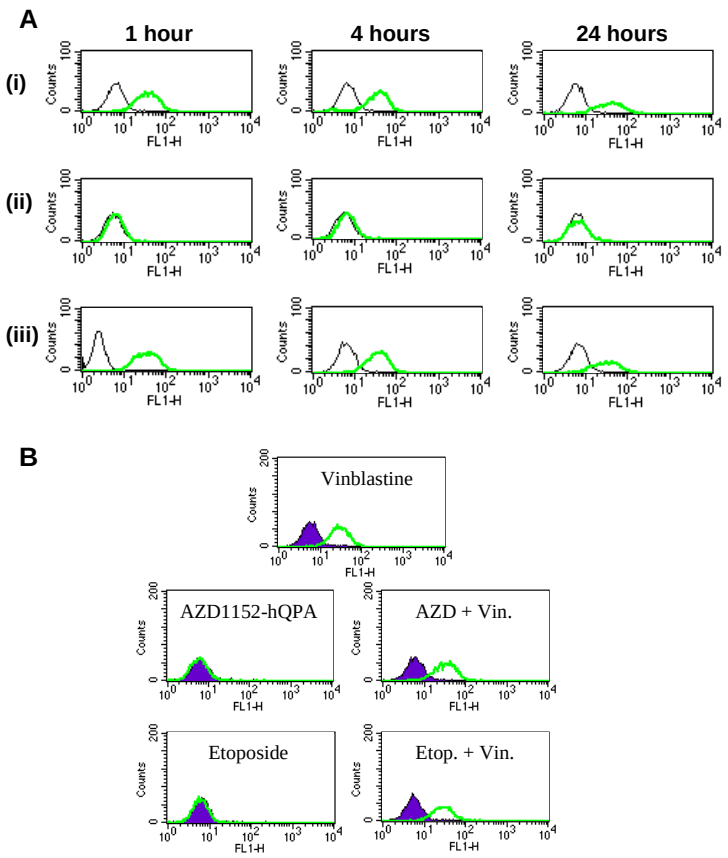

Figure 5.2 Flow cytometric histogram plots showing UIC2 binding in KG-1a cells in the presence or absence of 5µM vinblastine (i), 1µM AZD1152-hQPA (ii) or both (iii) (A). UIC2 binding in KG-1a cells in the presence of vinblastine, AZD1152-hQPA or 10µg/ml etoposide. The dark line is the diluent control and the green line indicates any shift. Plots are representative of a single experiment which was done in triplicate.

reactivity of the UIC2 antibody with Pgp is increased by the addition of Pgp transported compounds. AZD1152-hQPA was tested in the UIC2 shift assay using the Pgp positive KG-1a cell line and the known Pgp substrate vinblastine (Park *et al.*, 2003) as a positive control (Figure 5.2A). No shift in UIC2 binding was seen with AZD1152-hQPA treatment up to 24 hours. Also, co-incubation of AZD1152-hQPA and vinblastine failed to affect any shift seen with vinblastine alone.

This assay failed to show that AZD1152-hQPA is a Pgp substrate. However it did not prove the converse as a few Pgp substrates such as etoposide fail to alter UIC2 binding depending on their stoichiometry and Pgp ATPase activity (Mechetner *et al.*, 1997). This is demonstrated in figure 5.2B which shows that AZD1152-hQPA and etoposide both fail to produce a shift in UIC2 binding and that both fail to affect any shift seen with vinblastine alone.

5.3.ii Rhodamine 123 and Bodipy-prazosin accumulation assays

An additional possibility is that AZD1152-hQPA can modulate Pgp function without itself being a substrate. To determine whether AZD1152-hQPA is able to modulate Pgp or BCRP function it was compared to known modulators using fluorescent dye retention assays. AZD1152-hQPA had no effect on R123 retention in the Pgp positive OCI-AML3DNR cell line (Figure $5.3A_{(i)}$) in contrast to the marked increase in retention seen with CSA (Figure $5.3A_{(ii)}$). Likewise AZD1152-hQPA had no effect on BODIPY retention in the BCRP positive OCI-AML6.2 cell line (Figure $5.3B_{(i)}$) in contrast to the increase in retention seen with FTC (Figure $5.3B_{(ii)}$). In these assays AZD1152-hQPA did not appear to be a modulator of Pgp or BCRP function.

5.3.iii Radio-labelled drug accumulation assay

To categorically determine if AZD1152-hQPA was being effluxed by Pgp and BCRP, radio-labelled AZD1152-hQPA was used to measure the cellular retention

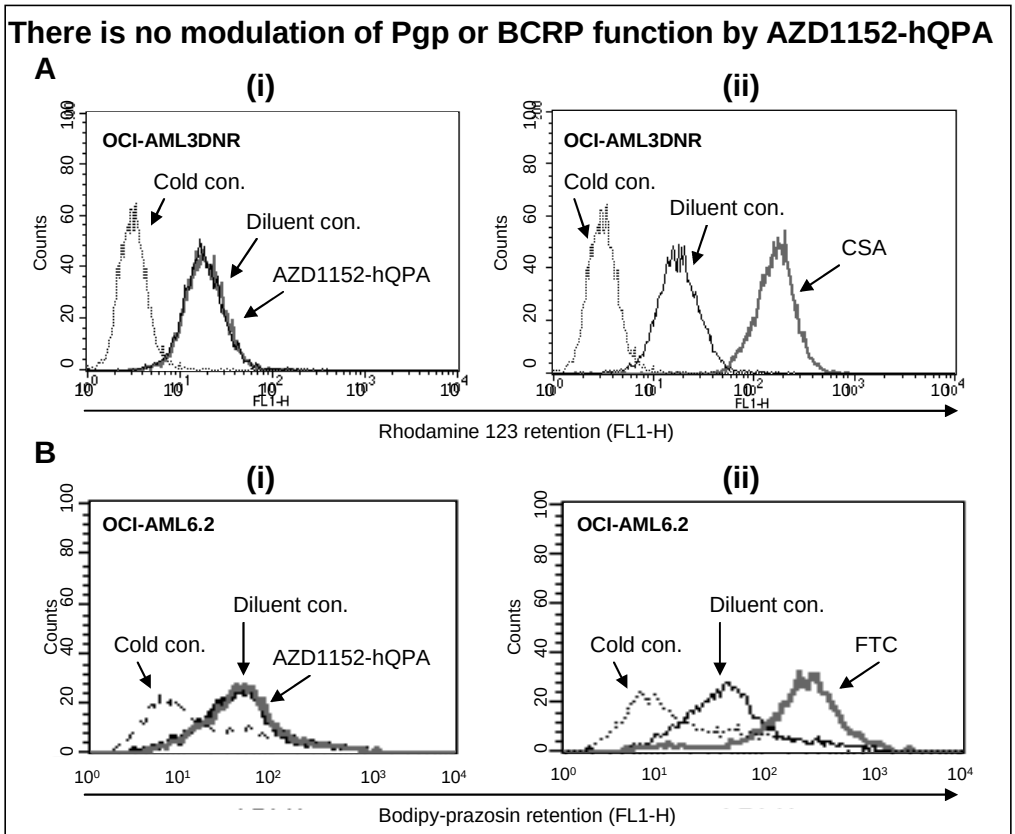

Figure 5.3 R123 accumulation in OCI-AML3DNR cells +/- 300nM AZD1152-hQPA (i) or 2.5µg/ml CSA (ii). The dotted lines are the 4°C R123 control. The solid black line is R123 + diluent control and the solid grey line R123 + AZD1152-hQPA (i) and R123 + CSA (ii) (A). BODIPY-prazosin accumulation in OCI-AML6.2 cells +/- 300nM AZD1152-hQPA (i) or 10µM FTC (ii). The dotted lines are the 4°C BODIPY control. The solid black line is BODIPY + diluent control and the solid grey line BODIPY + AZD1152-hQPA (i) and BODIPY + FTC (ii) (B). Plots are representative of a single experiment which was done in triplicate.

of the drug (Figure 5.4). In this assay CSA and FTC increased retention of [^{14}C]-AZD1152-hQPA in both OCI-AMLDNR ($p=0.004$) and OCI-AML6.2 ($p=0.005$) cells respectively. The modulators increased retention of [^{14}C]-AZD1152-hQPA to at least the concentration seen in the ABC transporter negative/AZD1152-hQPA sensitive OCI-AML3 cell line. This suggests that AZD1152-hQPA is being effluxed by Pgp and BCRP and explains why cell lines over-expressing these transporters are less sensitive to the drug.

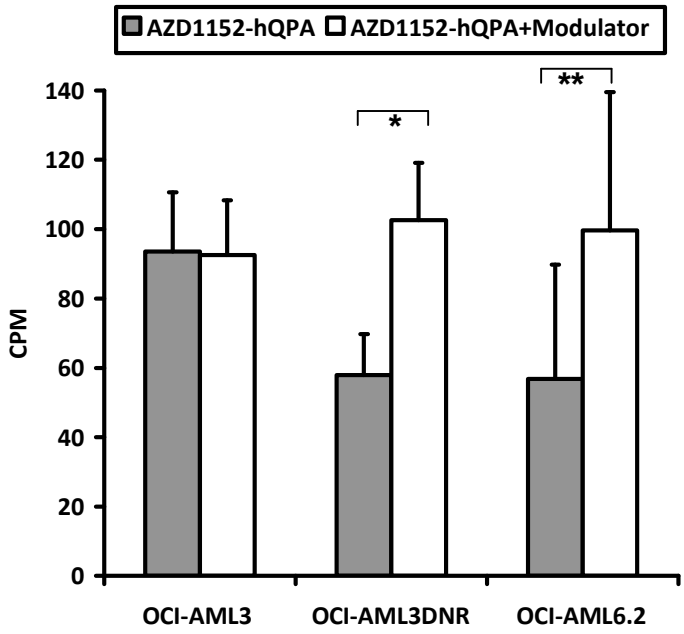

Figure 5.4 300nM [^{14}C]-AZD1152-hQPA uptake in Pgp expressing OCI-AML3DNR cells +/- the Pgp modulator CSA and in OCI-AML6.2 cells +/- the BCRP modulator FTC. Pgp/BCRP negative OCI-AML3 cells have been used as a positive control (*p=0.004/**p=0.005) (analyzed using paired samples t-test), +95% confidence interval). Diluent controls were included for each modulator. Columns, mean of three experiments; bars, SD.

5.4 Does culture with known drug efflux inhibitors enhance sensitivity to AZD1152-hQPA?

Sub-toxic doses of the Pgp inhibitor CSA or the BCRP inhibitor FTC were added to cell culture with 10-1000nM AZD1152-hQPA (Figure 5.5). Addition of CSA sensitizes the Pgp positive cell lines OCI-AML3DNR and KG-1a to pHH3 down-regulation with complete loss of pHH3 seen at 24 hours with 100nM AZD1152-hQPA (Figure 5.5A(i)). There is no statistical significance in the decrease in pHH3 at 10nM AZD1152-hQPA plus CSA in the OCI-AML3

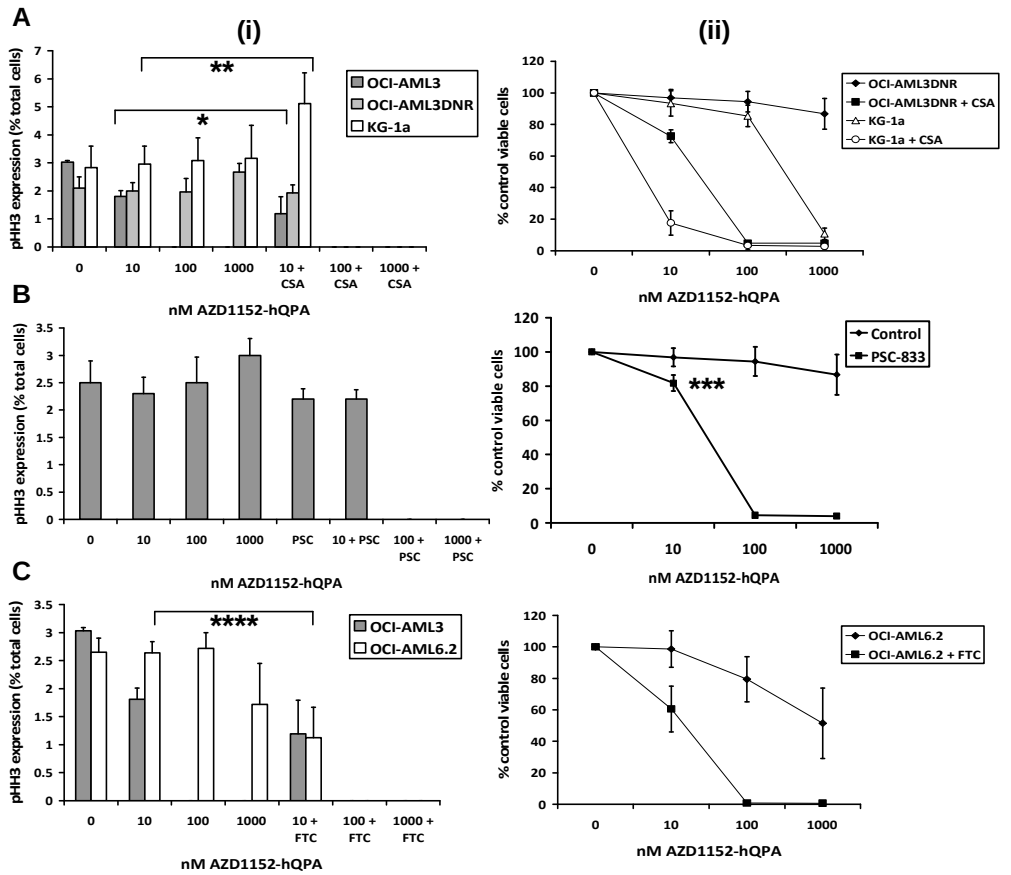

Figure 5.5 Effect of 24 hours AZD1152-hQPA exposure +/- 2.5µg/ml CSA on pHH3 expression in OCI-AML3, OCI-AML3DNR and KG-1a cells (*p=0.145/**p=0.145) (analyzed using paired samples t-test), +95% confidence interval) (i) and 72 hours viable cell count (ii) (A). Effect of 24 hours AZD1152-hQPA exposure +/- 1µM PSC-833 on pHH3 expression in OCI-AML3DNR cells (***p=0.021) (i) and 72 hours viable cell count (ii) (B) Effect of 24 hours AZD1152-hQPA exposure +/- 5µM FTC on pHH3 expression in OCI-AML3 and OCI-AML6.2 cells (****p=0.021) (i) and 72 hours viable cell count (ii) (C). Columns/lines, mean of three experiments; bars, SD.

cells, or in the increase in pHH3 in KG-1a cells with the same treatment, both p=0.145. The same effect is seen in 72 hour cell viability with a marked decrease in viability at 10nM and complete loss of cell viability at 100nM AZD1152-hQPA with the addition of CSA (Figure 5.5A(ii)). PSC-833 is a cyclosporine analogue with greater specificity for Pgp than CSA (Twentyman, 1991). CSA is a broad-spectrum MDR modulator, with effects on MDR-associated proteins including Pgp, MRP, and BCRP (Qadir *et al.*, 2005). In contrast, whereas PSC-833

effectively modulates Pgp, it has no effects on BCRP or MRP modulation (Qadir *et al.*, 2005). Addition of PSC-833 to the OCI-AML3DNR cells results in complete inhibition of pHH3 at 100nM AZD1152-hQPA (Figure 5.5B(i)), with significant (p=0.021) loss of viability seen at 10nM AZD1152-hQPA with the addition of PSC-833 (Figure 5.5B(ii)).

Addition of FTC also sensitizes the BCRP positive cell line OCI-AML6.2 to pHH3 down-regulation at AZD1152-hQPA concentrations as low as 10nM (p=0.021) with complete down-regulation of pHH3 seen at 100nM AZD1152-hQPA with the addition of FTC (Figure 5.5$C_{(i)}$). Complete loss of cell viability at 72 hours was achieved at 100nM AZD1152-hQPA with the addition of FTC (Figure 5.5$C_{(ii)}$).

The MRP inhibitor MK-571 did not sensitize OCI-AML3DNR cells to AZD1152-

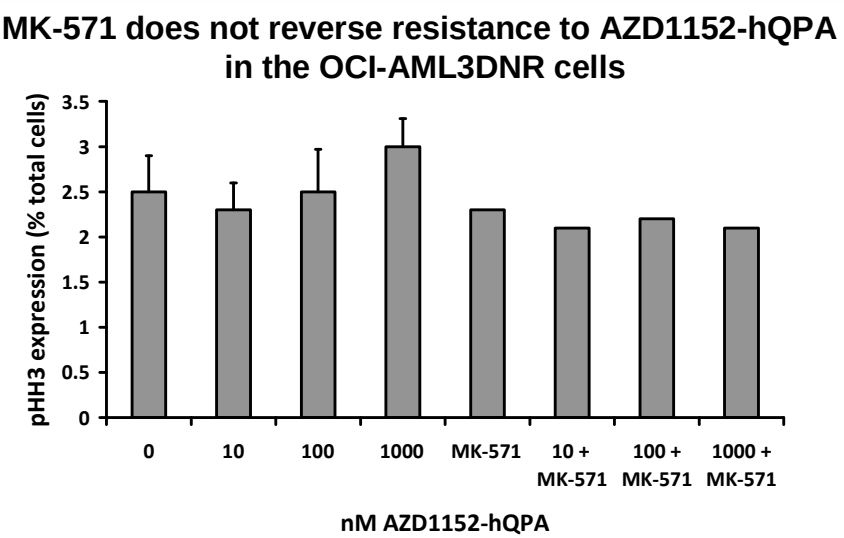

Figure 5.6 Flow cytometric measurement of pHH3 expression in OCI-AML3DNR cells after 24 hours AZD1152-hQPA exposure +/- 40μM MK-571. (n=1 for MK-571 addition) Columns/lines, mean of three experiments; bars, SD.

hQPA induced pHH3 inhibition confirming that resistance in the OCI-AML3DNR cells is not due to any elevated MRP expression (Figure 5.6).

Chapter Six
THE FLT3-ITD MUTATION IS A SECONDARY TARGET OF AZD1152-hQPA IN AML CELLS

6.1 Background

FLT3 mutations can be found in approximately 30% of AML patients, either as FLT3-ITD (24%) or FLT3 activation loop mutations (7%), making FLT3 one of the most commonly mutated genes in AML (Gilliland, 2002). Younger patients with AML have a high complete remission rate, but relapses occur in approximately 50% of cases overall and this figure rises to 70% in patients with FLT3-ITDs making the FLT3-ITD gene mutation a poor prognostic factor in AML (Grimwade *et al.*, 1998; Gale *et al.*, 2005).

6.2 AML cell lines with the FLT3-ITD mutation are particularly sensitive to AZD1152-hQPA

During the course of this study, it was noticed that the FLT3-ITD expressing MV4-11 and MOLM-13 cell lines were particularly sensitive to AZD1152-hQPA, with viability and pHH3 IC_{50}s below 10nM (Figure 6.1). Interestingly, VX-680 a selective inhibitor of all three aurora kinases also exhibits cross-inhibitory activity against the receptor tyrosine kinase FLT3 and ablated colony formation in primary AML cells with FLT3-ITD (Harrington *et al.*, 2004; Carvajal *et al.*, 2006). ITD mutation of FLT3 induces activating phosphorylation of the receptor in the absence of FL (Gilliland, 2002). With this in mind, it was decided to measure pFLT3 levels in the ITD cell lines after treatment with AZD1152-hQPA.

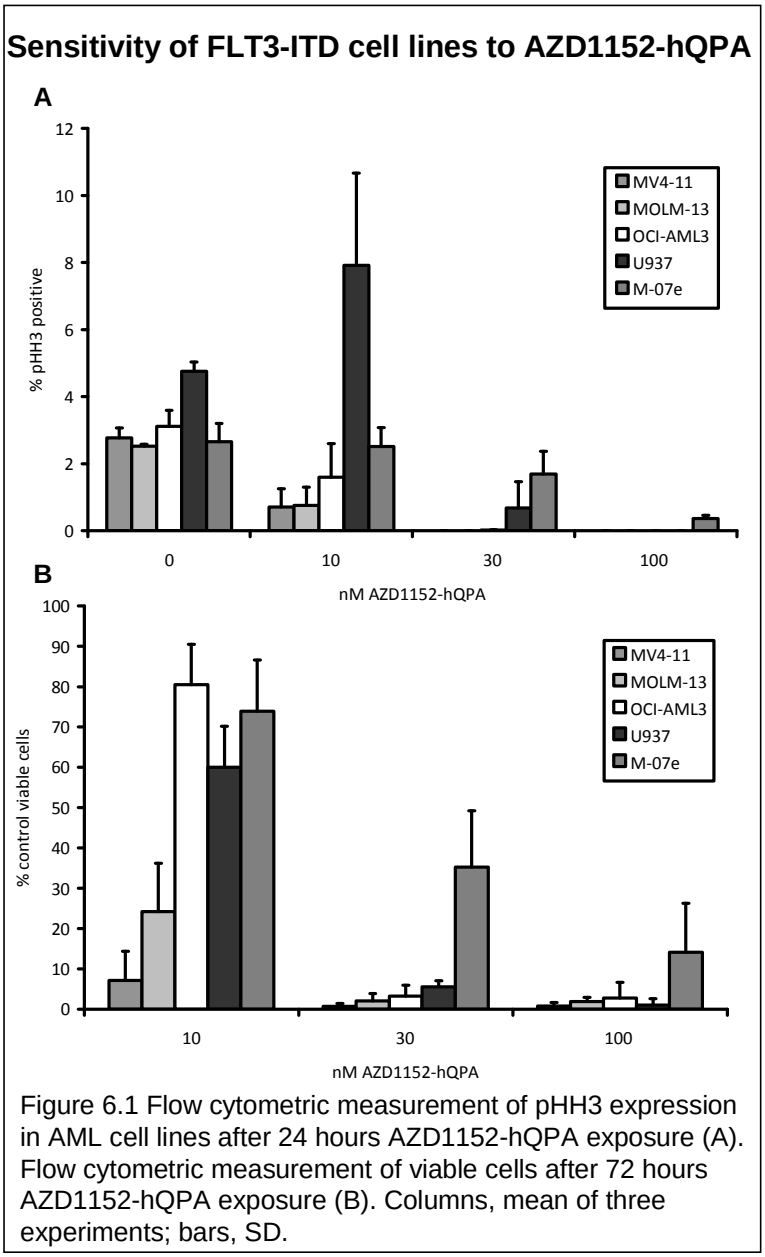

Figure 6.1 Flow cytometric measurement of pHH3 expression in AML cell lines after 24 hours AZD1152-hQPA exposure (A). Flow cytometric measurement of viable cells after 72 hours AZD1152-hQPA exposure (B). Columns, mean of three experiments; bars, SD.

6.3 pFLT3 inhibition by AZD1152-hQPA

The phosphorylated form of FLT3 was measured by immunoprecipitation in FLT3-ITD expressing cell lines initially treated for 24 hours with AZD1152-hQPA. A 77.7% and 86.9% decrease in phosphorylated FLT3 was seen in MOLM-13 and MV4-11 cells respectively (Figure 6.2). Data was obtained using

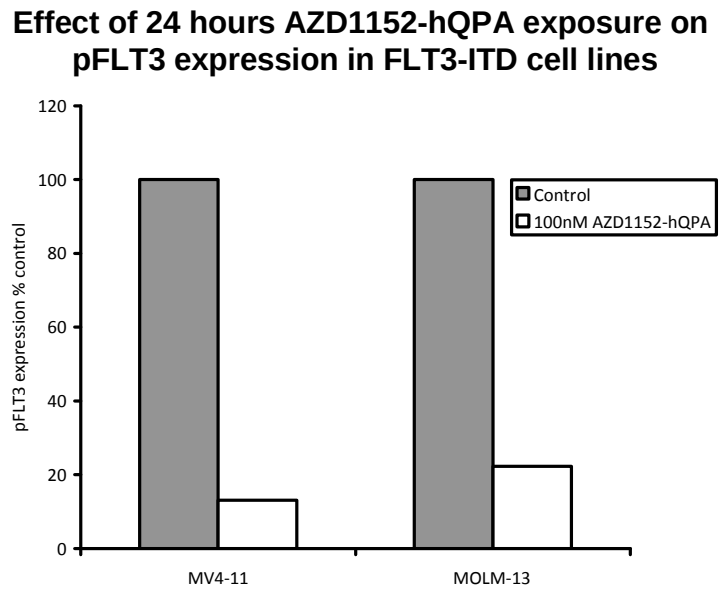

Figure 6.2 Effect of 24 hours AZD1152-hQPA exposure on pFLT3 expression measured by immunoblotting and normalized to total FLT3 expression. (n=1)

Genesnap software attached to a syngene spectrometer but the image itself was fairly messy and difficult to visualize (a clearer immunoblot is presented in a later section in Figure 6.5). The data was normalized to total FLT3 expression which was unaffected by the drug.

Encouraged by this result it was decided to measure the effect of phosphorylated signal transducer and activator of transcription 5 (pSTAT5) in the same FLT3-ITD cell lines. Oncogenic activation by FLT3-ITD mutation is known to activate aberrant signalling, including direct STAT5 activation (Choudhary *et al.*, 2007). pSTAT5 was measured by flow cytometry in the FLT3-ITD cell lines using an antibody specific for activated (tyrosine-phosphorylated) STAT5 (Figure 6.3). This assay is fairly rapid and requires far less material than for immunoblotting, which makes it potentially useful for patient material. Experiments confirmed the down-regulation of pSTAT5 after 24 hours of treatment with AZD1152-hQPA in

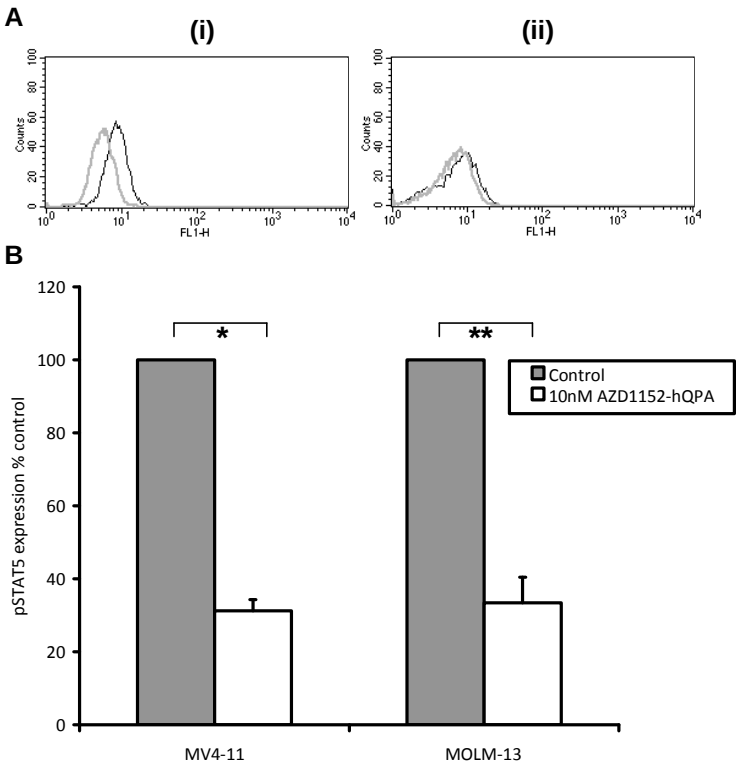

Figure 6.3 Flow cytometric histograms of 24 hour pSTAT5 expression in MV4-11 control cells (i) and 10nM AZD1152-hQPA exposure (ii) (A). The light line indicates the isotype control. Flow cytometric measurement of pSTAT5 expression in FLT3-ITD cell lines (*p=0.008/**p=0.007 (analyzed using paired samples t-test), +95% confidence interval) (B). Columns, mean of three experiments; bars, SD.

the FLT3-ITD cell lines. 10nM AZD1152-hQPA induced a 68.7% (p=0.008) and 66.5% (p=0.007) decrease in pSTAT5 expression in MV4-11 and MOLM-13 FLT3-ITD cell lines respectively (Figure 6.3).

6.4 Is AZD1152-hQPA targeting FLT3 directly or is it a result of Aurora B inhibition?

To determine whether AZD1152-hQPA is directly targeting pFLT3 and subsequently pSTAT5 in our FLT3-ITD cell lines it was decided to decrease the

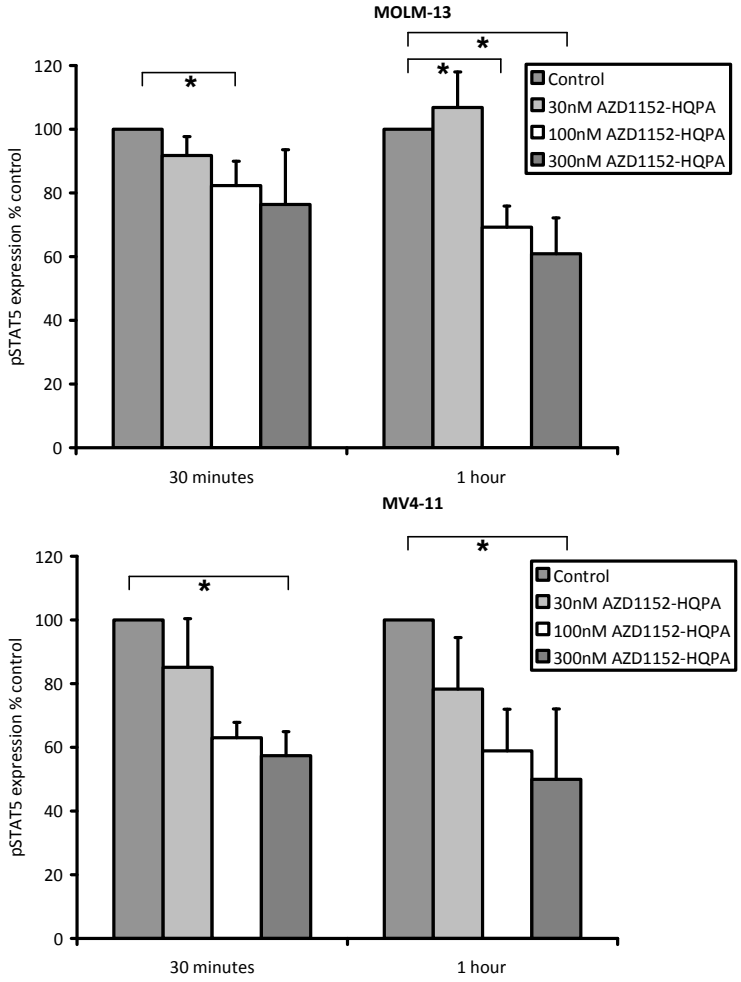

Figure 6.4 Effect of short term AZD1152-hQPA exposure on pSTAT5 expression measured by flow cytometry (*p<0.05 (analyzed using paired samples t-test), +95% confidence interval) . Columns, mean of three experiments; bars, SD.

incubation times with the drug. Because of the convenience of the assay in terms of time and material needed pSTAT5 expression was measured first in the cell lines. Experiments confirmed the down-regulation of pSTAT5 after 30 minutes and 1 hour treatment with AZD1152-hQPA in the FLT3-ITD cell lines in a dose dependent manner (Figure 6.4). Down-regulation of pFLT3 was confirmed using immunoblotting with down-regulation seen in the FLT3-ITD cell lines at concentrations as low as 30nM AZD1152-hQPA after 1 hour incubation (Figure

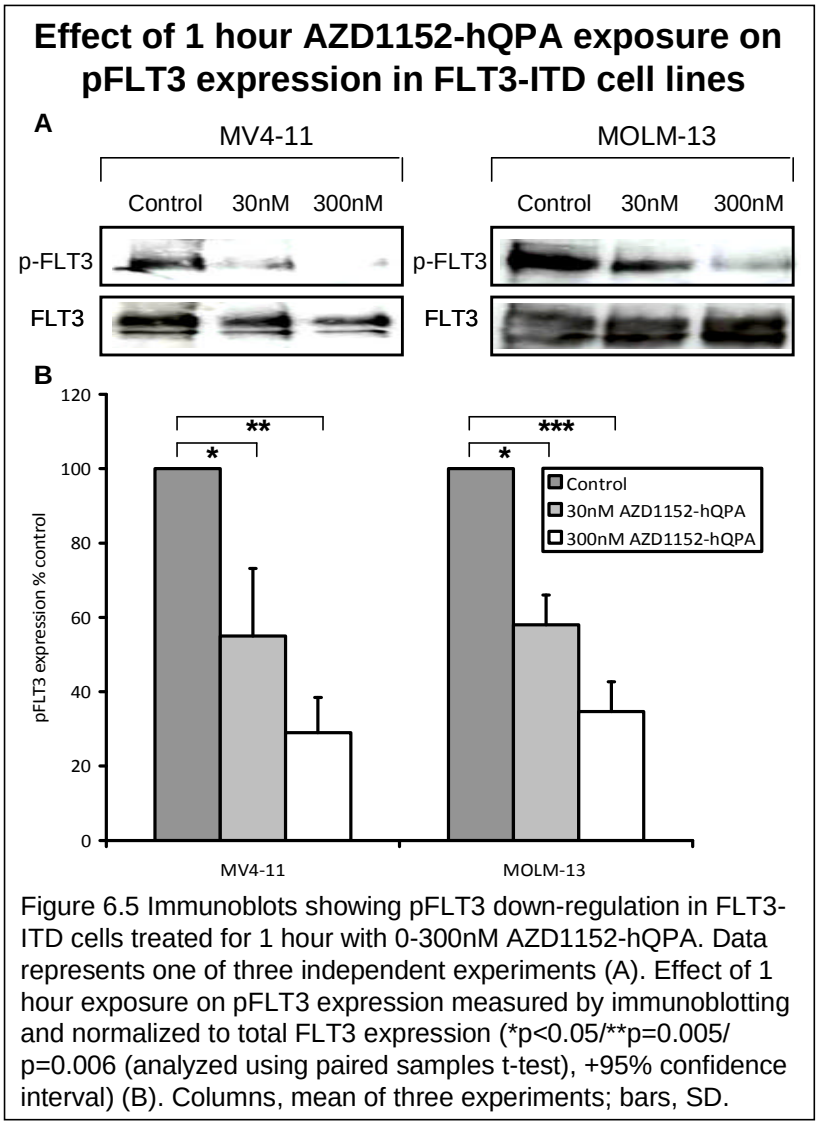

Figure 6.5 Immunoblots showing pFLT3 down-regulation in FLT3-ITD cells treated for 1 hour with 0-300nM AZD1152-hQPA. Data represents one of three independent experiments (A). Effect of 1 hour exposure on pFLT3 expression measured by immunoblotting and normalized to total FLT3 expression (*p<0.05/**p=0.005/ p=0.006 (analyzed using paired samples t-test), +95% confidence interval) (B). Columns, mean of three experiments; bars, SD.

6.5). 300nM AZD1152-hQPA induced a 71% (p=0.005) and 65.3% (p=0.006) decrease in pFLT3 expression in MV4-11 and MOLM-13 FLT3-ITD cell lines respectively (Figure 6.5).

The FLT3-ITD MV4-11 cell line is cytokine independent, but growth is enhanced in the presence of IL-3 (Santoli *et al.*, 1987). We therefore investigated whether sensitivity to AZD1152-hQPA is abrogated when alternative cytokine pathways

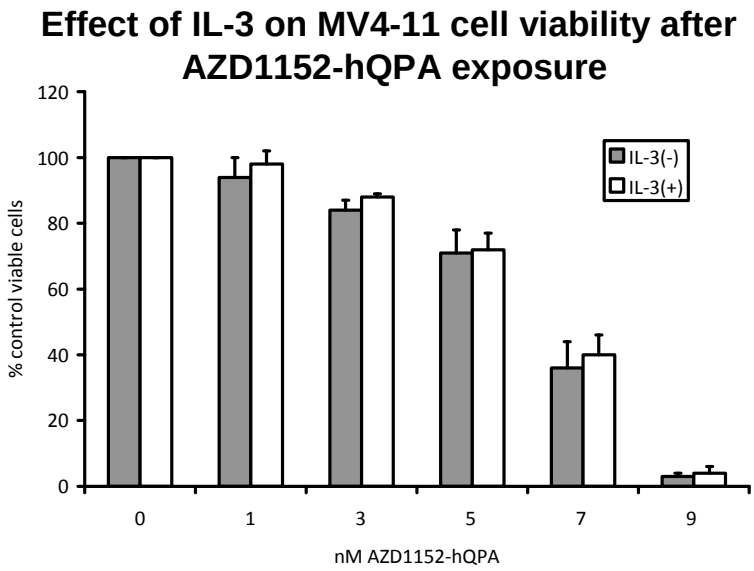

Figure 6.6 Effect of 72 hours AZD1152-hQPA exposure on MV4-11 viable cell count plus/minus incubation with 100u/ml IL-3. Columns, mean of three experiments; bars, SD.

are stimulated (Figure 6.6). Here we demonstrate that IL-3 does not protect MV4-11 cells from AZD1152-hQPA induced loss of viability.

Chapter Seven SPECIFICITY OF AZD1152-hQPA IN PRIMARY AML CELLS

7.1 Background

We have established that specificity of AZD1152-hQPA in AML cell lines is dependent on the Pgp, BCRP and FLT3 status of the cells. Our next aim was to investigate the specificity of AZD1152-hQPA in primary samples and determine whether the same predictors of response that were found in the cell lines are observed in these samples.

7.2 Establishment of proliferating primary AML cell cultures

The level of pHH3 detectable in untreated cell lines was low (2.5-4.8% of total cells; Figure 3.4) and expression in primary cells was expected to be even lower, as a very small population of cells are actively dividing at the time of sampling. Because of this we wanted to pre-incubate primary samples with a cytokine cocktail to drive the cells into cycle, allowing us to measure pHH3, and determine specificity of AZD1152-hQPA in the samples. The combination of cytokines used (20ng/ml IL-3, SCF, IL-6, and 25ng/ml G-CSF) for optimal 48 hour culture of leukaemic blasts has been previously reported by our lab (Mony *et al.*, 2008).

Cellular proliferation was measured in 65 primary AML samples using [^{3}H]-Tdr uptake with or without 48 hours pre-incubation with cytokine cocktail (Figure 7.1). Proliferation was confirmed in 51 (78.5%) of the samples when treated with cytokine cocktail for 48 hours and all proliferating samples showed increased [^{3}H]-Tdr uptake at 48 hours compared to basal proliferation measured at 6 hours (Figure 7.1$_{(A)}$).

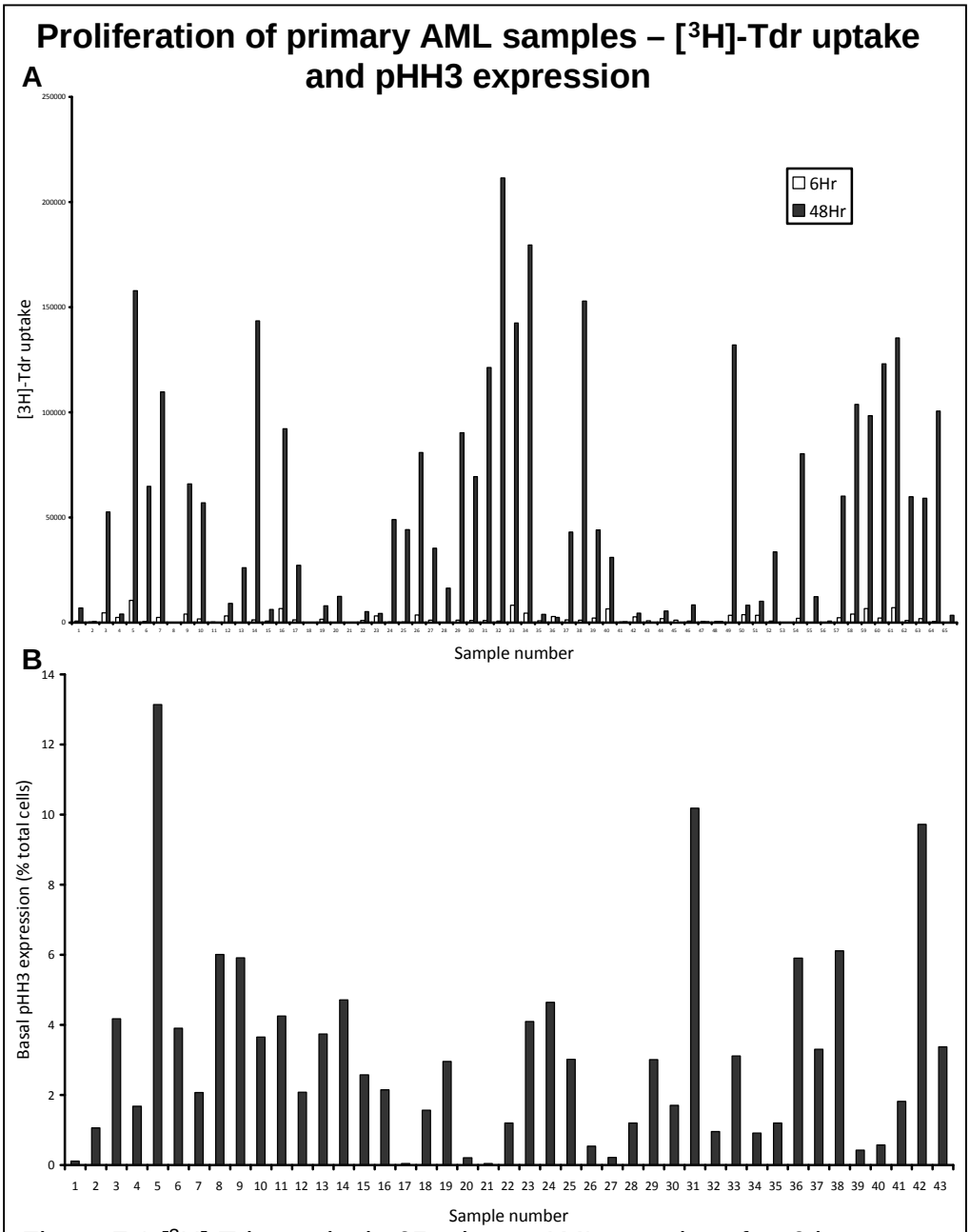

Figure 7.1 [^{3}H]-Tdr uptake in 65 primary AML samples after 6 hours without and 48 hours with cytokine cocktail pre-incubation (A). pHH3 expression in 43 primary samples after 48 hours pre-incubation with cytokine cocktail (B).

7.3 Can pHH3 be measured in primary samples and inhibited with AZD1152-hQPA?

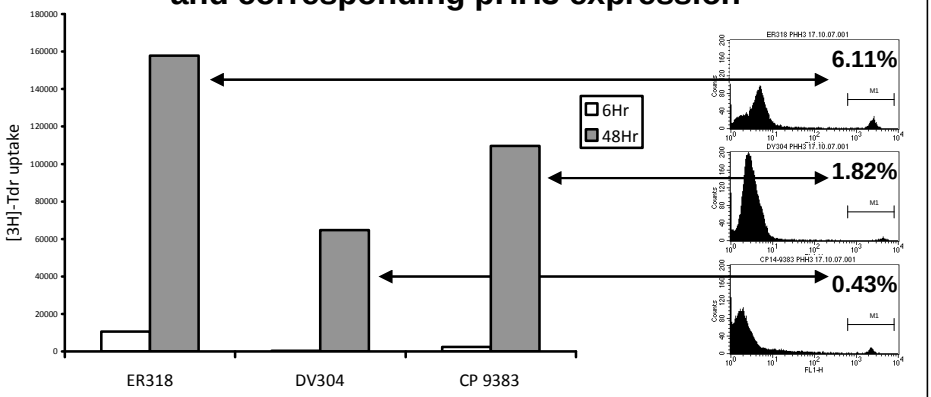

Figure 7.2 [^{3}H]-Tdr uptake in 3 primary AML samples after 6 hours and after 48 hours of pre-incubation with cytokine cocktail. The histograms show pHH3 expression in the corresponding samples after 48 hours cytokine cocktail pre-incubation.

Confident with the amount of proliferation seen at 48 hours we then went on to measure pHH3 under the same conditions and were able to measure pHH3 expression in 43 primary samples (Figure $7.1_{(B)}$). Mean basal pHH3 expression in the primary samples was 3.01% (range, 0.04-13.14%) of total cells which was comparable to the expression seen in cell lines. Basal pHH3 expression and the amount of proliferation shown by [^{3}H]-Tdr uptake was measured in 3 primary samples and corresponding values were seen (Figure 7.2).

Aurora-B mRNA levels were measured in 88 primary samples (Figure $7.3_{(A)}$) and as expected pHH3 expression in untreated primary samples correlated well with aurora-B mRNA levels ($p=0.015$, $R^2=0.2098$; Figure $7.3_{(B)}$). Our next aim was to try to inhibit pHH3 with AZD1152-hQPA in these primary samples. Significant pHH3 inhibition was achieved in cytokine-primed primary samples at short time periods with 300nM AZD1152-hQPA (Figure $7.4_{(A)}$). pHH3 expression was measured in 37 primary samples after 1 hours treatment with 300nM AZD1152-

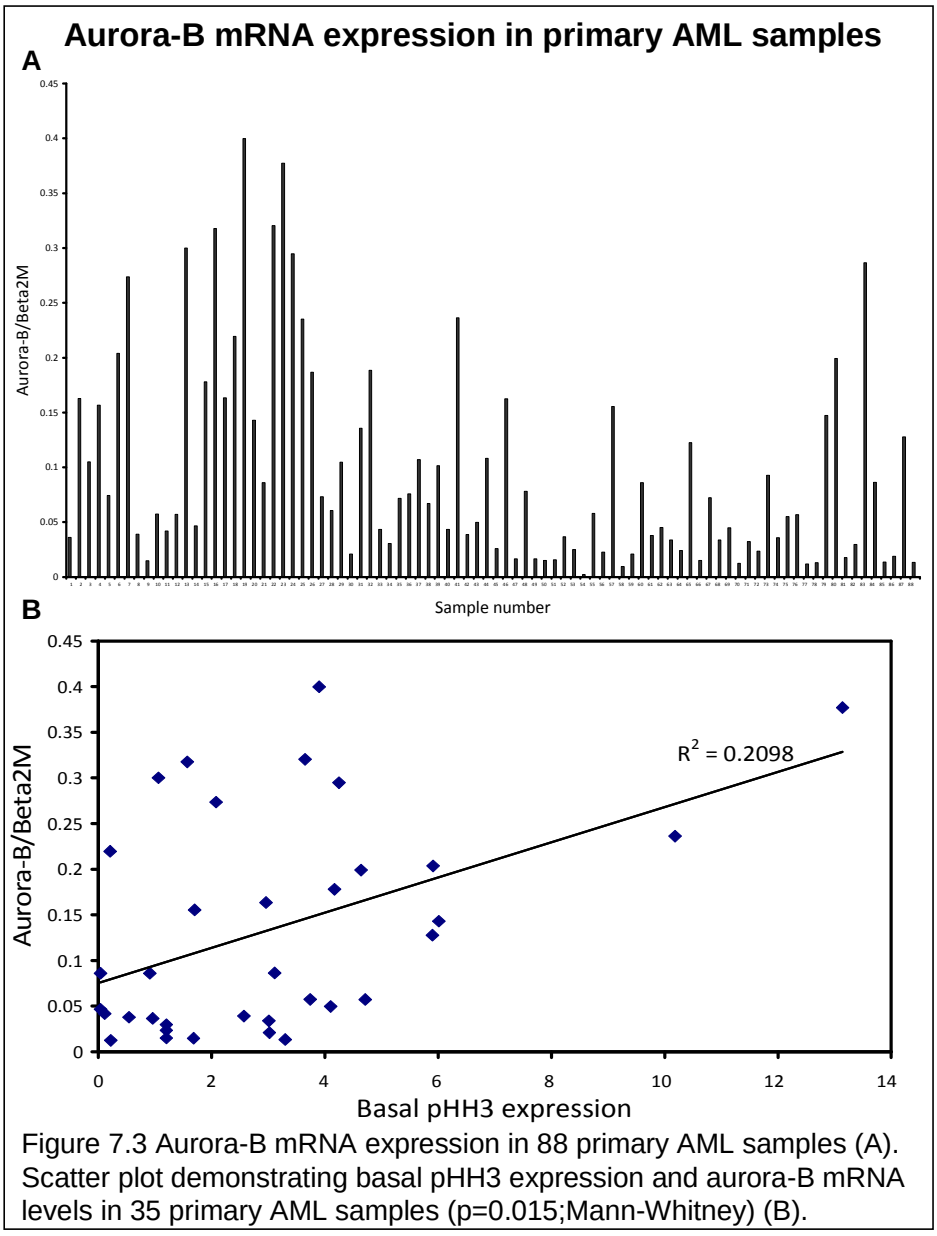

Figure 7.3 Aurora-B mRNA expression in 88 primary AML samples (A). Scatter plot demonstrating basal pHH3 expression and aurora-B mRNA levels in 35 primary AML samples (p=0.015;Mann-Whitney) (B).

hQPA (Figure $7.4_{(B)}$). IC_{50} was achieved in all but 2 samples (94.6%) with a mean down-regulation of 78% (Range, 32.7-100%).

7.4 Pgp and BCRP positive primary AML samples are less sensitive to AZD1152-hQPA induced pHH3 inhibition

Pgp and BCRP expression was measured in 37 primary AML samples. A study in

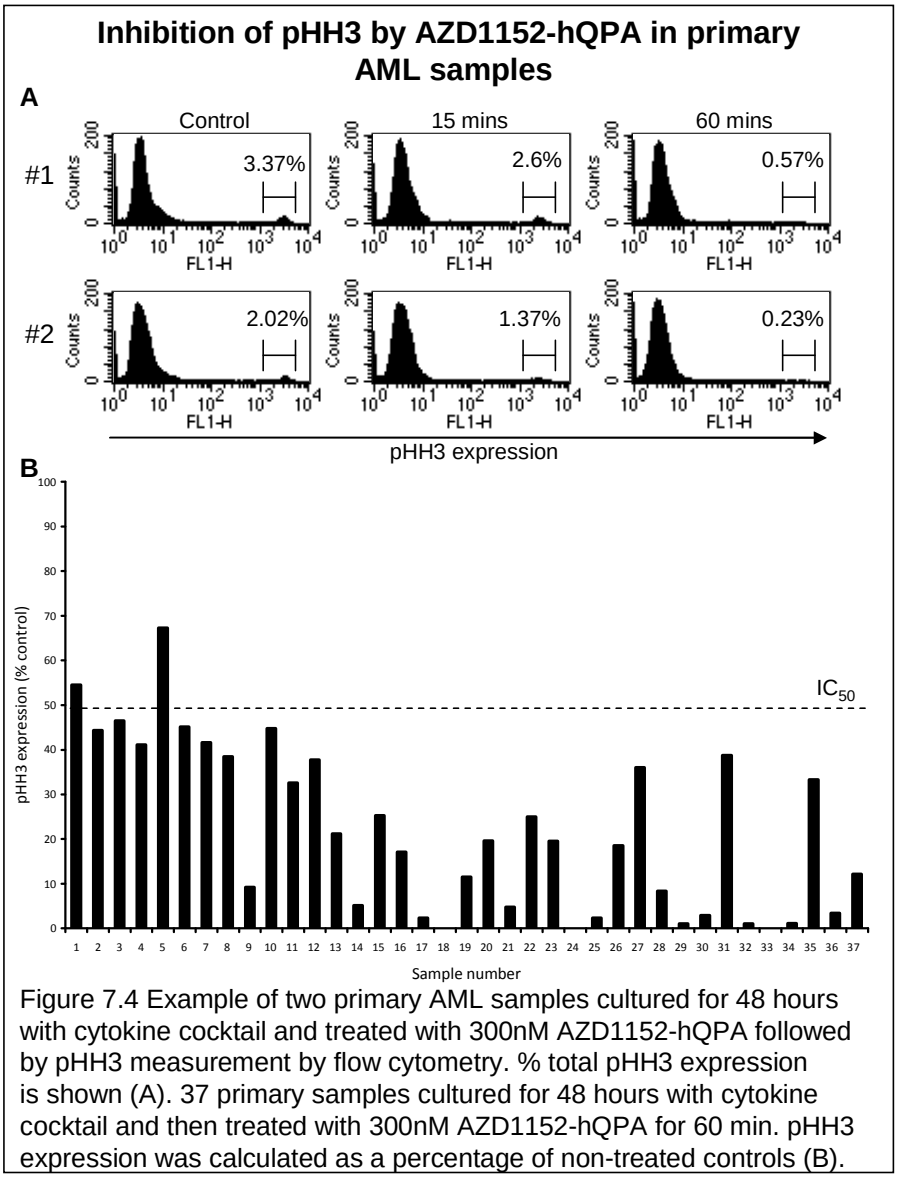

Figure 7.4 Example of two primary AML samples cultured for 48 hours with cytokine cocktail and treated with 300nM AZD1152-hQPA followed by pHH3 measurement by flow cytometry. % total pHH3 expression is shown (A). 37 primary samples cultured for 48 hours with cytokine cocktail and then treated with 300nM AZD1152-hQPA for 60 min. pHH3 expression was calculated as a percentage of non-treated controls (B).

2001 compared MRK-16, UIC2 and 15D3 monoclonal antibody staining in leukaemic blasts (Taylor *et al.*, 2001). They concluded that when assaying patient samples for Pgp expression and function using flow cytometry, the R123 functional assay should be performed in concert with MRK-16 antibody staining (Taylor *et al.*, 2001). Mean MRK-16 test/control mean fluorescence intensity (MFI) in the primary samples was 1.13 (range, 0.72-2.92). Pgp protein level was

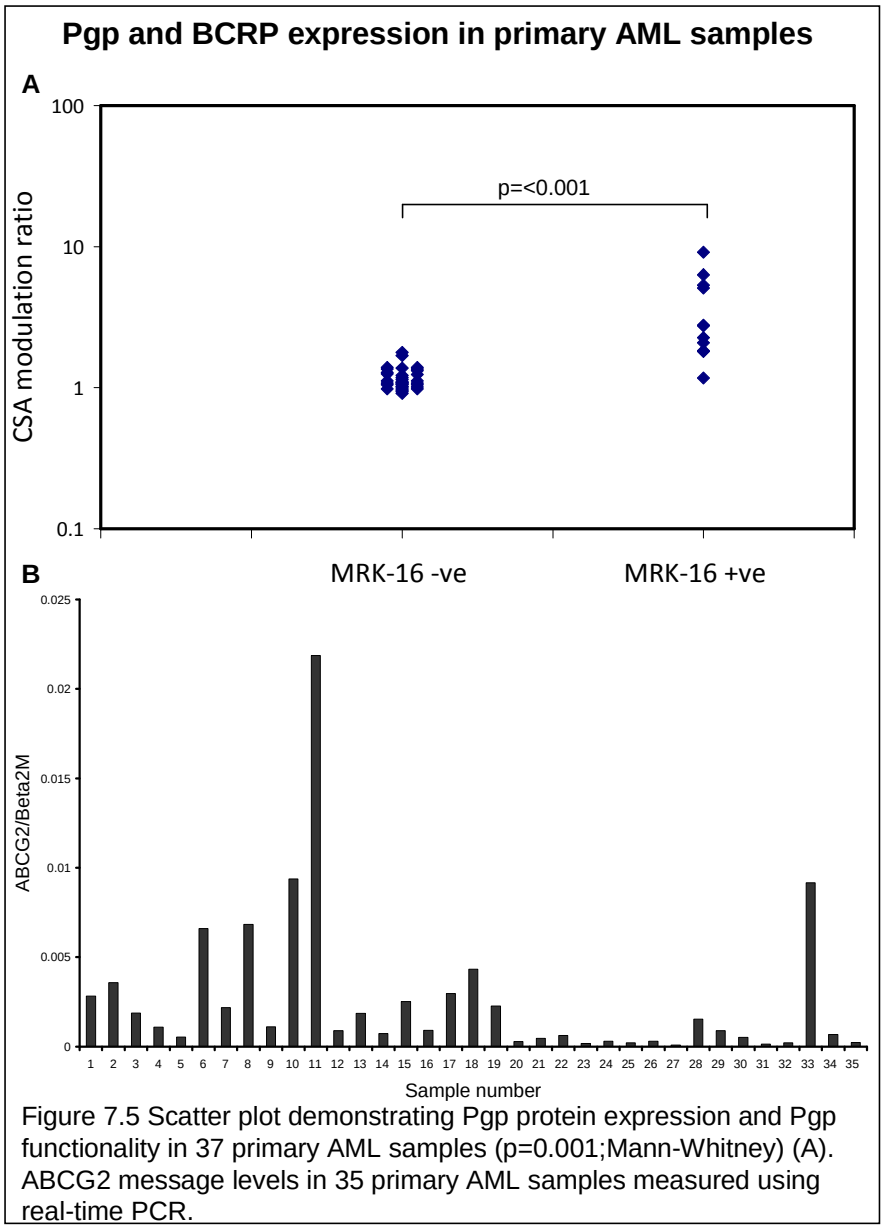

Figure 7.5 Scatter plot demonstrating Pgp protein expression and Pgp functionality in 37 primary AML samples (p=0.001;Mann-Whitney) (A). ABCG2 message levels in 35 primary AML samples measured using real-time PCR.

recorded as positive when the MRK-16 test/control value was ≥1.1 (based on data gathered during the AML14 and AML15 trials carried out in our lab). Mean CSA/R123 modulation ratio in the primary samples was 1.74 (range, 0.91-9.16). Pgp was recorded as functional when the CSA/R123 modulation ratio was ≥1.7 based on a previous study (Pallis *et al.*, 1999b). There was a significant correlation between Pgp protein expression and functional activity in our samples (p=0.001) (Figure $7.5_{(A)}$). ABCG2 message levels were measured in 35 patient samples using

real-time PCR (in 2 samples the cDNA was not amplified) (Figure $7.5_{(B)}$). The ABCG2 expression levels data was normally distributed, so for statistical purposes, values above and below the mean were used to classify samples as ABCG2 positive and negative respectively. Of the primary samples tested 9/37 (24.3%) were positive for Pgp and 9/35 (25.7%) were positive for BCRP. The 2 samples where an IC_{50} for pHH3 expression was not achieved were positive for both Pgp and BCRP expression (Figure 7.6). Five samples co-expressed Pgp and BCRP such that a significant correlation was found ($p=0.008$, $R^2=0.238$) between Pgp and BCRP expression in our primary samples. The percentage of Pgp and BCRP positive samples and the co-expression correlation agrees with previously published data (Damiani *et al.*, 2006).

Pgp positive samples were significantly ($p=<0.001$) less sensitive to AZD1152-

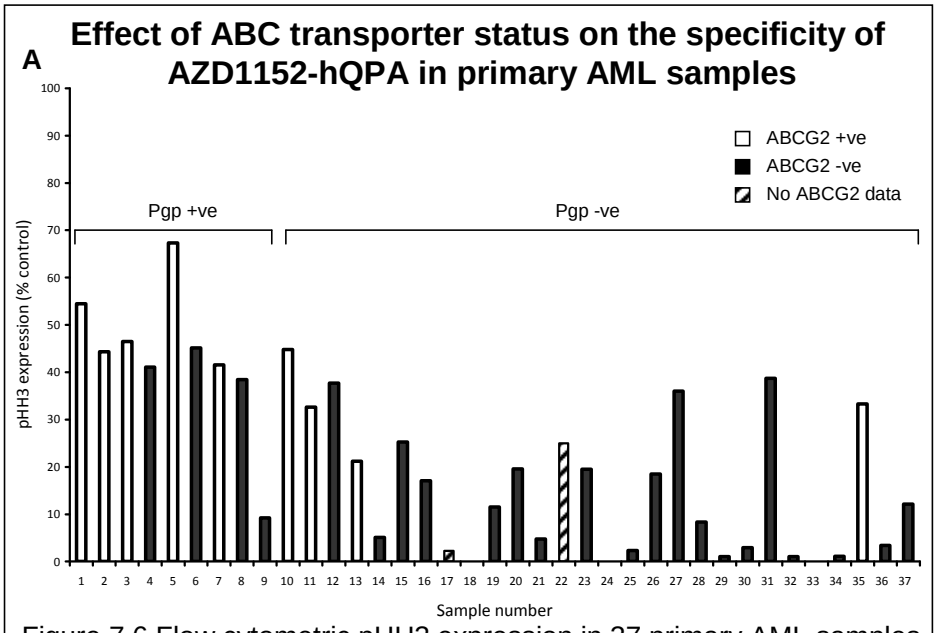

Figure 7.6 Flow cytometric pHH3 expression in 37 primary AML samples pre-incubated with cytokine cocktail for 48 hours and then treated with 300nM AZD1152-hQPA for 60 minutes.

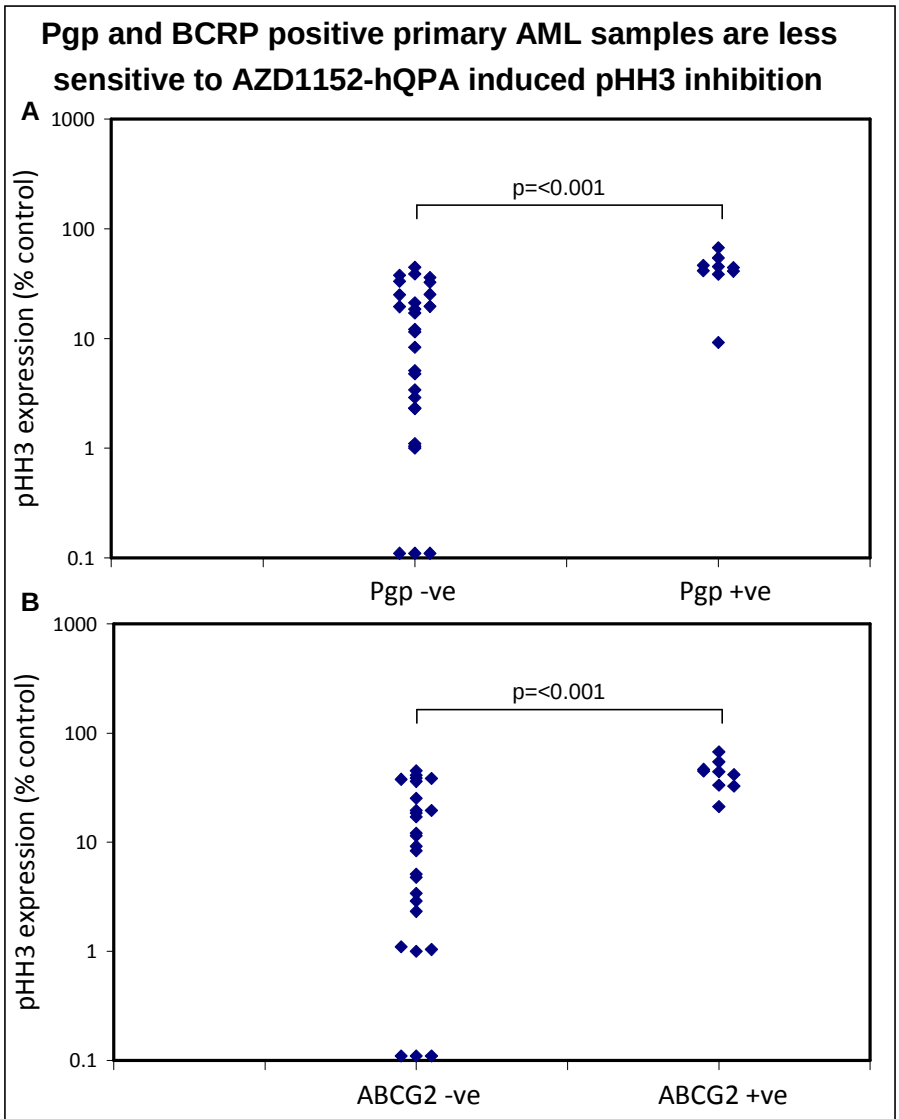

Figure 7.7 Scatter plot showing that Pgp positive primary samples are less sensitive to AZD1152-hQPA induced pHH3 inhibition than Pgp negative samples (p=<0.001;Mann-Whitney) (A). Scatter plot showing that BCRP positive primary samples are less sensitive to AZD1152-hQPA induced pHH3 inhibition than BCRP negative samples (p=<0.001) (B).

hQPA induced pHH3 inhibition than Pgp negative samples (Figure $7.7_{(A)}$). BCRP positive primary samples were also significantly (p=<0.001) less sensitive to AZD1152-hQPA induced pHH3 inhibition compared to BCRP negative samples (Figure $7.7_{(B)}$). However, a sharp distinction between cell lines and primary samples was noted. The transporter-expressing cell lines were insensitive to down-

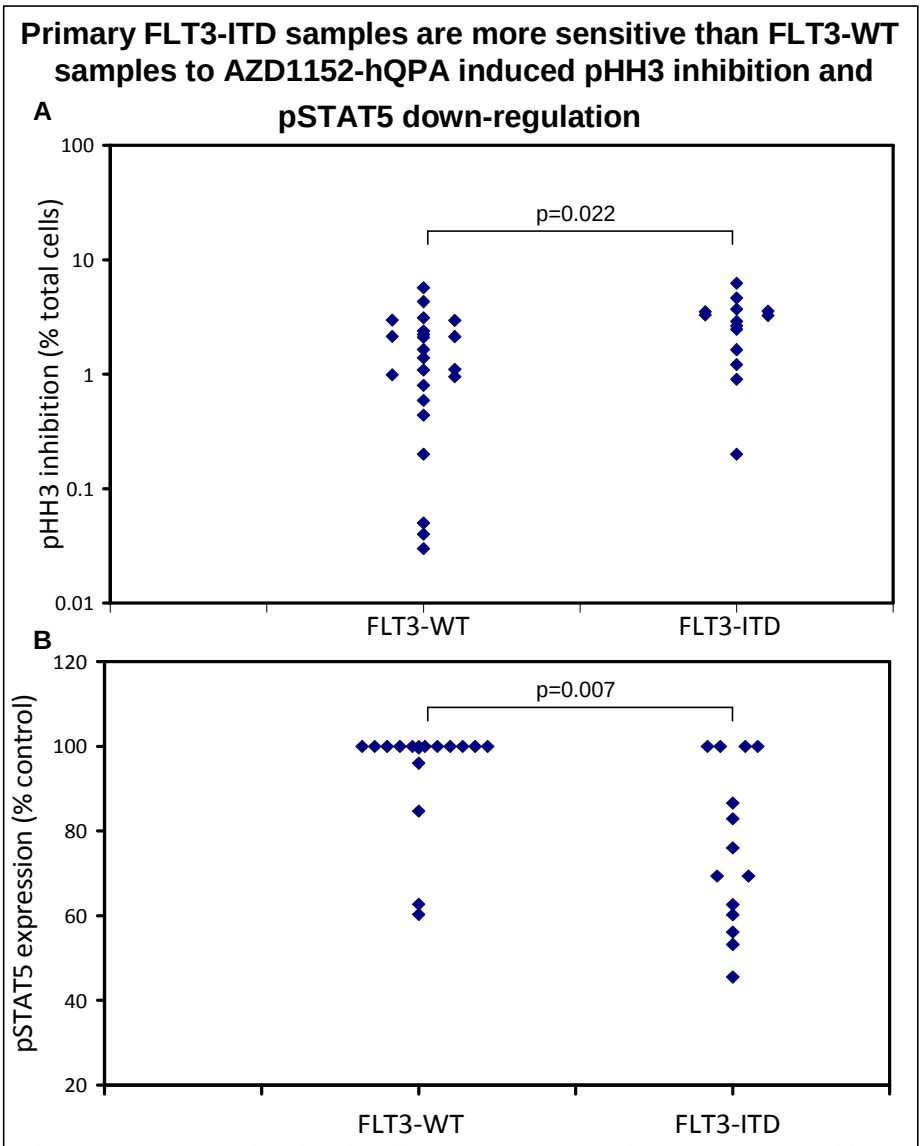

Figure 7.8 Scatter plot showing that FLT3-ITD samples are more sensitive to AZD1152-hQPA induced pHH3 inhibition than FLT3-WT samples (p=0.022;Mann-Whitney) (A). Scatter plot showing that FLT3-ITD primary samples are more sensitive to AZD1152-hQPA induced pSTAT5 down-regulation than FLT3-WT samples (p=0.007) (B).

regulation of pHH3 at concentrations of up to 1000nM AZD1152-hQPA even after 24 hours. In contrast 50% pHH3 inhibition was achieved in 94.6% of total primary samples at 300nM AZD1152-hQPA after only one hour incubation. Importantly, IC_{50} was also achieved in 77.78% (7/9) of Pgp positive samples and 77.78% (7/9) of BCRP positive samples. The two samples where an IC_{50} was not achieved co-

expressed both Pgp and BCRP, although it should be noted that IC_{50} was achieved in 3/5 (60%) samples that co-expressed Pgp and BCRP.

7.5 Primary FLT3-ITD samples are more sensitive to AZD1152-hQPA induced pHH3 down-regulation and pSTAT5 down-regulation compared to FLT3-WT samples

It was found that the FLT3-ITD mutation is a secondary target of AZD1152-hQPA, and because of the sensitivity of the FLT3-ITD cell lines to the drug, it was decided to screen our primary samples for FLT3 status. Forty two primary samples were screened for FLT3 mutation using genomic DNA fluorescent PCR amplification and analysis on a 3130 Genetic Analyzer. Seventeen (40.5%) of the samples had a FLT3-ITD mutation. Samples were pre-incubated with cytokine cocktail for 48 hours and then treated with 300nM AZD1152-hQPA for 1 hour.

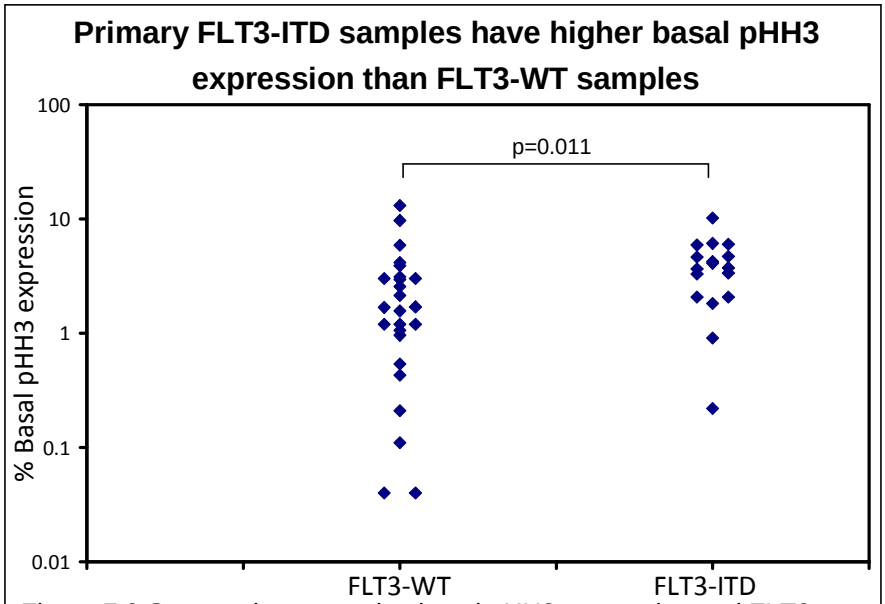

Figure 7.9 Scatter plot comparing basal pHH3 expression and FLT3 status in 42 primary AML samples (p=0.011;Mann-Whitney).

pHH3 expression was measured by flow cytometry and inhibition was calculated as a percentage of total pHH3 in untreated controls. The FLT3-ITD samples were more sensitive to AZD1152-hQPA induced pHH3 inhibition (p=0.022; Figure $7.8_{(A)}$).

Thirty-one primary AML samples were pre-incubated with cytokine cocktail for 48 hours and then treated with 300nM AZD1152-hQPA for 1 hour. pSTAT5 expression was measured by flow cytometry and inhibition was calculated as a percentage of total pSTAT5 in untreated controls. The FLT3-ITD samples were significantly more sensitive to AZD1152-hQPA induced pSTAT5 down-regulation (p=0.007; Figure $7.8_{(B)}$).

The presence of a FLT3-ITD results in an increased auto-phosphorylation of the FLT3 receptor tyrosine kinase and thereby increased cellular proliferation

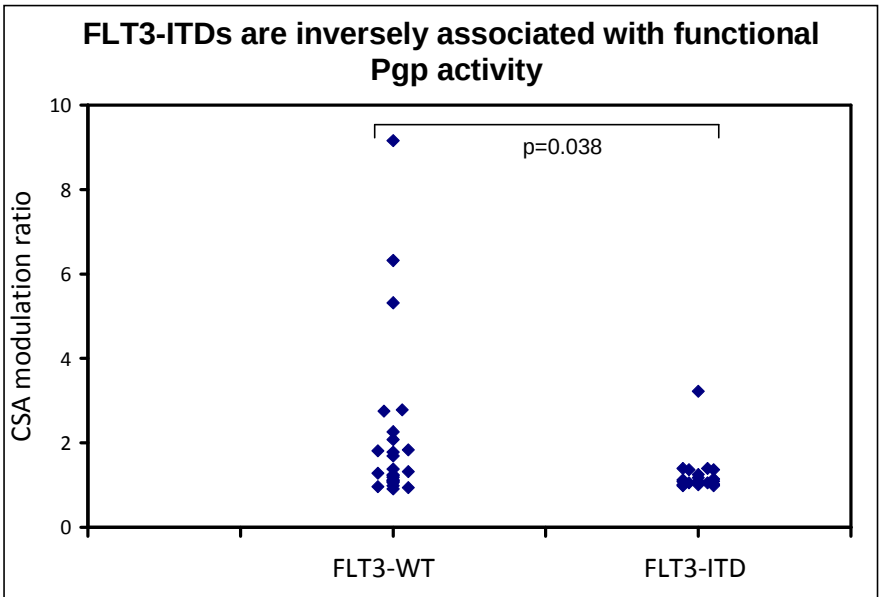

Figure 7.10 Scatter plot comparing FLT3 status and functional Pgp activity in 46 primary AML samples (p=0.038;Mann-Whitney).

(Gilliland, 2002). Expression of pHH3 is limited to mitosis and hence proliferating cells. We can demonstrate that our primary FLT3-ITD samples have higher basal pHH3 expression than FLT3-WT samples (p=0.011) (Figure 7.9). Previous work by our group has shown that FLT3-ITDs are inversely associated with functional Pgp activity (Pallis *et al.*, 2003b). The same was found in this sample population. Pgp was recorded as functional when the CSA modulation ratio was ≥1.7. Here, the mean modulation ratio in FLT3 wild-type samples was 2.13, and in ITD samples it was 1.27 (p=0.038) (Figure 7.10). Also, Pgp protein level was recorded as positive when the MRK-16 test/control value was ≥1.1. The mean MRK-16 test/control value in FLT3 wild-type samples was 1.18, and in ITD samples it was 1.06, although this was not statistically significant (p=0.137). Out of our fourteen FLT3-ITD samples only two samples (14.3%) were positive for Pgp expression and there was no statistical significance in terms of sensitivity to AZD1152-hQPA induced pHH3 inhibition in these samples (p=0.1) (Figure 7.11). There was also

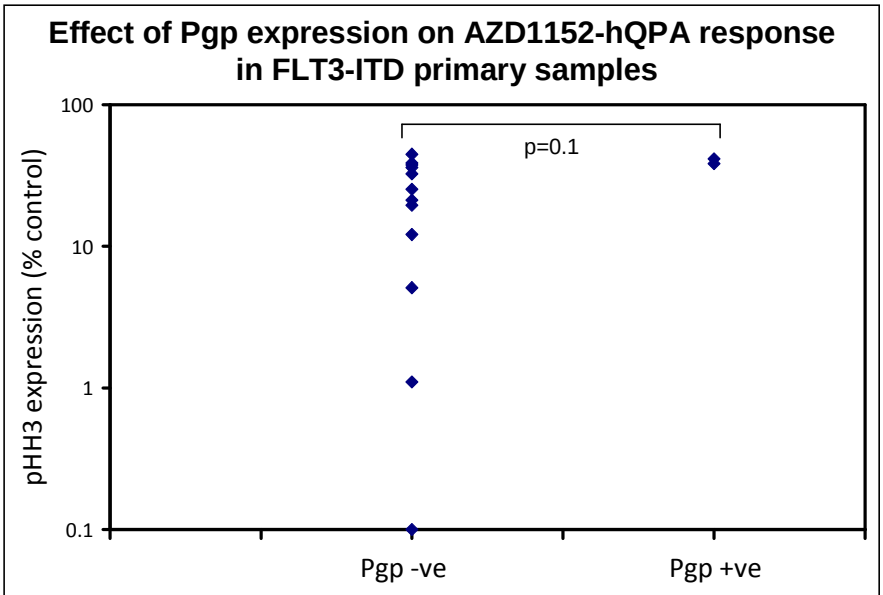

Figure 7.11 Scatter plot comparing Pgp status and AZD1152-hQPA induced pHH3 inhibition in 14 FLT3-ITD primary AML samples (p=0.1; Mann-Whitney).

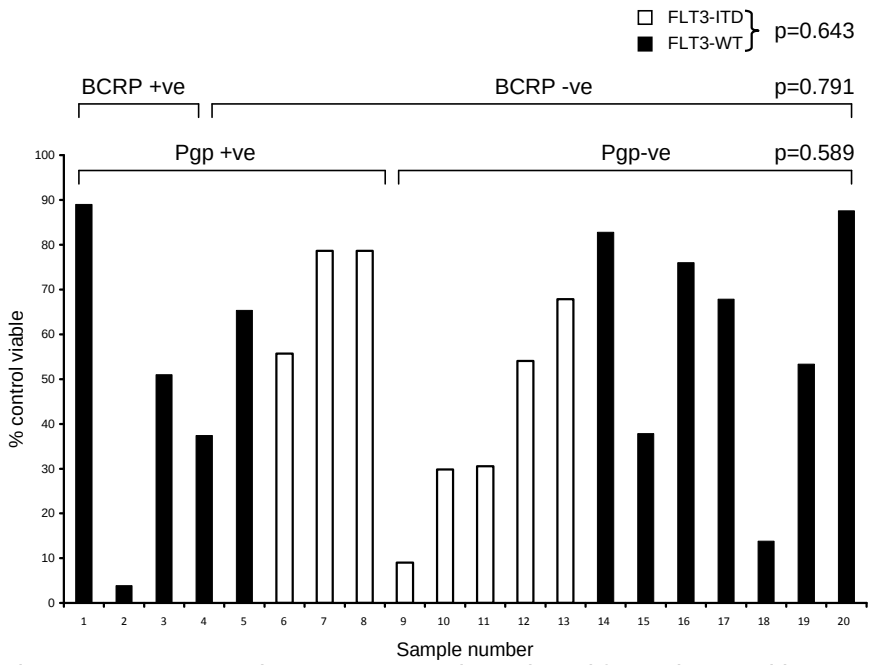

Figure 7.12 Twenty primary AML samples cultured for 48 hours with cytokine cocktail followed by 72 hours culture with 300nM AZD1152-hQPA. There is no significance between Pgp (p=0.589; Mann-Whitney), BCRP (p=0.791) or FLT3 (p=0.643) status of primary samples and viability in response to AZD1152-hQPA in this assay.

no correlation between FLT3 and BCRP status in this sample group (p=0.586).

7.6 Primary FLT3-ITD samples are more sensitive to AZD1152-hQPA induced growth inhibition compared to FLT3-WT samples

Initial experiments to examine the effects of AZD1152-hQPA on cell viability in primary samples were carried out in suspension culture. As previously described, samples were cultured for 48 hours in cytokine medium, and then cultured for a further 72 hours with 300nM AZD1152-hQPA. Cell viability was determined by

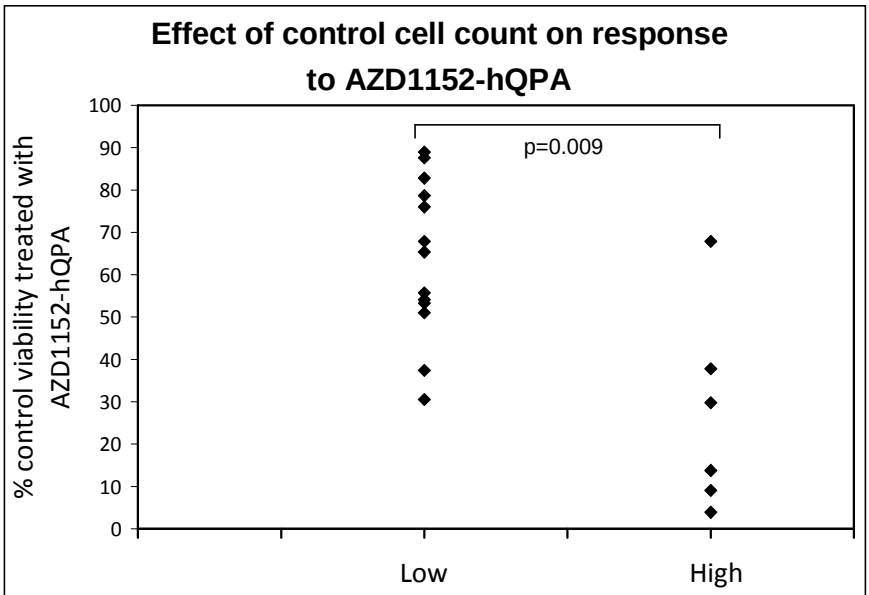

Figure 7.13 Effect of AZD1152-hQPA on viable/proliferating (High) and non-proliferating (Low) primary AML cells (p=0.009;Mann-Whitney).

flow cytometry using 7AAD to detect viable cells (Figure 7.12). There was no statistical significance between FLT3 (p=0.643), Pgp (p=0.589), or BCRP (p=0.791) status of primary samples and viability in response to AZD1152-hQPA in suspension culture. In this assay a reference to an internal standard of fixed and stained mononuclear cells is used. This allows us to determine the absolute number rather than the proportion of viable cells remaining at the end of the culture period. When control cell viability count as a percent of the starting concentration was examined and compared to the percent of control viability of cells treated with AZD1152-hQPA a statistical significance (p=0.009) was seen (Figure 7.13). The % untreated cells surviving data was normally distributed, so for statistical purposes, values above and below the mean were used to classify samples as high (viable/proliferating) or low (non-proliferating) respectively. Clearly then, a response to AZD1152-hQPA in suspension culture was seen predominantly in those primary samples that were viable/proliferating, regardless

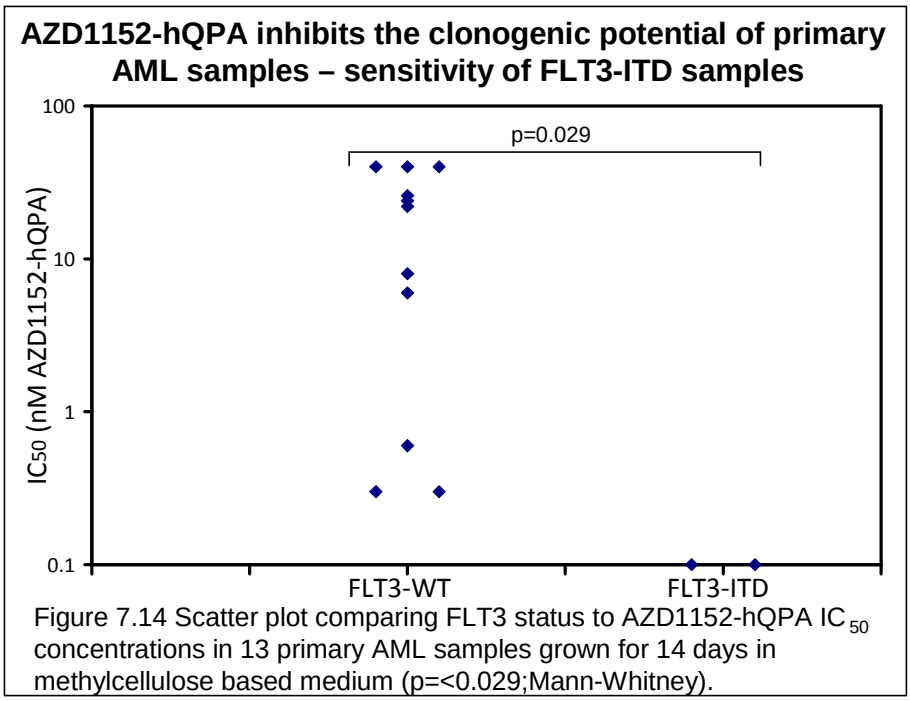

Figure 7.14 Scatter plot comparing FLT3 status to AZD1152-hQPA IC_{50} concentrations in 13 primary AML samples grown for 14 days in methylcellulose based medium (p=<0.029;Mann-Whitney).

of the FLT3, Pgp or BCRP status of the cells. There is no "gold standard" assay for primary AML cellular response to a drug in culture. It was decided to switch to a methylcellulose based colony forming assay to determine growth inhibition in response to AZD1152-hQPA in primary cells. This assay has the disadvantage that fresh samples are needed for optimal colony growth and these are in limited supply.

Consecutive fresh primary AML samples (20 FLT3-WT and 8 FLT3-ITD) were grown for 14 days in methylcellulose based medium containing 0-30nM AZD1152-hQPA. Colonies were counted under the microscope and growth was defined as greater than 12 colonies present in untreated wells. Colonies were detected in untreated samples from 11 FLT3-WT but only 2 FLT3-ITD cases. IC_{50} was calculated compared to untreated controls. The two FLT3-ITD samples were

both more sensitive to AZD1152-hQPA induced growth inhibition than any of the wild type samples (p=0.029) (Figure 7.14).

In this chapter the ability to measure the pHH3 biomarker and to target it in primary AML cells is demonstrated. Pgp and ABCG2 expressing primary samples are less sensitive to AZD1152-hQPA induced pHH3 inhibition although 50% inhibition of pHH3 was achieved in nearly 95% of these samples in contrast to the resistance seen in cell lines. FLT3-ITD primary samples are more sensitive to AZD1152-hQPA in terms of pHH3 and pSTAT5 inhibition and colony forming potential.

Chapter Eight
DISCUSSION

8.1 Study aims and objectives

The aurora kinase family members are essential for normal mitotic progression and have attracted great interest as potential new therapeutic targets (Kollareddy *et al.*, 2012). The aim of this study was to investigate the efficacy of the novel aurora-B kinase inhibitor AZD1152-hQPA in a panel of AML cell lines and primary samples. Initially, particular attention was paid to the ABC transporter status of AML cell lines and its effect on the sensitivity of AZD1152-hQPA, by measuring the biomarker pHH3. Our studies showed that AML cell lines with elevated ABC transporter expression were relatively resistant to AZD1152-hQPA (Chapter 3). The mode of cell death following treatment with AZD1152-hQPA in our cell lines was investigated and also whether p53 status affects cellular response to the drug (Chapter 3). With the development of the OCI-AML3DNR cell line we were able to demonstrate that AZD1152-hQPA is effluxed by Pgp along with BCRP in our cell lines (Chapters 4 and 5). Subsequent investigations revealed that mutant FLT3 was a secondary target of AZD1152-hQPA in our cell lines (Chapter 6). Response to AZD1152-hQPA in primary AML samples was subsequently investigated with particular emphasis on their ABC transporter and FLT3 status (Chapter 7).

8.2 Biomarker assay optimization and chemosensitivity of AML cells to AZD1152-hQPA

Aurora-B is known to phosphorylate Histone H3 (pHH3) at the Ser10 position during mitosis (Giet, 2001; Bhaumik et al., 2007) and previous reports have shown

inhibition of pHH3 following treatment with aurora kinase inhibitors (Ditchfield et al., 2003; Keen, 2004). Inhibition of pHH3 reflects aurora-B inhibition and as such can be considered a biomarker for aurora-B activity. A clinical marker for aurora-A inhibition is currently not available (Kitzen et al., 2010). To be able to use pHH3 as a biomarker for AZD1152-hQPA activity in our cell lines and patient samples, we needed to develop a method to measure its expression, and its inhibition by the drug. The development and technical validation of a biomarker assay, particularly in clinical samples, is important as it allows an early indication of drug efficacy and gives a rapid and valid endpoint for our cell based assays.

A flow cytometric method was subsequently developed to simultaneously measure pHH3 expression, and DNA content, in our cell lines (Figure 3.1). Initially PI was used to counter-stain for DNA content. However because of spectral overlap between PI in the PE and the pHH3 antibody in the FITC channel, the counter-stain was changed to 7-AAD which has minimal spectral overlap with FITC (Rabinovitch *et al.*, 1986). The level of pHH3 detectable in untreated cell lines was low and expression in primary cells was expected to be even lower as a very small population of cells is actively dividing at the time of sampling. With this in mind, it was decided to pre-incubate the AML blasts with a cytokine cocktail to drive the cells into cycle before treatment with AZD1152-hQPA. Proliferation was seen in 51 out of 65 primary samples as measured by [^{3}H]-Tdr uptake and levels of pHH3 were comparable to those found in cell lines (Figure 7.1). The pHH3 antibody stained with extreme brightness (Figure 3.1) and an initial publication of this method seems to have missed the pHH3 positive population entirely, reporting a

shift in autofluorescence as evidence of biomarker targeting (Yang *et al.,* 2007). A detailed protocol of the optimized assay is included in the appendix of this thesis. Real-time PCR confirmed that aurora-B mRNA levels correlated to basal pHH3 expression in primary AML blasts (Figure 7.3). This was to be expected as aurora-B is known to phosphorylate Histone H3 and both are indicative of cells in G_2/M (Giet, 2001; Bhaumik *et al.*, 2007). pHH3 inhibition was seen at short time periods after treatment with AZD1152-HQPA in all of the primary samples tested (Figure 7.4).

Treatment with AZD1152-hQPA resulted in inhibition of pHH3, accumulation of cells with >4N DNA content, and subsequent loss of viability in a panel of leukaemic cell lines (Figures 3.4-3.6). To determine mode of cell death, Annexin binding, along with active caspase-3 and 7A6 antigen expression were used, and it was shown that AZD1152-hQPA treated cell lines undergo apoptosis and that the polyploid population contained apoptotic cells (Figures 3.9-3.11). This agrees with previous studies which reported that aurora-B disruption in tumour cells forces cells through a catastrophic mitotic exit leading to polyploid cells that subsequently lose viability (Ditchfield *et al.,* 2003).

The way that AML is treated has changed little over the last thirty years and current chemotherapy is not cancer specific resulting in numerous unwanted side effects caused by damage to normal tissues, such as those of the bone marrow, gut mucosa and hair follicles. It is hoped that these toxic side effects can be minimized by using a drug with a specific target, such as aurora-B. Also it may be possible to

use a lower dose of current chemotherapy when used in combination with targeted drugs such as AZD1152-hQPA, again reducing toxicity. AZD1152-hQPA was compared in our cell lines to the standard chemotherapeutic agents used in AML, DNR and Ara-c, and a 72 hour IC_{50} was achieved in all but one cell line at lower concentrations of AZD1152-hQPA (Figure 3.7). The specificity of AZD1152-hQPA was significantly similar to that of DNR with the KG-1a cell line standing out as the most resistant to the two agents. DNR is known to be effluxed by Pgp in AML cells (Borg *et al.*, 2000) and the elevated expression of Pgp in the KG-1a cell line has been demonstrated. One group has published data suggesting that AZD1152-hQPA synergistically enhanced the anti-proliferative capacity of DNR in MOLM-13 cells (Ikezoe *et al.*, 2007). However, we found the opposite, in the same cell line using IC_{50} concentrations and calcusyn software to calculate a CI value; we found that there was moderate antagonism between the two agents (Figure 3.8). The cell line specificity profile of AZD1152-hQPA was significantly different to that of Ara-c. Promisingly, there was synergism between these two agents in the MOLM-13 cell line. One explanation for this could be the different modes of action of DNR and Ara-c. The anthracycline DNR forms a stable complex with DNA and interferes with nucleic acid synthesis but its cytotoxic effects are not cell cycle phase specific (Come *et al.*, 1999). The nucleoside analogue Ara-c is incorporated into newly synthesized DNA leading to chain termination and inhibition of DNA synthesis (Ravandi *et al.*, 2004). As such it exhibits cell cycle phase specificity and primarily kills cells undergoing DNA synthesis (S-phase). AZD1152-hQPA targets cells specifically in the G_2/M phase of the cell cycle so it is reasonable to presume that drugs that induce S-phase

inhibition should not necessarily be synergistic in combination with AZD1152-hQPA. However it may be this two pronged targeting of either ends of the cell cycle that accounts for the synergy between these two drugs. Also, this synergy was found in cell lines, which tend to be much more synchronized than cells *in vivo*, where this dual targeting of the cell cycle may be enhanced. Because of the small number of cells in G_2/M phase at any one time, as demonstrated by the amount of baseline cells expressing pHH3 (Figure 3.4 and Figure 7.1B), the drug should be administered as a continuous infusion over long time periods for maximal benefit. A phase II clinical trial in AML patients combining AZD1152-hQPA over 7 days continuous infusion with low dose Ara-c is currently ongoing (Clinicaltrials.Gov, April 2012).

8.3 p53 mutation and AZD1152-hQPA sensitivity in AML

The non-specific aurora kinase inhibitor, VX-680, has been shown to preferentially induce endoreduplication in cells with compromised p53 (Gizatullin *et al.*, 2006). The p53 tumour suppressor gene is mutated and/or deleted in more than 50% of solid tumours (Levine, 1997). It is possible then, that cells lacking functional p53 might be selectively sensitive to aurora kinase inhibition, providing a benefit for normal cells over tumour cells. However, haematological malignancies do not contain frequent alterations in the p53 gene, with one study detecting loss of p53 in only 5% of over two thousand adult AML patients (Fenaux *et al.*, 1992; Seifert *et al.*, 2009). Our cell lines were sequenced for p53 expression and their DNA content measured after treatment with AZD1152-hQPA (Figure

3.14). AZD1152-hQPA preferentially induced endoreduplication in the p53 compromised HL-60 and U937 cells in comparison to p53wt cells, findings that agree with reported data on VX-680 (Gizatullin *et al.*, 2006). However, although the p53wt cell lines were checked in comparison with p53-compromised cells, p53wt did not save our AZD1152-hQPA treated AML cell lines from massive endoreduplication and ultimate loss of viability. It appears then that p53 restrains endoreduplication after aurora-B inhibition by AZD152-hQPA. These findings are consistant with Ditchfield et al and their investigations with the dual aurora inhibitor ZM447439 in HeLa cells (Ditchfield *et al.*, 2003). Also, p53 compromised U937 cells acquired DNA damage quicker (in the G_1/S phase of the cell cycle) when compared to the p53wt MV4-11 and OCI-AML3 (Figure 3.12) cells indicating a role for p53 in DNA damage response to AZD1152-hQPA. Recently published data suggests a direct link to aurora-B and p53 via NIR (novel INHAT repressor), a transcriptional co-repressor with inhibitor of histone acetyltransferase activity, which is known to suppress p53 transcriptional activity and function (Wu *et al.*, 2011). This group demonstrate that aurora-B, NIR and p53 exist in a protein complex in which aurora-B binds to NIR and also phosphorylates p53 suppressing its activity (Wu *et al.*, 2011) (Figure 8.1). They also report that inhibition of aurora-B causes p53-dependent apoptosis and cell growth arrest, due to the up-regulation of p21 and Bax. This suggests a possible mechanism for the apoptosis seen in response to AZD1152-hQPA in our p53wt AML cell lines. Interestingly, VX-680 has been shown to act synergistically to induce apoptosis in p53wt AML cell lines with Nutlin-3, which is a small molecule antagonist of the p53 regulator Mdm2 (Kojima *et al.*, 2008). This

suggests a rationale for the dual targeting of aurora kinases and Mdm2 in AML where p53 mutations are rare and downstream p53 signalling is mostly intact.

8.4 The effect of ABC transporters on the efficacy of AZD1152-hQPA

Elevated expression of the MDR1 gene coding for the drug efflux pump Pgp and the ABCG2 gene encoding BCRP are both associated with worse remission rates in AML (Leith *et al.*, 1997; Damiani *et al.*, 2006). Any potential new drug for the treatment of AML should therefore be screened for its efficacy in patients expressing high levels of these drug transporters. Initial experiments showed that our Pgp positive (KG-1a) and BCRP positive (OCI-AML6.2) cell lines were much less sensitive to AZD1152-hQPA in comparison to transporter negative cell lines. This was seen at both the biomarker and subsequent viability level (Figure 4.1). Because there was no parental Pgp negative comparison for the KG-1a cell line, it was decided to create a Pgp expressing cell line from the OCI-AML3 cells. No increase in Pgp expression or function after our nucleofection MDR1 transfection assays was detected. Although the transfected cells grew in the presence of G418 (in contrast to the control cells), indicating that the cells retained the neomycin resistance gene, no increase in Pgp protein was observed, suggesting that the MDR1 gene may have been ejected by the cells. One explanation could be a problem with the pCMV promoter region and it has also been reported that viral gene transfer methods are more efficient in leukaemia and lymphoma cells (Schakowski *et al.*, 2004). Along with this a literature search reveals a paucity of

data where the MDR1 gene has been successfully transfected into AML cells. As such it was decided to try and select for elevated Pgp expression in the OCI-AML3 cell line using the known Pgp substrate DNR (Legrand *et al.*, 1999; Borg *et al.*, 2000). The subsequently developed OCI-AML3DNR cell line expressed significantly more Pgp both at the protein and functional level (Figures 4.7) and importantly no increase in BCRP or MRP expression was seen (Figures 4.7 and 4.8). Also, STR analysis of the OCI-AML3DNR cell line was identical to the parent cell line and the cell line phenotype and FLT3 status matched that of the parent cell line (Table 4.1). Therefore the OCI-AMLDNR cell line is a relatively clean model for measuring Pgp related MDR. The OCI-AMLDNR cell line was significantly more resistant to AZD1152-hQPA, in terms of biomarker inhibition and loss of viability, compared to the sensitive OCI-AML3 parent cells (Figure 5.1). Using the UIC2 shift assay and fluorescent dye accumulation assays it was shown that AZD1152-hQPA is neither a substrate of Pgp or modulates the function of Pgp or BCRP in the resistant cell lines (Figure 5.2 and 5.3). By using radioabelled ^{14}[C]-AZD1152-hQPA in combination with known Pgp and BCRP inhibitors it was shown definitively that the drug is being effluxed by these transporters in the OCI-AML3DNR and OCI-AML6.2 cells accounting for the resistance seen in both cell lines (Figure 5.4). The resistance to AZD1152-hQPA in the transporter positive cell lines was reversed when known inhibitors of Pgp and BCRP were co-cultured with AZD1152-hQPA (Figure 5.5).

8.5 The FLT3-ITD mutation is a secondary target of AZD1152-hQPA

Through the course of our studies, the particular sensitivity of the FLT3-ITD expressing MV4-11, and MOLM-13 cell lines, to AZD1152-hQPA was noticed. Both had IC_{50} values for viability and pHH3 inhibition of <10nM and were therefore the most sensitive of any of the lines tested (Figure 6.1). The FLT3 gene is one of the most commonly mutated genes in AML either as FLT3-ITD (24%) or FLT3 activation loop mutation (7%), and is associated with poor prognosis (Gilliland, 2002; Hunter *et al.*, 2004). Interestingly, VX-680, a selective inhibitor of all three aurora kinases, also exhibits cross-inhibitory activity against the receptor tyrosine kinase FLT3 and ablated colony formation in primary AML cells with FLT3-ITD (Harrington *et al.*, 2004; Carvajal *et al.*, 2006).

Because AZD1152-hQPA has been designed to specifically target aurora-B kinase, one of the questions that needed to be addressed was whether AZD1152-hQPA is also targeting FLT3 in the sensitive FLT3-ITD cell lines. AZD1152-hQPA has shown > 100-fold specificity for aurora B kinase in a panel of 50 other serine/threonine and tyrosine kinases, including FLT3, but its action against mutated FLT3 had not been reported (Keen *et al.*, 2005). ITD mutation of FLT3 induces activating phosphorylation of the receptor in the absence of ligand (Gilliland, 2002). Oncogenic activation by ITD mutation is also known to activate aberrant signalling, including direct STAT5 activation (Choudhary *et al.*, 2007), whilst ligand-induced FLT3-WT does not directly activate STAT5 (Mizuki *et al.*,

2000; Spiekermann *et al.,* 2003). Measurement of pSTAT5 can be performed by flow cytometry and requires relatively small amounts of cellular material so it was deemed important to optimize this assay for potential use with patient samples. One hour incubation at low doses of AZD1152-hQPA resulted in down-regulation of pSTAT5 in both the FLT3-ITD cell lines (Figure 6.4). Encouraged by this, pFLT3 expression was measured in the ITD cell lines by immunoblotting. FLT3 dephosphorylation is shown after 1 hour incubation at doses as low as 30nM AZD1152-HQPA (Figure 6.5). This was the first demonstration that AZD1152-hQPA inhibits pFLT3 in ITD cell lines along with its down-stream target pSTAT5.

The FLT3-ITD MV4-11 cell line is cytokine independent, but growth is enhanced in the presence of IL-3 (Santoli *et al.*, 1987). Also, the addition of IL-3 has been shown to rescue the growth of BaF3/ITD cells in the presence of the FLT3 inhibitor CEP-701 (Levis *et al.*, 2002). Activation of the IL-3 receptor induces the activity of the JAK/STAT (leading to STAT5 phosphorylation), Raf/MEK/ERK and PI3K/Akt pathways, which results in cell proliferation and prevention of apoptosis (Steelman *et al.*, 2004). It was demonstrated that IL-3 does not protect MV4-11 cells from AZD1152-hQPA induced loss of viability (Figure 6.6). So introducing pSTAT5 via an alternative pathway does not protect MV4-11 cells from the effects of AZD1152-hQPA suggesting it is the dual targeting of FLT3-ITD and aurora-B that is responsible for the enhanced sensitivity in these cells.

8.6 Effect of AZD1152-hQPA on primary AML cells

In our viability assays, a response was seen to AZD1152-hQPA in suspension culture predominantly in those primary samples that were viable and proliferating regardless of the Pgp, BCRP or FLT3 status of the cells (Figure 7.12 and 7.13). This demonstrates that cells need to go through the G_2/M phase to elicit a response from AZD1152-hQPA as only the proliferating cells were responding. Also, the quality of the sample in terms of its age and the effect of freeze/thawing could well have an effect on its ability to proliferate in suspension culture. Because of this priority was given to the pHH3 biomarker, over cell death, as a measure of response to AZD1152-hQPA in primary samples.

pHH3 expression was measured in 37 primary AML samples cultured for one hour with or without AZD1152-hQPA. 9/37 (24.3%) were positive for Pgp and 9/35 (25.7%) were positive for BCRP with a significant correlation ($p=0.008$, $R^2=0.238$) seen for co-expression. This data agrees with results seen previously (Damiani *et al.*, 2006). Pgp positive samples were significantly less sensitive to AZD1152-hQPA induced pHH3 inhibition compared to Pgp negative samples ($p=0.001$) as were BCRP positive samples compared to BCRP negative samples ($p=0.001$) (Figure 7.6 and 7.7). Importantly though, >50% inhibition of pHH3 was still seen in all but 2 primary samples (94.6%). So certainly at the level of the biomarker a much better response was seen in ABC transporter positive primary samples than in transporter positive cell lines at the corresponding dose of AZD1152-hQPA. Whereas in the transporter positive cell lines efflux of

AZD1152-hQPA using radio-labelled AZD1152-hQPA was demonstrated it is clear that all of our primary samples retained enough drug to target the pHH3 biomarker. This difference in response may be explained by the 'artificially' high transporter expression seen in the cell lines. For example, if we look at our measure of Pgp function, the mean CSA modulation ratio in our primary samples was 1.74. Four times this was seen in the Pgp expressing OCI-AML3DNR cell line and greater than seven times seen in the Pgp expressing KG-1a cell line. Likewise the amount of Pgp protein measured using the MRK-16 antibody was 2-fold higher in the OCI-AML3DNR cells and 7-fold higher in the KG-1a cells compared to the mean value of 1.13 seen in primary samples. A study of 149 AML patient samples reported that Pgp and BCRP expression was a prognostic factor and patients who co-expressed Pgp and BCRP had the poorest prognosis (Benderra *et al.*, 2004). It is demonstrated here that primary samples with high Pgp and/or BCRP expression, are less sensitive to AZD1152-hQPA, although an IC_{50} for pHH3 inhibition was achieved in 3/5 (60%) samples that co-expressed Pgp and BCRP. Clearly then, AZD1152-hQPA is able to enter these cells and target aurora-B and pHH3 in these primary samples, even when they express high levels of both Pgp and BCRP.

Results to support our findings have recently been reported in data from solid tumours. Using whole-genome microarray techniques to analyse two AZD1152-hQPA resistant colon and pancreatic cell lines it was discovered that it was amplification of genes that encode for Pgp and BCRP that conferred resistance to the drug (Guo *et al.*, 2009). Inhibiting Pgp as a way of reversing MDR has been

intensively studied for many years. Pharmacological inhibition of Pgp by small-molecule antagonists has been studied in several AML trials with various agents but only yielding little clinical success (Mahadevan, 2004; Szakacs *et al.*, 2006). Many of these agents are substrates for other transporters and enzyme systems resulting in unpredictable pharmacokinetic interactions in the presence of chemotherapy agents. Recently more specific so called third generation inhibitors of MDR, such as zosuquidar, have been developed that have the potential to minimize any drug-drug interactions (Lancet *et al.*, 2009). A combination of these inhibitors with AZD1152-hQPA could circumvent any problem of drug efflux by ABC transporters seen with this drug. Another strategy to overcome susceptibility to the effects of MDR would be to design a novel aurora kinase inhibitor whose activity is not influenced by drug efflux mediated by ABC transporters. One such inhibitor, AMG-900, is discussed later.

It was demonstrated that AZD1152-hQPA inhibits pFLT3 in ITD cell lines along with its down-stream target pSTAT5. AZD1152-hQPA caused growth inhibition of primary AML blasts in our colony formation assays and again the FLT3-ITD samples were the most sensitive of those tested (Figure 7.14). FLT3-ITD primary samples were also particularly sensitive to pSTAT5 down-regulation after treatment with AZD1152-hQPA, compared to FLT3-WT samples (Figure 7.8). FLT3-ITD primary samples were also found to be the most sensitive to AZD1152-hQPA induced pHH3 inhibition (Figure 7.8) which is intriguing as pHH3 is widely reported to be a direct substrate of aurora kinase B. One possible explanation for this could be the role of survivin, a member of the inhibitors-of-apoptosis protein

(IAPs) family, which has recently been demonstrated to lie downstream of FLT3-ITD signalling (Fukuda *et al.*, 2009). Survivin along with aurora-B, INCENP and borealin makes up the chromosomal passenger complex which plays a key role in mitotic progression. One study reported that treatment of FLT3-ITD MV4-11 leukaemia cells with the FLT3-ITD inhibitor SU5416 resulted in reduced survivin expression and inhibited cell proliferation (Fukuda *et al.*, 2009). Survivin is highly expressed in various malignant cells, including leukaemic cells, and small molecule (YM155), and antisense (SPC3042) inhibitors of survivin are currently in phase I and phase II clinical trials (Hansen *et al.*, 2008; Lewis *et al.*, 2009). It has recently been reported that survivin expression levels are prognostic in AML and that survivin is over-expressed in CD34+/CD38- AML stem/progenitor cells when compared to bulk AML blasts (Carter *et al.*, 2012). Survivin may therefore be an important target in AML therapy. Interestingly, AZD1152-hQPA has also been reported to inhibit survivin expression along with pHH3 and Rb protein in Burkitt's and Hodgkin's lymphoma cell lines (Mori *et al.*, 2011). This group demonstrated survivin inhibition in these cells followed by caspase-9 and caspase-3 activation with subsequent apoptosis (Figure 8.1). They also concluded that Rb inhibition in these cells resulted in the polyploid phenotype associated with aurora-B inhibition.

An important problem with the current crop of small molecule FLT3 inhibitors being tested in AML is mechanisms of acquired resistance. These include the development of secondary mutations in the FLT3 gene, elevated levels of FL after

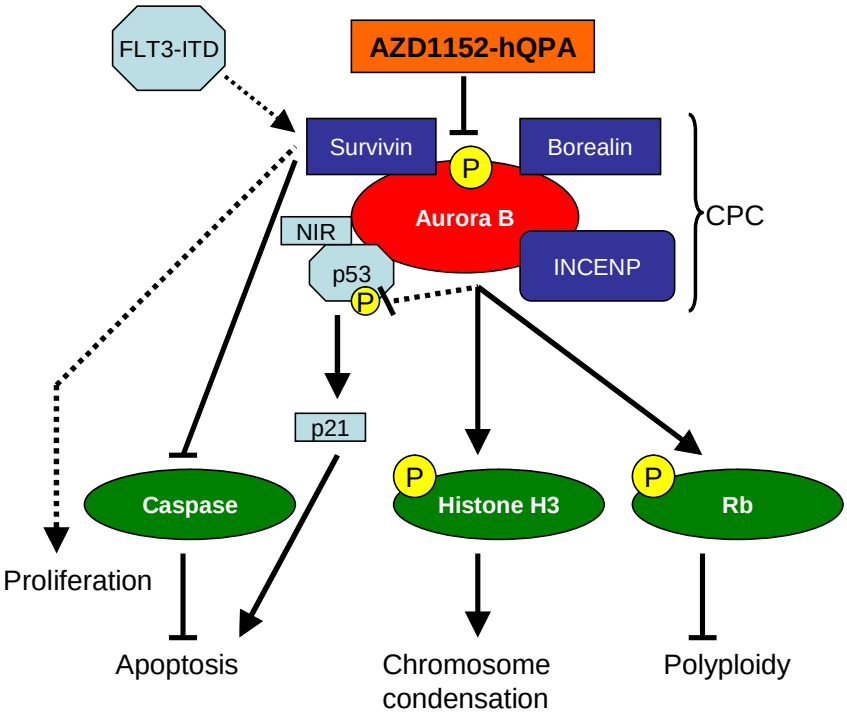

Figure 8.1 Interactions of aurora-B and the CPC. Adapted from Mori et al Biochem Pharmacol 2011.

chemotherapy and also over-expression of survivin (Zhou *et al.*, 2009; Sato *et al.*, 2011). An interesting study recently reported the effect of CCT241736 on MOLM-13 and MV4-11 AML cell lines selected for resistance against the FLT3 inhibitor MLN518 (tandutinib) (Moore *et al.*, 2011). Like AZD1152-hQPA, CCT241736 is a dual aurora kinase and FLT3-ITD inhibitor. Unlike the selective FLT3 inhibitors MLN518 and AC220, the in vitro cellular efficacy of CCT241736 was not affected by high levels of FL in AML cell lines. Furthermore, CCT241736 inhibited a wide range of FLT3 mutants, including FLT3-ITD, -D835Y, -D835H, -K663Q and –N841I.

The presence of a FLT3-ITD results in an increased auto-phosphorylation of the FLT3 receptor tyrosine kinase and thereby increased cellular proliferation

(Gilliland, 2002). pHH3 expression is limited to mitosis and therefore proliferating cells. It is demonstrated here that primary FLT3-ITD samples have statistically higher basal pHH3 expression than FLT3-WT samples thus rendering them more susceptible to AZD1152-hQPA (Figure 7.9). Of our primary samples, 40.5% had the FLT3-ITD mutation. This is more than the 24% expected and described in the literature (Gilliland, 2002). Occurrence of FTL3-ITD has been strongly associated with higher peripheral leukocyte count and higher blast percentages (Kottaridis *et al.*, 2001; Schnittger *et al.*, 2002). This means that in samples with a FLT3-ITD, we would expect a larger blast percentage available after separation over Histopaque, to be cryo-preserved for future use. So in effect we are selecting for FLT3-ITD samples in the lab giving a false positive percentage of these samples occurring in our frozen primary sample pool and hence the slightly higher than expected value of 37.8% in our primary samples. No FLT3-ALMs were detected in our primary sample group. This is not particularly surprising as only 7% of AML patients are reported to have this mutation (Gilliland, 2002) and in contrast to FLT3-ITD mutations, FLT3-ALMs are not associated with higher diagnostic white cell counts (Meshinchi *et al.*, 2006). The same argument applies to the percentage of Pgp positive samples that were seen (24.3%). Pgp has been reported to be expressed in 47% of elderly AML cases (Burnett *et al.*, 2009) compared to 34% in younger patients (Pallis *et al.*, 2011). High Pgp protein expression is associated with low WBC count (Seedhouse *et al.*, 2007) so it would be expected that there would be fewer cryo-preserved Pgp positive samples.

A recent study found that out of 171 AML patients, 2% had clones that co-expressed FLT3-ITDs and Pgp, and these patients had a very poor prognosis (Marzac *et al.*, 2006). In our sample group 5% (2/37) of the samples co-expressed a FLT3-ITD and Pgp. It should be noted that an IC_{50} for pHH3 inhibition was achieved in both these samples. It was also found that FLT3-ITDs are inversely associated with functional Pgp activity (Figure 7.10). The mean modulation ratio in FLT3 wild-type samples was 2.13, and in ITD samples it was 1.27 (p=0.038). These results agree with previous findings from our group (Pallis *et al.*, 2003b). In the two samples where FLT3-ITD was associated with high Pgp expression there was no statistical significance in terms of pHH3 response to AZD1152-hQPA. FLT3-ITD mutations are associated with higher proliferation and a higher diagnostic WBC, in contrast to the low WBC count associated with high Pgp expression (Kottaridis *et al.*, 2001; Seedhouse *et al.*, 2007). One explanation for this could be a loss of Pgp phenotype under increased proliferative capacity as reported by Smeets et al (Smeets *et al.*, 1999). The authors report that non-cycling progenitor cells, both normal and leukaemic, have a relatively high MDR functionality. A direct link between FLT3-ITD tyrosine kinase activity and Pgp expression has been suggested. Our group has recently identified FOXO1 as a gene co-expressed with ABCB1, and determined that manipulation of FOXO1 expression levels, leads to corresponding changes in Pgp expression (Seedhouse *et al.*, 2009). FOXO1 is a transcription factor that mediates a cellular stress response by inhibiting cell growth and up-regulating expression of molecules involved in apoptosis and antioxidant defences (Tothova, 2007). Seedhouse et al suggest that

FOXO1 acts on an axis with Pgp and FLT3, where FOXO1 up-regulates Pgp, and FLT3-ITDs suppress FOXO1 (Seedhouse *et al.*, 2009).

Tiribelli et al found a significant correlation between over-expression of FLT3-ITD and ABCG2 and that this subgroup of AML patients had a significantly worse prognosis (Tiribelli *et al.*, 2010). This group measured BCRP by flow cytometry using the BXP-34 antibody and they reported that 70% of their FLT3-ITD samples were associated with high BCRP expression. Four out of fourteen (26.6%) of our FLT3-ITD samples expressed high levels of ABCG2 such that no correlation between FLT3 and BCRP status was found in our sample group (p=0.586). This may be explained by our relatively small number (n=35) of patient samples compared to the 166 sampled by Tiribelli's group and also by the different methods of measuring BCRP/ABCG2 expression.

8.7 Aurora kinase inhibitors in clinical development

There are currently more than 30 aurora kinase inhibitors in various stages of pre-clinical and clinical studies and those in clinical development are listed in table 8.1 (Kollareddy *et al.*, 2012). Because of their diverse chemical structures many of these inhibitors have off-target activities, as has been demonstrated with AZD1152, and its activity against pFLT3. One of the most interesting and advanced of the aurora kinase inhibitors is PHA-739358 (Danusertib) which has been shown to have good pharmacokinetics and anticancer activity in patients with advanced solid tumours (Cohen *et al.*, 2009). Danusertib exhibits inhibitory

Table 8.1 – Aurora kinase inhibitors in clinical trials. (Adapted from (Kollareddy *et al.*, 2012)).

COMPOUND	IN VITRO POTENCY	CLINICAL DEVELOPMENT
PAN-AURORA KINASE INHIBITORS		
PHA-739358	Aurora $A_{(IC50)}$ - 13nM Aurora $B_{(IC50)}$ - 79nM Aurora $C_{(IC50)}$ - 61nM	Phase II – Advanced solid tumours and leukaemias.
CYC116	Aurora $A_{(IC50)}$ - 44nM Aurora $B_{(IC50)}$ - 19nM Aurora $C_{(IC50)}$ - 65nM	Phase I – Advanced solid tumours.
SNS-314	Aurora $A_{(IC50)}$ - 9nM Aurora $B_{(IC50)}$ - 31nM Aurora $C_{(IC50)}$ - 3nM	Phase I – Advanced solid tumours.
VX-680	Aurora $A_{(IC50)}$ - 0.7nM Aurora $B_{(IC50)}$ - 18nM Aurora $C_{(IC50)}$ - 4.6nM	Terminated due to severe toxicities.
R763	Aurora $A_{(IC50)}$ - 4nM Aurora $B_{(IC50)}$ - 4.8nM Aurora $C_{(IC50)}$ - 6.8nM	Phase I – Advanced solid tumours.
AT9283	Aurora $A_{(IC50)}$ - 3nM Aurora $B_{(IC50)}$ - 3nM	Phase II – Refractory solid tumours and leukaemias.
PF-03814375	Aurora $A_{(IC50)}$ - 5nM Aurora $B_{(IC50)}$ – 0.8nM	Phase I – Advanced solid tumours.
GSK1070916	Aurora $B_{(IC50)}$ – 3.5nM Aurora $C_{(IC50)}$ – 6.5nM	Phase I – Advanced solid tumours and leukaemias.
AMG-900	Aurora $A_{(IC50)}$ - 5nM Aurora $B_{(IC50)}$ - 4nM Aurora $C_{(IC50)}$ - 1nM	Phase I – Advanced solid tumours and acute leukaemias.
SPECIFIC AURORA KINASE INHIBITORS		
MLN8237	Aurora $A_{(IC50)}$ - 1nM	Phase II – Advanced solid tumours, AML and MDS.
ENMD-2076	Aurora $A_{(IC50)}$ - 14nM	Phase II – Refractory ovarian cancers.
MK-5108	Aurora $A_{(IC50)}$ – 0.064nM	Phase I – Advanced and refractory solid tumours.
AZD1152	Aurora $B_{(IC50)}$ – 0.37nM	Phase II – Advanced solid tumours, acute leukaemia and B-cell lymphoma.

activity against all three aurora kinases as well as other off-target oncogenic kinases such as Ret, FGFR-1 and Bcr-Abl tyrosine kinase including its multidrug resistant T315I mutant (Gontarewicz, 2010). This mutation is responsible for up to

25% of all clinically observed resistances in CML patients undergoing imatinib therapy and danusertib is currently in phase II studies in this group of CML patients (Paquette *et al.*, 2007). Along with all three aurora kinases CYC116 has been shown to inhibit VEGFR-2 which directly promotes angiogenesis (Kollareddy *et al.*, 2012). Inhibition of angiogenesis is a novel approach for suppressing metastasis in the treatment of solid tumours and this has encouraged further clinical development of CYC116. AT9283 is a multikinase inhibitor with activity against aurora-A and B and also JAK2 (janus kinase 2), JAK3 and Abl. Like Danusertib the compound was found to inhibit proliferation of cells with both wild type BCR-ABL and T315I BCR-ABL (Tanaka *et al.*, 2010). The pan-aurora kinase inhibitor AMG-900 has been shown to be broadly active in taxane resistant Pgp and BCRP expressing cell lines along with 3 multidrug resistant xenograft models (Payton *et al.*, 2010). This compound may therefore have an advantage over AZD1152 in its ability to negate any MDR conferred by high ABC transporter expression. Interestingly AMG-900 was more potent than AZD1152, VX-680 and danusertib when tested in P-gp expressing cell lines (Payton *et al.*, 2010). Two phase I studies are currently recruiting patients to study AMG-900 in AML and advanced solid tumours.

8.8 The future of AZD1152 (Barasertib)

AZD1152 (AZD1152-hQPA) has recently been given the international nonproprietary name of Barasertib (Barasertib-hQPA). A phase I/II study of AZD1152 was undertaken in a Western population of patients with advanced

AML or newly diagnosed patients for whom no standard therapies were anticipated to result in durable remission (Lowenberg *et al.*, 2009). AZD1152 had acceptable tolerability with the most commonly reported adverse effect being febrile neutropenia and stomatitis/mucosal inflammation which were generally manageable. The maximum tolerated dose (MTD) of AZD1152 given as a continuous intravenous infusion over 7 days was established as 1200mg with an overall haematological response rate of 25%. A similarly designed study in Japanese patients with advanced AML found a similar pharmacokinetic profile and minimal adverse effects with a 19% overall haematological response (Tsuboi *et al.*, 2011). The findings in both these studies are in contrast to previous studies of AZD1152 and other aurora kinase inhibitors in patients with solid tumours where only stable disease has generally been reported (Boss *et al.*, 2006; Steeghs *et al.*, 2009; Traynor *et al.*, 2011). A major topic of current research is the combination of other cytotoxic agents and radiotherapy with aurora kinase inhibitors. Two studies have reported that AZD1152 sensitizes cancer cells to ionizing radiation in prostate cancer (Niermann *et al.*, 2011) and colorectal and lung cancer cell lines (Tao *et al.*, 2008). There is pre-clinical data suggesting synergy between AZD1152 and the topoisomerase I poison CPT-11 (Irinotecan) in colon cancer xenograft models (Nair *et al.*, 2009). Another group found that AZD1152 enhanced the effectiveness of the alkylating agent oxaliplatin, and the nucleoside analogue gemcitabine, in colon and pancreatic cancer xenografts respectively (Azzariti *et al.*, 2011). Both studies state that the administration schedule of drug administration is crucial when combining AZD1152-hQPA with another chemotherapeutic agent. A further study, reported enhanced tumour growth

inhibition in human xenograft models, when AZD1152-hQPA was combined with the MEK1/2 inhibitor selumetinib compared with monotherapies (Holt *et al.*, 2012). This group also reported the importance of scheduling as AZD1152-hQPA before selumetinib was more beneficial than when selumetinib was dosed before AZD1152-hQPA. Synergism was found between AZD1152-hQPA and Ara-c in our cell lines. A multi-centre phase II clinical trial in patients aged over 60 with newly diagnosed AML is currently ongoing. Its aims are to assess the efficacy, safety, and tolerability of AZD1152 alone, and in combination with low dose Ara-c, in comparison with low dose Ara-c alone. Another phase II trial is similarly investigating the effects of AZD1152 in relapsed/refractory diffuse large B-cell lymphoma.

8.9 Conclusions and future work

It is commonly accepted that the AML phenotype results from multiple genetic/epigenetic lesions affecting differentiation, proliferation, and apoptosis. Consequently, targeting of a single aberrant protein is unlikely to eradicate the leukaemic clone. Furthermore, although several molecularly targeted therapies have been shown to be active in AML, it is clear from early clinical studies that most of these novel agents will need to be used in combination with conventional cytotoxic therapy. AZD1152 appears to be a promising new agent for treatment of individuals with AML because of its dual targeting of aurora-B and the FLT3-ITD. In particular, those patients who have an ITD mutation in the FLT3 gene should benefit, as we have demonstrated that these samples have high levels of pHH3

compared to FLT3-WT samples, and are less likely to have high levels of functional Pgp. MDR AML cell lines are a useful tool to model transporter mediated drug resistance but their efflux activity is extreme compared to that found in primary AML samples. Most clinical trials with Pgp modulators have been unsuccessful and thus the importance of efflux pumps in AML chemoresistance is unclear. Clinical trials with AZD1152 may help to resolve this issue, since pHH3 is such a clear-cut biomarker at the cellular level. In conclusion, Pgp and BCRP expression levels, and pHH3 down-regulation in patients treated with AZD1152 should be monitored in order to establish whether transporter-mediated efflux is sufficient to adversely impact on the efficacy of the agent.

References

ABBOTT, B. L. *et al.* Low levels of ABCG2 expression in adult AML blast samples. *Blood*, v. 100, n. 13, p. 4594-601, Dec 15 2002.

ABRAHAM, J. *et al.* A phase I study of the P-glycoprotein antagonist tariquidar in combination with vinorelbine. *Clin Cancer Res*, v. 15, n. 10, p. 3574-82, May 15 2009.

AMBUDKAR, S. V. *et al.* Biochemical, cellular, and pharmacological aspects of the multidrug transporter. *Annu Rev Pharmacol Toxicol*, v. 39, p. 361-98, 1999.

ANDREWS, P. D. *et al.* Mitotic mechanics: the auroras come into view. *Curr Opin Cell Biol*, v. 15, n. 6, p. 672-83, Dec 2003.

APPELBAUM, F. R. *et al.* Acute myeloid leukemia. *Hematology Am Soc Hematol Educ Program*, v., p. 62-86, 2001.

ATKINSON, A. J. *et al.* Biomarkers and surrogate endpoints: preferred definitions and conceptual framework. *Clin Pharmacol Ther*, v. 69, n. 3, p. 89-95, Mar 2001.

AZZARITI, A. *et al.* Aurora B kinase inhibitor AZD1152: determinants of action and ability to enhance chemotherapeutics effectiveness in pancreatic and colon cancer. *Br J Cancer*, v. 104, n. 5, p. 769-80, Mar 1 2011.

BAER, M. R. *et al.* Phase 3 study of the multidrug resistance modulator PSC-833 in previously untreated patients 60 years of age and older with acute myeloid leukemia: Cancer and Leukemia Group B Study 9720. *Blood*, v. 100, n. 4, p. 1224-32, Aug 15 2002.

BELLOC, F. *et al.* Flow cytometry detection of caspase 3 activation in preapoptotic leukemic cells. *Cytometry*, v. 40, n. 2, p. 151-60, Jun 1 2000.

BENDERRA, Z. *et al.* Breast cancer resistance protein and P-glycoprotein in 149 adult acute myeloid leukemias. *Clin Cancer Res*, v. 10, n. 23, p. 7896-902, Dec 1 2004.

BENDERRA, Z. *et al.* MRP3, BCRP, and P-glycoprotein activities are prognostic factors in adult acute myeloid leukemia. *Clin Cancer Res*, v. 11, n. 21, p. 7764-72, Nov 1 2005.

BHAUMIK, S. R. *et al.* Covalent modifications of histones during development and disease pathogenesis. *Nat Struct Mol Biol*, v. 14, n. 11, p. 1008-16, Nov 2007.

BISCHOFF, J. R. The Aurora/Ipl1p kinase family: regulators of chromosome segregation and cytokinesis. *Trends Cell Biol*, v. 9, n. 11, p. 454-9, Nov 1999.

BISCHOFF, J. R. *et al.* A homologue of Drosophila aurora kinase is oncogenic and amplified in human colorectal cancers. *Embo J*, v. 17, n. 11, p. 3052-65, Jun 1 1998.

BOESCH, D. *et al.* In vivo circumvention of P-glycoprotein-mediated multidrug resistance of tumor cells with SDZ PSC 833. *Cancer Res*, v. 51, n. 16, p. 4226-33, Aug 15 1991.

BONNET, D. Human acute myeloid leukemia is organized as a hierarchy that originates from a primitive hematopoietic cell. *Nat Med*, v. 3, n. 7, p. 730-7, Jul 1997.

BORG, A. G. *et al.* P-glycoprotein and multidrug resistance-associated protein, but not lung resistance protein, lower the intracellular daunorubicin accumulation in acute myeloid leukaemic cells. *Br J Haematol*, v. 108, n. 1, p. 48-54, Jan 2000.

BORG, A. G. *et al.* Overexpression of lung-resistance protein and increased P-glycoprotein function in acute myeloid leukaemia cells predict a poor response to chemotherapy and reduced patient survival. *Br J Haematol*, v. 103, n. 4, p. 1083-91, Dec 1998.

BOSS, D. S. *et al.* Clinical evaluation of AZD1152, an i.v. inhibitor of Aurora B kinase, in patients with solid malignant tumors. *Ann Oncol*, v., Oct 5 2006.

BRIZZI, M. F. *et al.* Expression and modulation of IL-3 and GM-CSF receptors in human growth factor dependent leukaemic cells. *Br J Haematol*, v. 76, n. 2, p. 203-9, Oct 1990.

BROXTERMAN, H. J. *et al.* Quality control of multidrug resistance assays in adult acute leukemia: correlation between assays for P-glycoprotein expression and activity. *Blood*, v. 87, n. 11, p. 4809-16, Jun 1 1996.

BURGER, H. *et al.* Imatinib mesylate (STI571) is a substrate for the breast cancer resistance protein (BCRP)/ABCG2 drug pump. *Blood*, v. 104, n. 9, p. 2940-2, Nov 1 2004.

BURNETT, A. K. *et al.* The Addition of Gemtuzumab Ozogamicin to Intensive Chemotherapy in Older Patients with AML Produces a Significant

Improvement in Overall Survival: Results of the UK NCRI AML16 Randomized Trial. v. 118. n. 212011a. p. 268-268.

BURNETT, A. K. *et al.* Identification of patients with acute myeloblastic leukemia who benefit from the addition of gemtuzumab ozogamicin: results of the MRC AML15 trial. *J Clin Oncol*, v. 29, n. 4, p. 369-77, Feb 1 2011b.

BURNETT, A. K. *et al.* The impact of dose escalation and resistance modulation in older patients with acute myeloid leukaemia and high risk myelodysplastic syndrome: the results of the LRF AML14 trial. *Br J Haematol*, v. 145, n. 3, p. 318-32, May 2009.

CARETA, F. P. *et al.* The Aurora A and B kinases are upregulated in bone marrow-derived chronic lymphocytic leukemia cells and represent potential therapeutic targets. *Haematologica*, v., Feb 13 2012.

CARMENA, M. The cellular geography of aurora kinases. *Nature Reviews Molecular Cell Biology*, v. 4, n. 11, p. 842-854, Nov 2003.

CARTER, B. Z. *et al.* Survivin Is Highly Expressed in AML Stem Cells and Predicts Poor Clinical Outcome. v. 118. n. 212012. p. 108-109.

CARVAJAL, R. D. *et al.* Aurora kinases: New targets for cancer therapy. *Clinical Cancer Research*, v. 12, n. 23, p. 6869-6875, Dec 2006.

CAZZANIGA, G. *et al.* Nucleophosmin mutations in childhood acute myelogenous leukemia with normal karyotype. *Blood*, v. 106, n. 4, p. 1419-22, Aug 15 2005.

CHAN, C. S. Isolation and characterization of chromosome-gain and increase-in-ploidy mutants in yeast. *Genetics*, v. 135, n. 3, p. 677-91, Nov 1993.

CHANG, T. T. Rational approach to the clinical protocol design for drug combinations: a review. *Acta Paediatr Taiwan*, v. 41, n. 6, p. 294-302, Nov-Dec 2000.

CHAPUY, B. *et al.* Intracellular ABC transporter A3 confers multidrug resistance in leukemia cells by lysosomal drug sequestration. *Leukemia*, v. 22, n. 8, p. 1576-86, Aug 2008.

CHIEFFI, P. *et al.* Aurora B expression directly correlates with prostate cancer malignancy and influence prostate cell proliferation. *Prostate*, v. 66, n. 3, p. 326-33, Feb 15 2006.

CHOUDHARY, C. *et al.* Activation mechanisms of STAT5 by oncogenic Flt3-ITD. *Blood*, v. 110, n. 1, p. 370-4, Jul 1 2007.

CLINICALTRIALS.GOV. Study to Investigate the Efficacy, Safety and Tolerability of AZD1152 Alone and in Combination With Low Dose Cytosine Arabinoside (LDAC) in Acute Myeloid Leukaemia (AML) Patients (SPARK-AML1). http://clinicaltrials.gov, April 2012.

COHEN, R. B. *et al.* A phase I dose-escalation study of danusertib (PHA-739358) administered as a 24-hour infusion with and without granulocyte colony-stimulating factor in a 14-day cycle in patients with advanced solid tumors. *Clin Cancer Res*, v. 15, n. 21, p. 6694-701, Nov 1 2009.

COME, M. G. *et al.* Dual mechanism of daunorubicin-induced cell death in both sensitive and MDR-resistant HL-60 cells. *Br J Cancer*, v. 79, n. 7-8, p. 1090-7, Mar 1999.

COSTELLO, R. T. *et al.* Human acute myeloid leukemia CD34+/CD38- progenitor cells have decreased sensitivity to chemotherapy and Fas-induced apoptosis, reduced immunogenicity, and impaired dendritic cell transformation capacities. *Cancer Res*, v. 60, n. 16, p. 4403-11, Aug 15 2000.

CRIPE, L. D. *et al.* Zosuquidar, a novel modulator of P-glycoprotein, does not improve the outcome of older patients with newly diagnosed acute myeloid leukemia: a randomized, placebo-controlled trial of the Eastern Cooperative Oncology Group 3999. *Blood*, v. 116, n. 20, p. 4077-85, Nov 18 2010.

CROSSMAN, L. C. Clinical results with imatinib in chronic myeloid leukaemia. *Leuk Res*, v. 28 Suppl 1, p. S3-9, May 2004.

DAMIANI, D. *et al.* The prognostic value of P-glycoprotein (ABCB) and breast cancer resistance protein (ABCG2) in adults with de novo acute myeloid leukemia with normal karyotype. *Haematologica*, v. 91, n. 6, p. 825-8, Jun 2006.

DAMIANI, D. *et al.* The role of MDR-related proteins in the prognosis of adult acute myeloid leukaemia (AML) with normal karyotype. *Hematol Oncol*, v. 25, n. 1, p. 38-43, Mar 2007.

DE GROUW, E. P. *et al.* Preferential expression of a high number of ATP binding cassette transporters in both normal and leukemic CD34+CD38- cells. *Leukemia*, v. 20, n. 4, p. 750-4, Apr 2006.

DE JONGE-PEETERS, S. D. *et al.* ABC transporter expression in hematopoietic stem cells and the role in AML drug resistance. *Crit Rev Oncol Hematol*, v. 62, n. 3, p. 214-26, Jun 2007.

DILLMAN, R. O. *et al.* A comparative study of two different doses of cytarabine for acute myeloid leukemia: a phase III trial of Cancer and Leukemia Group B. *Blood*, v. 78, n. 10, p. 2520-6, Nov 15 1991.

DITCHFIELD, C. *et al.* Aurora B couples chromosome alignment with anaphase by targeting BubR1, Mad2, and Cenp-E to kinetochores. *Journal of Cell Biology*, v. 161, n. 2, p. 267-280, Apr 2003.

DOGAN, A. L. *et al.* Evaluation and comparison of MRP1 activity with three fluorescent dyes and three modulators in leukemic cell lines. *Leuk Res*, v. 28, n. 6, p. 619-22, Jun 2004.

DOHNER, H. *et al.* Diagnosis and management of acute myeloid leukemia in adults: recommendations from an international expert panel, on behalf of the European LeukemiaNet. *Blood*, v. 115, n. 3, p. 453-74, Jan 21 2010.

DOYLE, L. A. *et al.* A multidrug resistance transporter from human MCF-7 breast cancer cells. *Proc Natl Acad Sci U S A*, v. 95, n. 26, p. 15665-70, Dec 22 1998.

ESTEY, E. Acute myeloid leukaemia. *Lancet*, v. 368, n. 9550, p. 1894-907, Nov 25 2006.

ESTEY, E. H. Acute myeloid leukemia: 2012 update on diagnosis, risk stratification, and management. *Am J Hematol*, v. 87, n. 1, p. 89-99, Jan 2012.

EVANS, R. P. *et al.* The selective Aurora B kinase inhibitor AZD1152 is a potential new treatment for multiple myeloma. *Br J Haematol*, v. 140, n. 3, p. 295-302, Feb 2008.

FENAUX, P. *et al.* Azacitidine prolongs overall survival compared with conventional care regimens in elderly patients with low bone marrow blast count acute myeloid leukemia. *J Clin Oncol*, v. 28, n. 4, p. 562-9, Feb 1 2010.

FENAUX, P. *et al.* Mutations of the P53 gene in acute myeloid leukaemia. *Br J Haematol*, v. 80, n. 2, p. 178-83, Feb 1992.

FERLAY, J. *et al.* Estimates of cancer incidence and mortality in Europe in 2008. *Eur J Cancer*, v. 46, n. 4, p. 765-81, Mar 2010.

FISCHER, T. *et al.* Phase IIB trial of oral Midostaurin (PKC412), the FMS-like tyrosine kinase 3 receptor (FLT3) and multi-targeted kinase inhibitor, in patients with acute myeloid leukemia and high-risk myelodysplastic syndrome with either wild-type or mutated FLT3. *J Clin Oncol*, v. 28, n. 28, p. 4339-45, Oct 1 2010.

FU, J. *et al.* Roles of Aurora kinases in mitosis and tumorigenesis. *Mol Cancer Res*, v. 5, n. 1, p. 1-10, Jan 2007.

FUKUDA, S. *et al.* Survivin mediates aberrant hematopoietic progenitor cell proliferation and acute leukemia in mice induced by internal tandem duplication of Flt3. *Blood*, v. 114, n. 2, p. 394-403, Jul 9 2009.

FULLER, B. G. *et al.* Midzone activation of aurora B in anaphase produces an intracellular phosphorylation gradient. *Nature*, v. 453, n. 7198, p. 1132-6, Jun 19 2008.

GALE, R. E. *et al.* No evidence that FLT3 status should be considered as an indicator for transplantation in acute myeloid leukemia (AML): an analysis of 1135 patients, excluding acute promyelocytic leukemia, from the UK MRC AML10 and 12 trials. *Blood*, v. 106, n. 10, p. 3658-65, Nov 15 2005.

GARCIA-MANERO, G. Demethylating agents in myeloid malignancies. *Curr Opin Oncol*, v. 20, n. 6, p. 705-10, Nov 2008.

GASSMANN, R. *et al.* Borealin: a novel chromosomal passenger required for stability of the bipolar mitotic spindle. *J Cell Biol*, v. 166, n. 2, p. 179-91, Jul 19 2004.

GEKELER, V. *et al.* The leukotriene LTD4 receptor antagonist MK571 specifically modulates MRP associated multidrug resistance. *Biochem Biophys Res Commun*, v. 208, n. 1, p. 345-52, Mar 8 1995.

GIET, R. Drosophila aurora B kinase is required for histone H3 phosphorylation and condensin recruitment during chromosome condensation and to organize the central spindle during cytokinesis. *J Cell Biol*, v. 152, n. 4, p. 669-82, Feb 19 2001.

GILLILAND, D. G. The roles of FLT3 in hematopoiesis and leukemia. *Blood*, v. 100, n. 5, p. 1532-42, Sep 1 2002.

GIRDLER, F. *et al.* Validating Aurora B as an anti-cancer drug target. *J Cell Sci*, v. 119, n. Pt 17, p. 3664-75, Sep 1 2006.

GIZATULLIN, F. *et al.* The Aurora kinase inhibitor VX-680 induces endoreduplication and apoptosis preferentially in cells with compromised p53-dependent postmitotic checkpoint function. *Cancer Res*, v. 66, n. 15, p. 7668-77, Aug 1 2006.

GLOVER, D. M. *et al.* Mutations in aurora prevent centrosome separation leading to the formation of monopolar spindles. *Cell*, v. 81, n. 1, p. 95-105, Apr 7 1995.

GONTAREWICZ, A. Danusertib (formerly PHA-739358)--a novel combined pan-Aurora kinases and third generation Bcr-Abl tyrosine kinase inhibitor. *Recent Results Cancer Res*, v. 184, p. 199-214, 2010.

GOTTESMAN, M. M. Overview: ABC transporters and human disease. *J Bioenerg Biomembr*, v. 33, n. 6, p. 453-8, Dec 2001.

GOTTESMAN, M. M. *et al.* Multidrug resistance in cancer: role of ATP-dependent transporters. *Nat Rev Cancer*, v. 2, n. 1, p. 48-58, Jan 2002.

GREENBERG, P. L. *et al.* Mitoxantrone, etoposide, and cytarabine with or without valspodar in patients with relapsed or refractory acute myeloid leukemia and high-risk myelodysplastic syndrome: a phase III trial (E2995). *J Clin Oncol*, v. 22, n. 6, p. 1078-86, Mar 15 2004.

GRIMWADE, D. *et al.* The importance of diagnostic cytogenetics on outcome in AML: analysis of 1,612 patients entered into the MRC AML 10 trial. The Medical Research Council Adult and Children's Leukaemia Working Parties. *Blood*, v. 92, n. 7, p. 2322-33, Oct 1 1998.

GULLY, C. P. *et al.* Antineoplastic effects of an Aurora B kinase inhibitor in breast cancer. *Mol Cancer*, v. 9, p. 42, 2010.

GUO, J. *et al.* Identification of genes that confer tumor cell resistance to the Aurora B kinase inhibitor, AZD1152. *Pharmacogenomics J*, v. 9, n. 2, p. 90-102, Apr 2009.

HAMADA, H. Functional role for the 170- to 180-kDa glycoprotein specific to drug-resistant tumor cells as revealed by monoclonal antibodies. *Proc Natl Acad Sci U S A*, v. 83, n. 20, p. 7785-9, Oct 1986.

HAN, H. *et al.* Identification of differentially expressed genes in pancreatic cancer cells using cDNA microarray. *Cancer Res*, v. 62, n. 10, p. 2890-6, May 15 2002.

HANSEN, J. B. *et al.* SPC3042: a proapoptotic survivin inhibitor. *Mol Cancer Ther*, v. 7, n. 9, p. 2736-45, Sep 2008.

HARRINGTON, E. A. *et al.* VX-680, a potent and selective small-molecule inhibitor of the Aurora kinases, suppresses tumor growth in vivo. *Nature Medicine*, v. 10, n. 3, p. 262-267, Mar 2004.

HAUF, S. *et al.* The small molecule Hesperadin reveals a role for Aurora B in correcting kinetochore-microtubule attachment and in maintaining the spindle assembly checkpoint. *Journal of Cell Biology*, v. 161, n. 2, p. 281-294, Apr 2003.

HOFFBRAND, A. V. *Essential haematology*. 5th. ed. Oxford: Blackwell Pub, 2006. (Essential series).

HOLT, S. V. *et al.* The MEK1/2 inhibitor, selumetinib (AZD6244; ARRY-142886), enhances anti-tumour efficacy when combined with conventional chemotherapeutic agents in human tumour xenograft models. *Br J Cancer*, v. 106, n. 5, p. 858-66, Feb 28 2012.

HSU, J. Y. *et al.* Mitotic phosphorylation of histone H3 is governed by Ipl1/aurora kinase and Glc7/PP1 phosphatase in budding yeast and nematodes. *Cell*, v. 102, n. 3, p. 279-91, Aug 4 2000.

HU, H. M. *et al.* Genomic organization, expression, and chromosome localization of a third aurora-related kinase gene, Aie1. *DNA Cell Biol*, v. 19, n. 11, p. 679-88, Nov 2000.

HUANG, X. F. *et al.* Aurora kinase inhibitory VX-680 increases Bax/Bcl-2 ratio and induces apoptosis in Aurora-A-high acute myeloid leukemia. *Blood*, v. 111, n. 5, p. 2854-65, Mar 1 2008.

HUNTER, H. M. *et al.* The expression of P-glycoprotein in AML cells with FLT3 internal tandem duplications is associated with reduced apoptosis in response to FLT3 inhibitors. *British Journal of Haematology*, v. 127, n. 1, p. 26-33, Oct 2004.

IKEZOE, T. *et al.* A novel treatment strategy targeting Aurora kinases in acute myelogenous leukemia. *Mol Cancer Ther*, v. 6, n. 6, p. 1851-7, Jun 2007.

IKEZOE, T. *et al.* p53 is critical for the Aurora B kinase inhibitor-mediated apoptosis in acute myelogenous leukemia cells. *Int J Hematol*, v., Dec 16 2009.

ISMAIL, I. H. The gamma-H2A.X: is it just a surrogate marker of double-strand breaks or much more? *Environ Mol Mutagen*, v. 49, n. 1, p. 73-82, Jan 2008.

JABBOUR, E. *et al.* A phase 1-2 study of a farnesyltransferase inhibitor, tipifarnib, combined with idarubicin and cytarabine for patients with newly diagnosed acute myeloid leukemia and high-risk myelodysplastic syndrome. *Cancer*, v. 117, n. 6, p. 1236-44, Mar 15 2011.

JAWAD, M. *et al.* Analysis of factors that affect in vitro chemosensitivity of leukaemic stem and progenitor cells to gemtuzumab ozogamicin (Mylotarg) in acute myeloid leukaemia. *Leukemia*, v. 24, n. 1, p. 74-80, Jan 2009.

JEMAL, A. *et al.* Cancer Statistics, 2010. *CA Cancer J Clin*, v., Jul 7 2010.

JOEL, S. P. *et al.* The activity of the novel aurora kinase B inhibitor AZD1152 in acute myeloid leukaemia cells. *Blood*, v. 106, n. 11, p. 943A-943A, Nov 2005.

JORDAN, M. A. Microtubules as a target for anticancer drugs. ***Nat Rev Cancer*****, v. 4, n. 4, p. 253-65, Apr 2004.**

JULIANO, R. L. A surface glycoprotein modulating drug permeability in Chinese hamster ovary cell mutants. ***Biochim Biophys Acta*****, v. 455, n. 1, p. 152-62, Nov 11 1976.**

KARP, J. E. ***et al.*** **Multi-institutional phase 2 clinical and pharmacogenomic trial of tipifarnib plus etoposide for elderly adults with newly diagnosed acute myelogenous leukemia.** ***Blood*****, v. 119, n. 1, p. 55-63, Jan 5 2012.**

KATAYAMA, H. Aurora kinase inhibitors as anticancer molecules. ***Biochim Biophys Acta*****, v. 1799, n. 10-12, p. 829-39, Oct-Dec 2010.**

KATAYAMA, H. ***et al.*** **Mitotic kinase expression and colorectal cancer progression.** ***J Natl Cancer Inst*****, v. 91, n. 13, p. 1160-2, Jul 7 1999.**

KEEN, N. Aurora-kinase inhibitors as anticancer agents. ***Nature Reviews Cancer*****, v. 4, n. 12, p. 927-936, Dec 2004.**

KEEN, N. ***et al.*** **Biological characterisation of AZD1152, a highly potent and selective inhibitor of Aurora kinase activity. v. 11. n. 242005. p. 9086S-9086S.**

KITZEN, J. J. ***et al.*** **Aurora kinase inhibitors.** ***Crit Rev Oncol Hematol*****, v. 73, n. 2, p. 99-110, Feb 2010.**

KIYOI, H. ***et al.*** **Prognostic implication of FLT3 and N-RAS gene mutations in acute myeloid leukemia.** ***Blood*****, v. 93, n. 9, p. 3074-80, May 1 1999.**

KNAPPER, S. The clinical development of FLT3 inhibitors in acute myeloid leukemia. ***Expert Opin Investig Drugs*****, v. 20, n. 10, p. 1377-95, Oct 2011.**

KNAPPER, S. ***et al.*** **A phase 2 trial of the FLT3 inhibitor lestaurtinib (CEP701) as first-line treatment for older patients with acute myeloid leukemia not considered fit for intensive chemotherapy.** ***Blood*****, v. 108, n. 10, p. 3262-70, Nov 15 2006.**

KOJIMA, K. ***et al.*** **Concomitant inhibition of Mdm2-p53 interaction and Aurora kinases activates the p53-dependent postmitotic checkpoints and synergistically induces p53-mediated mitochondrial apoptosis along with reduced endoreduplication in acute myelogenous leukemia.** ***Blood*****, v. 112, n. 7, p. 2886-95, Oct 1 2008.**

KOLLAREDDY, M. ***et al.*** **Aurora kinase inhibitors: Progress towards the clinic.** ***Invest New Drugs*****, v., Feb 18 2012.**

KORNBERG, R. D. Chromatin structure: a repeating unit of histones and DNA. *Science*, v. 184, n. 139, p. 868-71, May 24 1974.

KOTTARIDIS, P. D. *et al.* The presence of a FLT3 internal tandem duplication in patients with acute myeloid leukemia (AML) adds important prognostic information to cytogenetic risk group and response to the first cycle of chemotherapy: analysis of 854 patients from the United Kingdom Medical Research Council AML 10 and 12 trials. *Blood*, v. 98, n. 6, p. 1752-9, Sep 15 2001.

KRISHNAMACHARY, N. *et al.* Analysis of MRP gene expression and function in HL60 cells isolated for resistance to adriamycin. *Oncol Res*, v. 6, n. 3, p. 119-27, 1994.

LAMPSON, M. A. Sensing centromere tension: Aurora B and the regulation of kinetochore function. *Trends Cell Biol*, v. 21, n. 3, p. 133-40, Mar 2010.

LANCET, J. E. *et al.* A phase I trial of continuous infusion of the multidrug resistance inhibitor zosuquidar with daunorubicin and cytarabine in acute myeloid leukemia. *Leuk Res*, v. 33, n. 8, p. 1055-61, Aug 2009.

LAUPEZE, B. *et al.* High multidrug resistance protein activity in acute myeloid leukaemias is associated with poor response to chemotherapy and reduced patient survival. *Br J Haematol*, v. 116, n. 4, p. 834-8, Mar 2002.

LEGRAND, O. *et al.* Simultaneous activity of MRP1 and Pgp is correlated with in vitro resistance to daunorubicin and with in vivo resistance in adult acute myeloid leukemia. *Blood*, v. 94, n. 3, p. 1046-56, Aug 1 1999.

LEISCHNER, H. *et al.* SRC is a signaling mediator in FLT3-ITD- but not in FLT3-TKD-positive AML. *Blood*, v. 119, n. 17, p. 4026-33, Apr 26 2012.

LEITH, C. P. *et al.* Frequency and clinical significance of the expression of the multidrug resistance proteins MDR1/P-glycoprotein, MRP1, and LRP in acute myeloid leukemia. A Southwest Oncology Group Study. *Blood*, v. 94, n. 3, p. 1086-1099, Aug 1999.

LEITH, C. P. *et al.* Acute myeloid leukemia in the elderly: assessment of multidrug resistance (MDR1) and cytogenetics distinguishes biologic subgroups with remarkably distinct responses to standard chemotherapy. A Southwest Oncology Group study. *Blood*, v. 89, n. 9, p. 3323-9, May 1 1997.

LEVINE, A. J. p53, the cellular gatekeeper for growth and division. *Cell*, v. 88, n. 3, p. 323-31, Feb 7 1997.

LEVIS, M. *et al.* A FLT3-targeted tyrosine kinase inhibitor is cytotoxic to leukemia cells in vitro and in vivo. *Blood*, v. 99, n. 11, p. 3885-91, Jun 1 2002.

LEVIS, M. *et al.* Internal tandem duplications of the FLT3 gene are present in leukemia stem cells. *Blood*, v. 106, n. 2, p. 673-80, Jul 15 2005.

LEVIS, M. *et al.* Results from a randomized trial of salvage chemotherapy followed by lestaurtinib for patients with FLT3 mutant AML in first relapse. *Blood*, v. 117, n. 12, p. 3294-301, Mar 24 2011.

LEWIS, K. D. *et al.* A multi-center phase II evaluation of the small molecule survivin suppressor YM155 in patients with unresectable stage III or IV melanoma. *Invest New Drugs*, v. 29, n. 1, p. 161-6, Feb 2009.

LEY, T. J. *et al.* DNMT3A mutations in acute myeloid leukemia. *N Engl J Med*, v. 363, n. 25, p. 2424-33, Dec 16 2010.

LIST, A. F. *et al.* Benefit of cyclosporine modulation of drug resistance in patients with poor-risk acute myeloid leukemia: a Southwest Oncology Group study. *Blood*, v. 98, n. 12, p. 3212-20, Dec 1 2001.

LIZARD, G. *et al.* Evaluation of multidrug resistant phenotype by flow cytometry with monoclonal antibodies and functional tests. *Bull Cancer*, v. 82, n. 3, p. 211-7, Mar 1995.

LOWENBERG, B. *et al.* Acute myeloid leukemia and acute promyelocytic leukemia. *Hematology Am Soc Hematol Educ Program*, v., p. 82-101, 2003.

LOWENBERG, B. *et al.* Phase I/II Study to Assess the Safety and Efficacy of the Aurora B Kinase Inhibitor, AZD1152, in Patients with Advanced Acute Myeloid Leukemia. v. 114. n. 222009. p. 2080-.

MAHADEVAN, D. Targeting the multidrug resistance-1 transporter in AML: molecular regulation and therapeutic strategies. *Blood*, v. 104, n. 7, p. 1940-51, Oct 1 2004.

MAO, Q. Role of the breast cancer resistance protein (ABCG2) in drug transport. *Aaps J*, v. 7, n. 1, p. E118-33, 2005.

MARCUCCI, G. *et al.* Molecular genetics of adult acute myeloid leukemia: prognostic and therapeutic implications. *J Clin Oncol*, v. 29, n. 5, p. 475-86, Feb 10 2011.

MARQUES, D. S. *et al.* Relationships between multidrug resistance (MDR) and stem cell markers in human chronic myeloid leukemia cell lines. *Leuk Res*, v. 34, n. 6, p. 757-62, Jun 2010.

MARZAC, C. *et al.* ATP Binding Cassette transporters associated with chemoresistance: transcriptional profiling in extreme cohorts and their

prognostic impact in a cohort of 281 acute myeloid leukemia patients. *Haematologica*, v. 96, n. 9, p. 1293-301, Sep 2011.

MARZAC, C. *et al.* Flt3 internal tandem duplication and P-glycoprotein functionality in 171 patients with acute myeloid leukemia. *Clin Cancer Res*, v. 12, n. 23, p. 7018-24, Dec 1 2006.

MECHETNER, E. B. *et al.* P-glycoprotein function involves conformational transitions detectable by differential immunoreactivity. *Proc Natl Acad Sci U S A*, v. 94, n. 24, p. 12908-13, Nov 25 1997.

MESHINCHI, S. Structural and functional alterations of FLT3 in acute myeloid leukemia. *Clin Cancer Res*, v. 15, n. 13, p. 4263-9, Jul 1 2009.

MESHINCHI, S. *et al.* Clinical implications of FLT3 mutations in pediatric AML. *Blood*, v. 108, n. 12, p. 3654-61, Dec 1 2006.

MILLIGAN, D. W. *et al.* Guidelines on the management of acute myeloid leukaemia in adults. *Br J Haematol*, v. 135, n. 4, p. 450-74, Nov 2006.

MIZUKI, M. *et al.* Flt3 mutations from patients with acute myeloid leukemia induce transformation of 32D cells mediated by the Ras and STAT5 pathways. *Blood*, v. 96, n. 12, p. 3907-14, Dec 1 2000.

MONY, U. *et al.* Resistance to FLT3 inhibition in an in vitro model of primary AML cells with a stem cell phenotype in a defined microenvironment. *Leukemia*, v. 22, n. 7, p. 1395-401, Jul 2008.

MOORE, A. S. *et al.* Resistance to Selective FLT3 Inhibitors, Driven by FLT3 Ligand and FLT3 Point Mutations, Can Be Overcome with the Dual FLT3-Aurora Kinase Inhibitor CCT241736. v. 118. n. 212011. p. 1490-1490.

MORI, N. *et al.* Effects of AZD1152, a selective Aurora B kinase inhibitor, on Burkitt's and Hodgkin's lymphomas. *Biochem Pharmacol*, v., Mar 1 2011.

MORTLOCK, A. A. *et al.* Discovery, synthesis, and in vivo activity of a new class of pyrazoloquinazolines as selective inhibitors of aurora B kinase. *J Med Chem*, v. 50, n. 9, p. 2213-24, May 3 2007.

NAGAHARA, Y. *et al.* Mechanism of mitochondrial 7A6 antigen exposure triggered by distinct apoptotic pathways: involvement of caspases. *Cytometry A*, v. 71, n. 4, p. 232-41, Apr 2007.

NAIR, J. S. *et al.* Aurora B kinase regulates the postmitotic endoreduplication checkpoint via phosphorylation of the retinoblastoma protein at serine 780. *Mol Biol Cell*, v. 20, n. 8, p. 2218-28, Apr 2009.

NAKAO, M. *et al.* Internal tandem duplication of the flt3 gene found in acute myeloid leukemia. *Leukemia*, v. 10, n. 12, p. 1911-8, Dec 1996.

NIERMANN, K. J. *et al.* Enhanced radiosensitivity of androgen-resistant prostate cancer: AZD1152-mediated Aurora kinase B inhibition. *Radiat Res*, v. 175, n. 4, p. 444-51, Apr 2011.

OKE, A. *et al.* AZD1152 Rapidly and Negatively Affects the Growth and Survival of Human Acute Myeloid Leukemia Cells In vitro and In vivo. *Cancer Res*, v., Apr 14 2009.

PALLIS, M. Flow cytometric measurement of functional and phenotypic P-glycoprotein. *Methods Mol Med*, v. 111, p. 167-81, 2005.

PALLIS, M. *et al.* Reproducible measurements of AML blast p-glycoprotein function in 2 center analyses. *Blood*, v. 105, n. 3, p. 1367-1368, Feb 2005.

PALLIS, M. *et al.* Analysis of the interaction of induction regimens with p-glycoprotein expression in patients with acute myeloid leukaemia: results from the MRC AML15 trial. *Blood Cancer Journal*. v. 1, 2011.

PALLIS, M. *et al.* Flow cytometric measurement of phosphorylated STAT5 in AML: lack of specific association with FLT3 internal tandem duplications. *Leukemia Research*, v. 27, n. 9, p. 803-805, Sep 2003a.

PALLIS, M. *et al.* Flow cytometric chemosensitivity analysis of blasts from patients with acute myeloblastic leukemia and myelodysplastic syndromes: the use of 7AAD with antibodies to CD45 or CD34. *Cytometry*, v. 37, n. 4, p. 308-13, Dec 1 1999a.

PALLIS, M. *et al.* Resistance to spontaneous apoptosis in AML blasts is associated with p-glycoprotein expression and function, but not with the presence of FLT3 internal tandem duplications. *Blood*, v. 100, n. 11, p. 747A-748A, Nov 2002.

PALLIS, M. *et al.* Resistance to spontaneous apoptosis in acute myeloid leukaemia blasts is associated with p-glycoprotein expression and function, but not with the presence of FLT3 internal tandem duplications. *British Journal of Haematology*, v. 120, n. 6, p. 1009-1016, Mar 2003b.

PALLIS, M. *et al.* Reproducible flow cytometric methodology for measuring multidrug resistance in leukaemic blasts. *Adv Exp Med Biol*, v. 457, p. 77-88, 1999b.

PALLISGAARD, N. *et al.* Rapid and sensitive minimal residual disease detection in acute leukemia by quantitative real-time RT-PCR exemplified by

t(12;21) TEL-AML1 fusion transcript. *Genes Chromosomes Cancer*, v. 26, n. 4, p. 355-65, Dec 1999.

PAQUETTE, R. L. *et al.* PHA-739358, an aurora kinase inhibitor, induces clinical responses in chronic myeloid leukemia harboring T315I mutations of BCR-ABL. v. 110. n. 112007. p. 312A-312A.

PARK, S. W. *et al.* Analysis of P-glycoprotein-mediated membrane transport in human peripheral blood lymphocytes using the UIC2 shift assay. *Cytometry A*, v. 53, n. 2, p. 67-78, Jun 2003.

PASCHKA, P. *et al.* Adverse prognostic significance of KIT mutations in adult acute myeloid leukemia with inv(16) and t(8;21): a Cancer and Leukemia Group B Study. *J Clin Oncol*, v. 24, n. 24, p. 3904-11, Aug 20 2006.

PAYTON, M. *et al.* Preclinical evaluation of AMG 900, a novel potent and highly selective pan-aurora kinase inhibitor with activity in taxane-resistant tumor cell lines. *Cancer Res*, v. 70, n. 23, p. 9846-54, Dec 1 2010.

PEETERS, S. D. *et al.* Selective expression of cholesterol metabolism genes in normal CD34+CD38- cells with a heterogeneous expression pattern in AML cells. *Exp Hematol*, v. 34, n. 5, p. 622-30, May 2006.

PEPPER, C. *et al.* Flow cytometric assessment of three different methods for the measurement of in vitro apoptosis. *Leuk Res*, v. 22, n. 5, p. 439-44, May 1998.

QADIR, M. *et al.* Cyclosporin A is a broad-spectrum multidrug resistance modulator. *Clin Cancer Res*, v. 11, n. 6, p. 2320-6, Mar 15 2005.

RAAIJMAKERS, M. H. ATP-binding-cassette transporters in hematopoietic stem cells and their utility as therapeutical targets in acute and chronic myeloid leukemia. *Leukemia*, v. 21, n. 10, p. 2094-102, Oct 2007.

RABINDRAN, S. K. *et al.* Fumitremorgin C reverses multidrug resistance in cells transfected with the breast cancer resistance protein. *Cancer Res*, v. 60, n. 1, p. 47-50, Jan 1 2000.

RABINOVITCH, P. S. *et al.* Simultaneous cell cycle analysis and two-color surface immunofluorescence using 7-amino-actinomycin D and single laser excitation: applications to study of cell activation and the cell cycle of murine Ly-1 B cells. *J Immunol*, v. 136, n. 8, p. 2769-75, Apr 15 1986.

RANDLE, R. A. *et al.* Role of the highly structured 5'-end region of MDR1 mRNA in P-glycoprotein expression. *Biochem J*, v. 406, n. 3, p. 445-55, Sep 15 2007.

RAVANDI, F. *et al.* Progress in the treatment of acute myeloid leukemia. *Cancer*, v. 110, n. 9, p. 1900-10, Nov 1 2007.

RAVANDI, F. *et al.* New agents in acute myeloid leukemia and other myeloid disorders. *Cancer*, v. 100, n. 3, p. 441-54, Feb 1 2004.

ROBAK, T. Current and emerging therapies for acute myeloid leukemia. *Clin Ther*, v. 31 Pt 2, p. 2349-70, 2009.

ROGAKOU, E. P. *et al.* Initiation of DNA fragmentation during apoptosis induces phosphorylation of H2AX histone at serine 139. *J Biol Chem*, v. 275, n. 13, p. 9390-5, Mar 31 2000.

ROLLIG, C. *et al.* Survey and analysis of the efficacy and prescription pattern of sorafenib in patients with acute myeloid leukemia. *Leuk Lymphoma*, v., Dec 7 2011.

SAIJO, N. Critical comments for roles of biomarkers in the diagnosis and treatment of cancer. *Cancer Treat Rev*, v., Jun 6 2011.

SANTOLI, D. *et al.* Synergistic and antagonistic effects of recombinant human interleukin (IL) 3, IL-1 alpha, granulocyte and macrophage colony-stimulating factors (G-CSF and M-CSF) on the growth of GM-CSF-dependent leukemic cell lines. *J Immunol*, v. 139, n. 10, p. 3348-54, Nov 15 1987.

SANZ, M. A. *et al.* Management of acute promyelocytic leukemia: recommendations from an expert panel on behalf of the European LeukemiaNet. *Blood*, v. 113, n. 9, p. 1875-91, Feb 26 2009.

SARNO, S. *et al.* The novel aurora kinase inhibitor AS703569 shows potent anti-tumor activity in acute myeloid leukemia (AML). v. 110. n. 112007. p. 279A-279A.

SASAI, K. *et al.* Aurora-C kinase is a novel chromosomal passenger protein that can complement Aurora-B kinase function in mitotic cells. *Cell Motil Cytoskeleton*, v. 59, n. 4, p. 249-63, Dec 2004.

SATO, T. *et al.* FLT3 ligand impedes the efficacy of FLT3 inhibitors in vitro and in vivo. *Blood*, v. 117, n. 12, p. 3286-93, Mar 24 2011.

SCHAKOWSKI, F. *et al.* Novel non-viral method for transfection of primary leukemia cells and cell lines. *Genet Vaccines Ther*, v. 2, n. 1, p. 1, Jan 12 2004.

SCHARENBERG, C. W. *et al.* The ABCG2 transporter is an efficient Hoechst 33342 efflux pump and is preferentially expressed by immature human hematopoietic progenitors. *Blood*, v. 99, n. 2, p. 507-12, Jan 15 2002.

SCHINKEL, A. H. Mammalian drug efflux transporters of the ATP binding cassette (ABC) family: an overview. *Adv Drug Deliv Rev*, v. 55, n. 1, p. 3-29, Jan 21 2003.

SCHNITTGER, S. *et al.* Analysis of FLT3 length mutations in 1003 patients with acute myeloid leukemia: correlation to cytogenetics, FAB subtype, and prognosis in the AMLCG study and usefulness as a marker for the detection of minimal residual disease. *Blood*, v. 100, n. 1, p. 59-66, Jul 1 2002.

SCHNITTGER, S. *et al.* Nucleophosmin gene mutations are predictors of favorable prognosis in acute myelogenous leukemia with a normal karyotype. *Blood*, v. 106, n. 12, p. 3733-9, Dec 1 2005.

SCHUURHUIS, G. J. *et al.* Functional multidrug resistance phenotype associated with combined overexpression of Pgp/MDR1 and MRP together with 1-beta-D-arabinofuranosylcytosine sensitivity may predict clinical response in acute myeloid leukemia. *Clin Cancer Res*, v. 1, n. 1, p. 81-93, Jan 1995.

SEEDHOUSE, C. *et al.* Regulation of ABCB1 (p-glycoprotein) by the FOXO1 Transcription Factor in Acute Myeloid Leukemia. v. 114. n. 222009. p. 244-245.

SEEDHOUSE, C. H. *et al.* Sequential influences of leukemia-specific and genetic factors on p-glycoprotein expression in blasts from 817 patients entered into the National Cancer Research Network acute myeloid leukemia 14 and 15 trials. *Clin Cancer Res*, v. 13, n. 23, p. 7059-66, Dec 1 2007.

SEGERS, S. A. *et al.* Aurora Kinases in Childhood Acute Leukemia: The Promise of Aurora Kinase B As a Drugable Target. v. 118. n. 212011. p. 641-641.

SEIFERT, H. *et al.* The prognostic impact of 17p (p53) deletion in 2272 adults with acute myeloid leukemia. *Leukemia*, v. 23, n. 4, p. 656-63, Apr 2009.

SHEN, Y. *et al.* Gene mutation patterns and their prognostic impact in a cohort of 1,185 patients with acute myeloid leukemia. *Blood*, v., Aug 31 2011.

SMEETS, M. E. *et al.* Triggering noncycling hematopoietic progenitors and leukemic blasts to proliferate increases anthracycline retention and toxicity by downregulating multidrug resistance. *Blood*, v. 94, n. 7, p. 2414-23, Oct 1 1999.

SMITH, B. D. *et al.* Single-agent CEP-701, a novel FLT3 inhibitor, shows biologic and clinical activity in patients with relapsed or refractory acute myeloid leukemia. *Blood*, v. 103, n. 10, p. 3669-76, May 15 2004.

SONCINI, C. *et al.* PHA-680632, a novel Aurora kinase inhibitor with potent antitumoral activity. *Clin Cancer Res*, v. 12, n. 13, p. 4080-9, Jul 1 2006.

SONNEVELD, P. Chemotherapy resistance in acute myeloid leukaemia. *Best Pract Res Clin Haematol*, v. 14, n. 1, p. 211-33, Mar 2001.

SPIEKERMANN, K. *et al.* Overexpression and constitutive activation of FLT3 induces STAT5 activation in primary acute myeloid leukemia blast cells. *Clin Cancer Res*, v. 9, n. 6, p. 2140-50, Jun 2003.

STASI, R. *et al.* Gemtuzumab ozogamicin in the treatment of acute myeloid leukemia. *Cancer Treat Rev*, v. 34, n. 1, p. 49-60, Feb 2008.

STEEGHS, N. *et al.* Phase I pharmacokinetic and pharmacodynamic study of the aurora kinase inhibitor danusertib in patients with advanced or metastatic solid tumors. *J Clin Oncol*, v. 27, n. 30, p. 5094-101, Oct 20 2009.

STEELMAN, L. S. *et al.* JAK/STAT, Raf/MEK/ERK, PI3K/Akt and BCR-ABL in cell cycle progression and leukemogenesis. *Leukemia*, v. 18, n. 2, p. 189-218, Feb 2004.

STEINBACH, D. *et al.* ABCA3 as a possible cause of drug resistance in childhood acute myeloid leukemia. *Clin Cancer Res*, v. 12, n. 14 Pt 1, p. 4357-63, Jul 15 2006.

STONE, R. M. *et al.* Patients with acute myeloid leukemia and an activating mutation in FLT3 respond to a small-molecule FLT3 tyrosine kinase inhibitor, PKC412. *Blood*, v. 105, n. 1, p. 54-60, Jan 1 2005.

STONE, R. M. *et al.* Acute myeloid leukemia. *Hematology Am Soc Hematol Educ Program*, v., p. 98-117, 2004.

SUVANNASANKHA, A. *et al.* Breast cancer resistance protein (BCRP/MXR/ABCG2) in acute myeloid leukemia: discordance between expression and function. *Leukemia*, v. 18, n. 7, p. 1252-7, Jul 2004.

SZAKACS, G. *et al.* Targeting multidrug resistance in cancer. *Nat Rev Drug Discov*, v. 5, n. 3, p. 219-34, Mar 2006.

TALLMAN, M. S. *et al.* All-trans retinoic acid in acute promyelocytic leukemia: long-term outcome and prognostic factor analysis from the North American Intergroup protocol. *Blood*, v. 100, n. 13, p. 4298-302, Dec 15 2002.

TANAKA, R. *et al.* Activity of the multitargeted kinase inhibitor, AT9283, in imatinib-resistant BCR-ABL-positive leukemic cells. *Blood*, v. 116, n. 12, p. 2089-95, Sep 23 2010.

TAO, Y. *et al.* Enhancement of radiation response in p53-deficient cancer cells by the Aurora-B kinase inhibitor AZD1152. *Oncogene*, v. 27, n. 23, p. 3244-55, May 22 2008.

TAYLOR, B. J. *et al.* Detection of P-glycoprotein in cell lines and leukemic blasts: failure of select monoclonal antibodies to detect clinically significant Pgp levels in primary cells. *Leuk Res*, v. 25, n. 12, p. 1127-35, Dec 2001.

THOMAS, H. Overcoming multidrug resistance in cancer: an update on the clinical strategy of inhibiting p-glycoprotein. *Cancer Control*, v. 10, n. 2, p. 159-65, Mar-Apr 2003.

THOMAS, J. *et al.* Active transport of imatinib into and out of cells: implications for drug resistance. *Blood*, v. 104, n. 12, p. 3739-45, Dec 1 2004.

TIRIBELLI, M. *et al.* Concomitant ABCG2 overexpression and FLT3-ITD mutation identify a subset of acute myeloid leukemia patients at high risk of relapse. *Cancer*, v. 117, n. 10, p. 2156-62, May 15 2010.

TONG, T. *et al.* Overexpression of Aurora-A contributes to malignant development of human esophageal squamous cell carcinoma. *Clin Cancer Res*, v. 10, n. 21, p. 7304-10, Nov 1 2004.

TOTHOVA, Z. FoxO transcription factors and stem cell homeostasis: insights from the hematopoietic system. *Cell Stem Cell*, v. 1, n. 2, p. 140-52, Aug 16 2007.

TRAN, H. Clofarabine in the treatment of newly diagnosed acute myeloid leukemia in older adults. *Ann Pharmacother*, v. 46, n. 1, p. 89-96, Jan 2012.

TRAYNOR, A. M. *et al.* Phase I dose escalation study of MK-0457, a novel Aurora kinase inhibitor, in adult patients with advanced solid tumors. *Cancer Chemother Pharmacol*, v. 67, n. 2, p. 305-14, Feb 2011.

TSUBOI, K. *et al.* A Phase I study to assess the safety, pharmacokinetics and efficacy of barasertib (AZD1152), an Aurora B kinase inhibitor, in Japanese patients with advanced acute myeloid leukemia. *Leuk Res*, v. 35, n. 10, p. 1384-9, Oct 2011.

TWENTYMAN, P. R. Resistance modification by PSC-833, a novel non-immunosuppressive cyclosporin [corrected]. *Eur J Cancer*, v. 27, n. 12, p. 1639-42, 1991.

UGGLA, B. *et al.* BCRP mRNA expression v. clinical outcome in 40 adult AML patients. *Leuk Res*, v. 29, n. 2, p. 141-6, Feb 2005.

VAN DER KOLK, D. M. *et al.* Activity and expression of the multidrug resistance proteins P-glycoprotein, MRP1, MRP2, MRP3 and MRP5 in de novo and relapsed acute myeloid leukemia. *Leukemia*, v. 15, n. 10, p. 1544-53, Oct 2001.

VAN DER KOLK, D. M. *et al.* P-glycoprotein and multidrug resistance protein activities in relation to treatment outcome in acute myeloid leukemia. *Clinical Cancer Research*, v. 6, n. 8, p. 3205-3214, Aug 2000.

VAN DER POL, M. A. *et al.* Function of the ABC transporters, P-glycoprotein, multidrug resistance protein and breast cancer resistance protein, in minimal residual disease in acute myeloid leukemia. *Haematologica*, v. 88, n. 2, p. 134-47, Feb 2003.

VAN HOOSER, A. *et al.* Histone H3 phosphorylation is required for the initiation, but not maintenance, of mammalian chromosome condensation. *J Cell Sci*, v. 111 (Pt 23), p. 3497-506, Dec 1998.

WALSBY, E. *et al.* The aurora kinase inhibitor AZD1152 causes perturbation of cell cycle distribution in cell lines and primary AML samples. *Blood*, v. 106, n. 11, p. 774A-774A, Nov 2005.

WARNER, S. L. *et al.* Comparing Aurora A and Aurora B as molecular targets for growth inhibition of pancreatic cancer cells. *Mol Cancer Ther*, v. 5, n. 10, p. 2450-8, Oct 2006.

WEI, Y. *et al.* Phosphorylation of histone H3 is required for proper chromosome condensation and segregation. *Cell*, v. 97, n. 1, p. 99-109, Apr 2 1999.

WEISBERG, E. *et al.* Inhibition of mutant FLT3 receptors in leukemia cells by the small molecule tyrosine kinase inhibitor PKC412. *Cancer Cell*, v. 1, n. 5, p. 433-43, Jun 2002.

WILKINSON, R. W. *et al.* AZD1152, a selective inhibitor of Aurora B kinase, inhibits human tumor xenograft growth by inducing apoptosis. *Clin Cancer Res*, v. 13, n. 12, p. 3682-8, Jun 15 2007.

WU, L. *et al.* Aurora B interacts with NIR-p53, leading to p53 phosphorylation in its DNA-binding domain and subsequent functional suppression. *J Biol Chem*, v. 286, n. 3, p. 2236-44, Jan 21 2011.

YAN, X. *et al.* Aurora C is directly associated with Survivin and required for cytokinesis. v. 10. n. 62005. p. 617-26.

YANG, H. *et al.* Mitotic requirement for aurora A kinase is bypassed in the absence of aurora B kinase. *FEBS Lett*, v. 579, n. 16, p. 3385-91, Jun 20 2005.

YANG, J. *et al.* AZD1152, a novel and selective aurora B kinase inhibitor, induces growth arrest, apoptosis, and sensitization for tubulin depolymerizing agent or topoisomerase II inhibitor in human acute leukemia cells in vitro and in vivo. *Blood*, v., May 10 2007.

ZHANG, S. *et al.* Essential role of signal transducer and activator of transcription (Stat)5a but not Stat5b for Flt3-dependent signaling. *J Exp Med*, v. 192, n. 5, p. 719-28, Sep 4 2000.

ZHOU, J. *et al.* Enhanced activation of STAT pathways and overexpression of survivin confer resistance to FLT3 inhibitors and could be therapeutic targets in AML. v. 113. n. 172009. p. 4052-62.

ZHU, X. *et al.* Novel agents and regimens for acute myeloid leukemia: 2009 ASH annual meeting highlights. *J Hematol Oncol*, v. 3, p. 17, 2009.

Appendix

Protocol for measuring phospho-Histone H3 expression and DNA content in primary AML cells and cell lines

Reagents:
PBSAA buffer (PBS with 1%BSA and 0.1% sodium azide)
Cell permeabilization kit (Abd Serotec) containing reagent A and reagent B.
Anti-phospho-Histone H3 (Ser 10) clone 3H10 mouse monoclonal $IgG1_k$ (Upstate) 1mg/ml
Mouse IgG1 (Dako) 100µg/ml
Polyclonal Goat anti-mouse IgG FITC $F(ab`)_2$ (Dako) 1mg/ml

1. Prepare primary samples or cell lines as described.
2. Re-suspend cells at $3x10^6$/ml in 1ml PBSAA, put 100µl ($3x10^5$ cells) into each of two tubes.
3. Add 20µl reagent A to each tube.
4. Incubate 15 for minutes at room temperature in the dark.
5. Whilst vortexing add 3ml of ice cold methanol to each tube and incubate for 10 minutes on ice.
6. Pellet and then wash once in 3ml PBSAA. Tip off supernatant and re-suspend.
7. Add 20µl Reagent B to each tube.
8. Add 1^{st} layer abs:
   Add 200µl Anti-phospho-Histone H3 Ab (Diluted 1:290 in PBSAA) to Tube 1.
   Add 200µl Mouse IgG1 control (Diluted 1:24) to Tube 2.
   Vortex 1-2 seconds.
9. Incubate for 2 hours at room temperature.
10. Wash twice in PBSAA. Tip off supernatant and re-suspend.
11. Add 3µl Polyclonal Goat anti-mouse IgG FITC $F(ab`)_2$ to each tube.
12. Vortex and incubate for one hour at room temperature in the dark.
13. Wash twice in PBSAA. Tip off supernatant and follow protocol A or B.

    A Re-suspend the pellet in 20µl PBSAA and add to a slide to air dry. Add 10µl DAPI stain to a cover-slip, add the slide and seal with varnish. View under the fluorescence microscope to asses the percentage of cells positive for pHH3.

    B Add 300ul of 25µg/ml 7AAD.
    Incubate at room temperature in the dark for 15 minutes and FACS (collecting 25000 events).